PERTURBATION OF RENEWAL PROCESSES

Osman Caglar Akin, B.Sc.,M.Sc.

Dissertation Prepared for the Degree of

DOCTOR OF PHILOSOPHY

UNIVERSITY OF NORTH TEXAS

May 2008

APPROVED:

Paolo Grigolini, Major Professor
William D. Deering, Committee Member
Arkadii Krokhin, Committee Member
James Roberts, Committee Member
Chris L. Littler, Chair of the Department
 of Physics
Sandra L. Terrell, Dean of the Robert B.
 Toulouse School of Graduate
 Studies

Akin, Osman Caglar. <u>Perturbation of renewal processes</u>. Doctor of Philosophy (Physics), May 2008, 140 pp., 43 illustrations, references, 109 titles.

Renewal theory began development in the early 1940s, as the need for it in the industrial engineering sub-discipline operations research had risen. In time, the theory found applications in many stochastic processes. In this thesis I investigated the effect of seasonal effects on Poisson and non-Poisson renewal processes in the form of perturbations. It was determined that the statistical analysis methods developed at UNT Center for Nonlinear Science can be used to detect the effects of seasonality on the data obtained from Poisson/non-Poisson renewal systems. It is proved that a perturbed Poisson process can serve as a paradigmatic model for a case where seasonality is correlated to the noise and that diffusion entropy method can be utilized in revealing this relation. A renewal model making a connection with the stochastic resonance phenomena is used to analyze a previous neurological experiment, and it was shown that under the effect of a nonlinear perturbation, a non-Poisson system statistics may make a transition and end up in the of Poisson basin of statistics. I determine that nonlinear perturbation of the power index for a complex system will lead to a change in the complexity characteristics of the system, i.e., the system will reach a new form of complexity.

ACKNOWLEDGEMENTS

CONTENTS

LIST OF FIGURES

CHAPTER 1

INTRODUCTION

The research work whose results are illustrated in this thesis has been originally mo-
tivated by the statistical analysis of data produced by complex processes, with clear sign
of time periodicity. A paradigmatic case is given by the data, recently analyzed by the
researchers of the UNT and TWU Centers for Nonlinear Science, on the number of
babies born per day to teenager mothers in Texas. These data exhibit a clear annual
periodicity, and the UNT and TWU researchers have been trying to assess which is the
real complexity of this sociological system. The annual periodicity may generate the
false impression that the system is complex. Complexity, in fact, is supposed to be a
consequence of the spontaneous sociological self-organization, which is expected to be
independent of the annual periodicity. Annual periodicity, on the other hand, is a form of
deterministic process that may influence the evaluation of the delicate balance between
order and disorder, which is the main purpose of the research work of the researchers of
the UNT and TWU Centers for Nonlinear Science.

For this reason the first part of this thesis discusses the case of a Poisson system under
the influence of a periodic perturbation. To deal with this important issue we I establish
a close connection with the popular phenomenon of stochastic resonance (SR). I study
the condition under which the sequence of the time intervals between two consecutive
events exhibit evident signs of periodicity, and study these sequences with the diffusion
entropy method, originally proposed by the researchers of the UNT and TWU Centers
for Nonlinear Science, to analyze data of sociological interest. I consequently recognize
a way to establish whether the unperturbed process is complex or not.

An important discovery made in the first part of this thesis is the exponential cascade
effect, corresponding to the experimental observation made via the experiments of Siegel
and Moss and co-workers more than a decade ago. These authors applied a strong

harmonic perturbation to a neuron system and found that the histogram of the time distances between two consecutive firing events is a sequel of equally spaced peaks, whose intensity decays exponentially in time, thereby justifying the adoption of the term exponential cascade to denote the effect.

The second part of this thesis illustrates the research work done to establish if the exponential cascade is a compelling evidence of the Poisson nature of the unperturbed system. For this reason, in the second part of this thesis, I address the problem, more difficult from both theoretical and numerical point of view, of the harmonic perturbation of a non-Poisson renewal system.

The second part of the thesis contains several important results. The first, of interest for the original problem, is that the diffusion entropy method allows us in this case to establish the complexity of the unperturbed system, without operating any de-trending process.

In addition to this important result I notice that the exponential cascade phenomenon is not a compelling signature of the Poisson nature of the unperturbed system. The adoption of strong perturbation may have the effect of producing the exponential cascade phenomenon, even in the non-Poisson case. However, the exponential cascade in some cases is the signature of a genuine transition from non-Poisson statistics, whereas in other cases the adoption of the diffusion entropy method reveals that the system maintains its original non-Poisson character.

I recognize a third case, where the joint action of harmonic perturbation and non-Poisson unperturbed statistics produces a new form of complexity that is totally unexpected. This phenomenon is a clear indication that the complexity evaluation must be operated without using any de-trending procedure. The action of a harmonic perturbation on a complex system does not generate the trivial superposition of two distinct contributions, but a new form of complexity that may be the indication that a complex system, under the influence of a harmonic perturbation, evolves towards a different form of complexity.

CHAPTER 2

SCALING AND SELF SIMILARITY IN PHYSICS

2.1. Introduction

In this chapter, I discuss the basic concepts of self similarity and scaling in physics since it applies to our tools of time series analysis in the science of Complexity. I first discuss the observed power laws in nature, since such distributions are based on some peculiarities, and manifests a basic difference form the famous exponential distribution of the Poisson processes observed in radioactive decay processes where each constituent acts independently from the other so as to form a constant rate Poisson process with a exponential decay of the waiting times. The power laws are important as physical laws since they lack a characteristic scale. At this point we can make the connection with the concept of scaling where the solution of a differential equation may be scaling as functions of the time variable or space variable or some other derived parameters. Scaling concepts are important from the point of view of time series analysis since a distribution function, which might as well be the probability distribution function of some variables like space and time, $p(x, t)$, may possess a functional form, so as to satisfy a scaling relationship. I cover the basic scaling concepts in physics making the connection to the following statement: if a function satisfies the scaling condition, having known its distribution at some point in time, one may infer the expected form of the distribution function at a different time. I later discuss how to determine whether the scaling condition is satisfied by a certain time series and if it is satisfied what should be the particular constants of scaling to form the diffusion process under consideration in later chapters.

2.2. Power Laws in Nature

There are very well established arguments that say that systems in thermodynamic equilibrium have correlations which decay exponentially over space and time. The decay

3

rates are given as the reciprocals of the correlation length and the correlation time, and they are a measure of how big a typical fluctuation should be. [1]. But systems that are non-equilibrium systems like the turbulent flow regime,or systems like those on the verge of a phase transition i.e., critical systems, have fluctuations which decay as power laws. For that matter, systems in phase transition and those far from equilibrium are considered complex systems. So, where ever we see power laws, there is a common consensus that something interesting and complex must be in play.

Exponential distribution tell us about a natural scale of the physical phenomenon to occur but power laws do not, because in Power laws there are no natural scale parameters. This property of the power laws have obvious connections with fractals observed in nature since they also lack a natural scale parameter over a wide scale range of size distributions and possess the property of self similarity , or some sort of self similarity with some modifications (self affinity). And on the other hand, there are lots and lots of power laws observed in nature in statistical data, from earthquakes to blinking quantum dots, and even to some econo-physics phenomena or some social processes, and for that reason they are also referred to as Pareto distributions after the sociologist Vilfredo Pareto.

Vilfredo Pareto was among the first researchers to notice the universality of power laws in economics. While giving a talk in the first years of the 20th century in Geneva [2], Pareto was attacked by the German sociologist Gustav von Schmoller during a conference. During Pareto's presentation Schmoller attacked Pareto's ideas about the existence of mathematical laws in Economics. Next day, posing as a beggar, Pareto approaches Schmoller asking "Sir, is there a restaurant around here where I can eat for nothing?". As Schmoller responds "My dear man, there are no such restaurants, but there is a place around the corner where you can have good meal pretty cheaply","Aha" said Pareto,"So there are laws in economics".

And indeed there are mathematical laws in economics . Price movement distributions for stocks in New York and NASDAQ stock exchanges when plotted on a log-log plot reveals a very nice power law distribution, where the price movement for each stock is normalized by dividing the standard deviation in price movement for that stock. It has

4

been shown that calm time intervals, defined as the time interval between two successive price changes above a fixed threshold obeys a power law decay. It has also been shown that the power law exponent monotonically decreases with respect to the threshold [3]. Historically, the very first power law observed (in 1897) by Vilfredo Pareto was for the distribution of income in UK, and subsequently in Prussia, Saxony, Paris and some Italian cities [4].

Pareto was not the only person to notice power laws in nature. What is known as Zipf's law refers to the size of an occurrence of an event relative to its rank. As a Linguistic Professor at University of Harvard, George Kingsley Zipf was investigating the ranking of words in languages according to their usage. He was concerned with how many times a certain word was being used in the languages and wanted to rank these words. What he noticed was a power law relation between the frequency of usage of the word and its ranking as $y \sim r^b$ where y stands for the frequency, r for ranking of the word and b is the exponent close to but usually slightly larger than 1 in this particular case [5].

The power law distribution of various variables is abundant in nature. To note some of them [6], the distribution of city populations, moon craters, size distributions of earthquakes, the size distribution of moon craters and solar flares, computer files, wars, the distribution of number of papers scientists publish per capita, the number of citations received by papers, the number of hits on web pages, the number of species in biological taxa, distribution of peoples annual incomes, the size distribution of frequency changes of the neutron star pulses which are attributable to the quakes at neutron stars (which are also referred to as star-quakes) [7], all show power law distributions.. As will be discussed on the part concerning the renewal processes, what is expected is if there is no organization between the constituents of a physical system, and that the rate of the stochastic process is a constant and hence anytime is as good as any other time for an event to occur, such systems result in an exponential probability distribution. So the mere fact that we have power laws for the probability distribution functions instead of exponentials makes us alert about the fact that we are faced with a system in which the

interactions and cooperations between the constituents of a system play a crucial role, and/or the system is in a phase transition state being far from the conditions of statistical equilibrium. One such system is that of turbulence, in which a large number of molecules cooperate in such a way as to form curls and then turbulence where as there seems to be no such reason for the individual molecules making up the system to collaborate. And there is also the fact that, the time distribution of intermittent behavior in a fluid flow also possesses power law distributed behavior, which has no correlations in time in and amongst themselves whatsoever, and therefore seems to reveal renewal properties.

It appears that the number copies of books sold over a few decades in the U.S. also displays a power law distribution [6],[8]. The cumulative distribution of the number of calls arriving at each phone number in the U.S. displays a power law distribution [6],[9] as well. Note that this is not the number of calls arriving at the central, since for reasons explained in the part concerning the Poisson renewal Processes, the waiting time distribution between successive calls arriving at the central displays an exponential distribution, because each and every subscriber does not interact with another and the call may come at any time, if we ignore the obvious time dependencies like day and night etc. The power law distribution is also the case for the number of e-mails received and sent by individuals [6],[10]. In social life, apparently power laws find their place easily, as it goes, the number of actors that has links to k others decay following a power law, if we consider the link as between the actors acting in the same movie, just like the number of connections of an airport to other airports, the histogram will display a power law.

There is yet another case where we define the Erdos number based on the links to reach the papers published by the famous mathematician Paul Erdos in the Mathematicians community, a common publication with him referring to an Erdos number of 1, a publication with someone who has co-authored with Erdos having and Erdos number of 2 etc. If we plot the histogram for the number of mathematicians versus their Erdos number it calls for a power law as well.

Power laws, just like scaling relationships are scale invariant,they display invariance under scale change. In a relationship of the form $f(x) = \beta x^{\alpha}$, if we set, $x'^{\alpha} \rightarrow \lambda^{\alpha} x^{\alpha}$ and

$f(x') \to \lambda^{\alpha} f(x)$, the functional relationship is preserved as $f(x') = \beta(x')^{\alpha}$. A change in the scale of the independent variable preserves the functional form of the original equation. This implies that such relationships are not associated with a particular scale, so they are scale free and true on all scales, possess the same statistical properties on any scale. Near phase transition systems, or the onset of magnetization when temperature is changed or the transition between dynamical regimes via bifurcations in deterministic systems that are essentially deterministic, become critical and adequate quantities to describe their dynamics such as the magnitude of fluctuations of the correlation lengths become power laws. A system can reach this critical condition via changes of an external parameter such as temperature, or that it may reach this state through a change in the internal dynamics of the system, where we name the state of the system as self organized criticality. Theoretical and empirical investigations suggest that biological and ecological systems seem to operate near a critical state, which results in the abundance of power laws in their dynamics [11].

One should keep in mind that criticality is not necessarily the only means of generating power laws in systems. There are well established theories of Renewal, Modulation and Superstatistics that lead to power laws[12]. And also Tsallis statistics, which is a recipe for rearranging and modifying normal statistical mechanics by means of a parameter q so that it produces power law distributions [13]. In our work we investigate renewal (or in other cases modulation) systems as generating power law distributions of the kind

$$(2.1) \qquad \psi(\tau) = (\mu_0 - 1) \frac{T_0^{\mu_0 - 1}}{(\tau + T_0)^{\mu_0}}$$

which is observed many times in nature in the sojourn times for the occurrence of intermittent eddies in fluid flow and fluorescence intermittency in blinking quantum dots and single molecule spectroscopy.

2.3. Scaling Concepts in Physics

There are very well established Scaling or in other words Power Law relations in Physics, a few examples are as follows [14]

7

- The scaling law for the breathing rate ϱ of the animals $\varrho(M) = AM^n$. where M is the body mass of the animal and A and n are constants.
- The scaling law for the velocity distribution $v(d)$ near a wall in a turbulent shear flow. $v(d) = Ad^n$, where again A and n are constants.
- The scaling law for the radius of the shock wave after a nuclear explosion $\mathcal{R}_f(t) = (\frac{Et}{\rho_a})^{\frac{1}{5}}$, where $\mathcal{R}_f$ denotes the radius of the wavefront, E for energy, t for the time after the explosion and ρ_a is the density of the air.

Scaling laws reproduce themselves in all scales as a consequence of their built in self-similarity, in a sense they reproduce themselves in space and in time. One of the first scaling laws ever to enter into the discussion of mathematical physics was that derived by J.B.J. Fourier in 1822, for the phenomenon of heat conduction. Solving the partial differential equation for heat conduction [18]

$$(2.2) \qquad\qquad \partial_t \Theta = \partial_{xx}^2 \Theta$$

Fourier arrived at the equation

$$(2.3) \qquad\qquad \Theta(x, t) = \frac{\mathcal{A}}{\sqrt{t}} e^{-\frac{x^2}{4t}} = \frac{\mathcal{A}}{\sqrt{t}} f(\frac{x}{\sqrt{t}})$$

where $\mathcal{A}$ is a constant, Θ is time and space dependent variable temperature, x and t denote the variables for space and time respectively. The function f here could have assumed other forms, yet the important thing is that the solution to the partial differential equation can be written in terms of a variable which could be re-scaled, namely $f(x, t) = f(\frac{x}{\sqrt{t}})$. In self-similar coordinates, $(\Theta\sqrt{t}, \frac{x}{\sqrt{t}})$, once the dependence of the variable Θ is solved for a particular time t, it could simply be inferred from the self similar form of the solution for a later, or an earlier t'. So obtaining self-similar solutions in the form of the above scaling form is very important for it comes up with a lot of practical advantages in science. In general we will refer to solutions of the form

$$(2.4) \qquad\qquad T(x, t) = \frac{\mathcal{A}}{t^\delta} f(\frac{x}{t^\delta})$$

8

as satisfying scaling relations, where the values for $\delta \neq 0.5$ will be referred to as satisfying anomalous scaling conditions. Such scaling relations with anomalous scaling coefficients have been derived as early as 1942 by Guderley [15][14] where he studied a very intense implosion wavefront being in the form of a converging spherical or cylindrical shock wave, and also by Weizsacker (1954) [14][16] and Zeldovich (1956) in the problem of an *impulsive loading*, the plane analogue of the implosion wavefront problem. In these problems the self similar solution came in the form of a scaling relation with some certain values of the scaling coefficient δ not only different from 0.5 but also in the form of some transcendental numbers.

In a different sense one also notices that diffusion processes also satisfy a self similar solution but sometimes with an anomalous scaling as well, in which case if $\delta < 0.5$ we will refer to the anomalous diffusion process as sub-diffusion, and for $\delta > 0.5$ as super-diffusion.

2.4. Fractals and Self-Similarity in Nature

In colloquial usage, a *fractal* is "a rough or fragmented geometric shape which can be subdivided into smaller parts where each of these smaller parts is at least approximately a reduced size or copy of the whole". Mathematically a *fractal* is a set of points whose fractal dimension (the meaning of which is to be discussed below), exceeds its topological dimension [19].The term is defined by Benoit Mandelbrot in 1975 and was derived from the Latin word *fractus* meaning broken or fractured [20] . This root in Latin is a fecund one in physics cause the term refraction of the refraction index also comes from a similar word in Latin, *frangare* which means to break [21]. Where a function "breaks," it is not differentiable, and first ever fractal was discovered on this key issue by Karl Weierstrass investigating the everywhere continuous but nowhere differentiable function in the year 1861. [22].

Benoit Mandelbrot realized that in nature the ideal shapes like perfect spheres, infinite lines and circles are rare, what is more common however, is the shapes like that of trees, coasts mountains, often irregular looking and certainly very difficult to express in terms

of Euclidean geometry. If you look closer to a circle it looks like a line and if you look closer to a line it appears straight as a line again. Likewise, if you look closer with a birdseye view to a coast, it looks crinkly and if you look closer again it looks similar, as you come closer you will see similar structures with identical degree of crinkliness. Fractals are those shapes that have such structures, that have essentially similar features at smaller scales with identical (self-similar) or similar (self-affine) degrees of crinkliness.

In fact nature hardly resembles Plato's world of ideal shapes. He was Mandelbrot to first make this concept popular in science. Mandelbrot was born to a Lithuanian-Jewish family in Poland in 1924. When he was 12 his family had to leave Poland for Paris because of the rise of Nazism in Germany. His family was smart to foresee the possible consequences of a Nazi invasion in Warshaw, which by then had a Jewish population of about half a million. He had to leave Paris during the war for Tulle, and when the war was over he started at Ecole Polytechnique, where he was working as a student of Paul Levy and Gaston Julia. It turned out that having had to migrate to France and then to U.S. for Mandelbrot has been very fruitful for the advancement of science of fractals after all, since he learnt about the mathematical background in France From Levy and Julia, and had a chance to use the IBM computers for the experimental investigation in the U.S.

2.5. Generic examples of self similarity

2.6. Sierpinski Gasket

Nature presents us with some structures which possess self similar structures. This is so even when the way to construct the structures appears arbitrary, somewhat chaotic so to speak. Let us play "the chaos game" [23] [24] [25] proposed by Dr. Michael F. Barnsley at this point. Here are the rules for any triangle chosen as the playground:

- Step 1. Take a starting point anywhere on the triangle, randomly
- Step 2. Randomly choose a number from 1,2 and 3 where each point of the triangle is denoted with one of these numbers.

- Step 3. Move halfway from the starting point towards the corner denoted by the number in Rule 2. This new point will act as the new starting point for the next step.

- Step 4. Go to Step 2 and repeat the iteration.

As this procedure involves randomness at the beginning, choosing an arbitrary point on the triangle, and randomness at each iteration, choosing the corner to approach randomly, one might be compelled to think that the resulting pattern formed by the set of points emerging from the iteration will smear inside the triangle arbitrarily. On the contrary, Barnsley points out to the fact that, even if the iterations contain a good degree of randomness the resulting system forms an Affine transformation which even when we start with arbitrary initial conditions will lead us to some sort of a Strange Attractor for these rules, which , is shown in the figure for an isosceles triangle, and is named A Sierpinski Gasket, denoted usually by S. Sierpinski gasket has interesting properties, like if you take a smaller triangle inside the main triangle and magnify it you will see exactly the same picture, henceforth the structure is a self-similar one.

(a)   (b)
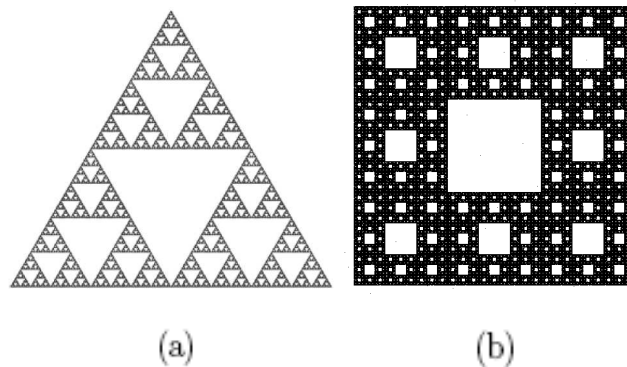
Figure 2.1.   Sierpinski gasket (a) and Sierpinski carpet (b).

Figures possessing fractal properties are centuries old. In 1525, the German artist Albrecht Duerer published *The Painters Manual* containing a section named "tile patterns formed by pentagons" [22]. Dueres pentagons largely resembles the Sierpinski carpet Figure.(2.1.b) formed with squares, replacing squares with pentagons. The first mathematical fractal was discovered in 1861 by Karl Weierstrass. He was obsessed with rigor,

and his quest led to the nowhere differentiable continuous function, a curve consisting of corners and corners only. Its rate of change at any particular point was impossible to define, and there was no smoothness anywhere. At the time, scientists were inclined to think that Weierstarss function was an aberration of the mind and nothing more than a pathology and it is not to be found in nature. But they could not have been more far from reality.

One can talk about a typical size of an object like a pen. However, it is not always possible to talk about a typical cloud, since it consists of parts similar to itself in a broad scale. Is there really a typical dimension for clouds? Is a lump here have dimensions of 30m, or could it be 300m or may be it is 3km or why not 30km? Since a part of a cloud is still a cloud, and they look quite similar on a very large range of scales, it does not really make sense to speak about typical dimensions of a cloud. For that matter clouds will form a good example of self similarity in nature. Any object we put in between two parallel mirrors will form self similar patters, smaller and smaller reflections,which goes *ad infinitum*. When we use the concept in the context of fractals, self similarity means that " a part of the whole looks like the whole itself," and this concept is ubiquitous in nature too. A part of a cloud often has very similar features as the whole. Apart of a border looks like its smaller parts. And a terrain forms similar features as the mountains.

An arc of a circle itself is not a circle. If we take a side of a triangle it is not triangular. Yet in nature self similarity is abundant. Trees, clouds and mountains all resemble smaller parts of themselves. Most Euclidian shapes do not have this property of self similarity. But then again, in nature what we see is often not Euclidian shapes, perfect lines or circles. What we see instead are self similar structures like the coast patterns on an extended range. If we take a look at smaller pieces of borders or coast lines, which are not perfect lines themselves, we see that at a smaller scale the structure looks similar. Those shapes are incredibly complicated if we try to describe them with Euclidian terms. Still they share an affinity with the so-called pathological shapes of modern mathematics, displaying an infinite series of motifs repeating itself on finer and finer scales.

2.6.1. *Koch Island*

One such example is a construct initially used to model a snowflake by Helge von Koch (1870-1924) in 1904 [26]. The shape utilized has an infinite length but being contained in a finite area. It has no tangent or smoothness anywhere. Taking a snapshot of smaller and smaller areas of the Koch curve, one will notice that a structure repeats itself so we may call it a self similar structure. The so called Koch curve or Koch snowflake has infinite circumference but a finite area, for this reason some curves having similar properties are referred to as "monster curves."

The generation of Koch curve is illustrated in Figure.(2.6.1) as follows. Let's commence with a line segment of length 1 shown in Figure.(2.6.1) by $n = 0$. The next step will be taking of the middle one third of the line segment out and replace it with two other parts each one of the same length instead, each in a position to form the sides of an isosceles triangle as shown in Figure.(2.6.1) by $n = 1$. So at this point it has a total length of $\frac{4}{3}$. The same procedure can be applied again to each one of the pieces and then the total length length will still be increased by a factor of $\frac{4}{3}$ yet again, which is illustrated in Figure.(2.6.1) by $n = 2$. In each and every iteration the total length will be multiplied by the same factor of $\frac{4}{3}$, *ad infinitum*, and in the limit as $n \to \infty$ the Koch curve emerges. The circumference of the Koch island is thus

$$(2.5) \qquad \lim_{n \to \infty} L = 3(\frac{4}{3})^n \to \infty$$

So, measuring the Koch curve in terms of length is not quite possible. So let us consider Koch curve from a point of view of its space filling properties. This kind of reasoning is developed by Felix Hausdorff (1869-1942). In this regard, let's take a look at Figure.(2.6.1) which I drew using Micrographix Designer 4.1 program, and consider the area covered by the boundary. Let us start by covering the perimeter with $N_0 = 3$ circles of radii $r_0 = \frac{1}{2}$ as shown in Figure.(2.6.1). There are $N_1 = 12$ circles of radii $r_1 = \frac{1}{6}$ for the second approximation. For the third approximation the number of circles

13

is $N_3 = 48$ while the radii of the circles is $r_2 = \frac{1}{18}$. It is evident that if one proceeds with the same method always using circles of smaller radii which follows

$$(2.6) \qquad r_n = \frac{1}{2 * (3^n)}$$

and increasing in number as

$$(2.7) \qquad N_n = 3 * (4^n)$$

the area covered by the circles at the nth iteration as n tends to infinity reads

$$(2.8) \qquad \lim_{n \to \infty} A_n = \lim_{n \to \infty} \frac{3}{4}\pi(\frac{4}{9})^n \to 0$$

So considered in terms of area, the boundary has zero area, but when considered in terms of its length the circumference of the Koch island, namely the length of the boundary is infinite! It simply means that the size of the boundary can neither be measured in terms of length nor in terms of area. Hence this might imply that the perimeter of the Koch island, has a dimension somewhere in between one and two dimensional objects.

So let's evaluate the number of circles necessary to fill the area on the circumference N_n in terms of the radius r_n using Eq.(2.6) and Eq.(2.7)

$$(2.9) \qquad N(r_n) = 3 * (4^n) = 3 * (4^{-\frac{log(2r_n)}{log(3)}}) = 3(2r_n^{-\frac{log(4)}{log(3)}}) \sim r_n^{-D}$$

where $D = \frac{log(4)}{log(3)} \sim 1.26$. Now let's notice that for a line $N(r_n) \sim \frac{1}{r_n}$ and for an area $N(r_n) \sim \frac{1}{r_n^2}$. Suppose $N(r_n)$ is the minimum number of balls of radius r_n required for covering a set, and $N(r_n) \sim r_n^{-D}$ where D is not an integer. In this case we call the set a *fractal* with a *fractal dimension* of D. Now we can come back to the definition of what a fractal is and we can quote Sornette at this point to illuminate a little bit more the definition, "The definition based solely on dimension is too narrow, and it is better to view a fractal set as possessing a fine structure, too much irregularity to be discussed in traditional geometric language, both locally and globally, some form of self similarity, a

fractal dimension somehow defined, which is greater than its topological dimension, and a simple usually recursive definition" [19]
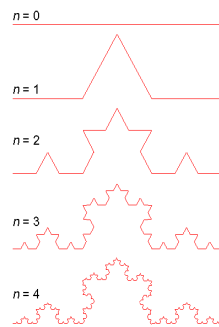
Figure 2.2.   Generation of the Koch curve starting from a line segment of length l.
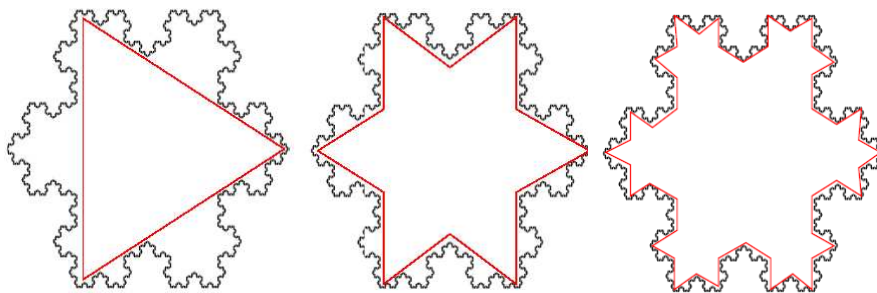
Figure 2.3.   Circumference of the Koch island in the first, second and third approximations.
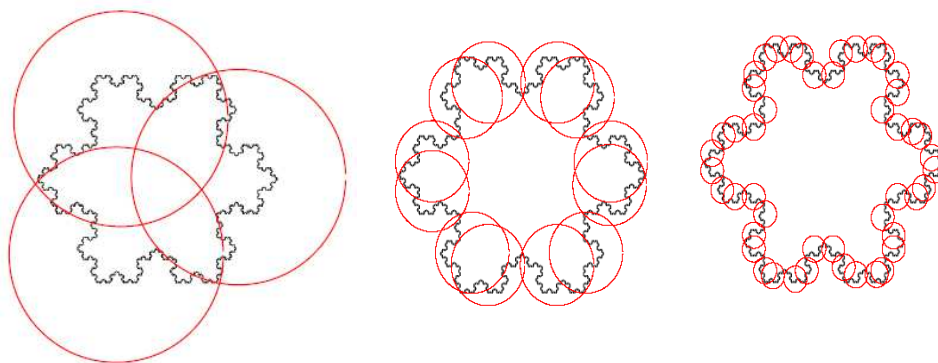
Figure 2.4.   Area of the Koch island in the first second and third approximations.

2.7. Coasts and Borders as Self-Similar Structures

The statistics of war has been studied by L.F. Richardson [27] and in it has been detected that the number of wars initiated globally in any given interval of time follows

a Poisson distribution [28]. It has also been realized that the number of wars waged in a certain period when plotted in chronological order is akin to a rate modulated Poisson process [29]. This suggests that the onset of war is essentially a random process [30]. Richardson's data, when analyzed based on two warring countries, of 94 wars between 2 countries only 12 were not neighboring countries, suggesting that sharing a common border is one of the main reasons to go to war, implying that war is basically a neighbor affair [30].

But the question how one determines the border between two countries is a basic question to ask [28]. Yet, if one has ever been to the Aegean coast, it is almost inevitable to ask the question, "How long this entire coast should be?" because the coast is one of the most crinkly coasts of all in the entire world. It is interesting to note that the same kind of question is also asked by Penck in 1894. He noticed that the scale of measurement affects the result of the total measurement, in other words, the length of the coastlines or the length of borders between countries depends on the length of the yardstick one uses [28].

L.F.Richardson also pointed out that reported borderlines by the neighboring countries are different, like Spanish-Portuguese border was reported to be 987 km by the Spanish and 1214km by the Portuguese. He reported that the differences might be due to the length of the measurement stick length used. Paul Addison [31] gives a prescription for the relationship between the length of a coastline or borderline and the measurement scale as follows.

- set the yardstick length to λ
- Plot the total length L in a $\log(L)$ versus $\log(\lambda)$ graph, where $L = N\lambda$, N is the coast length in units of λ.
- The resulting graph displays a $\log(L) = H * log(\lambda)$ form.

Such plots are called Richardson plots. If in Richardson plot, for a certain range of λ one can define a slope H_1 on the plot, and another slope H_2 for another range of λ, we refer to such structures as multi-fractals since different fractal structures are intertwined

16

in the overall structure. Of course the slope H will be a tool to define for us the fractal dimension, much like the Koch island structure defines for us a certain fractal dimension. For all that matters, fractals will obey power law forms, or put in a more neat way, fractals are one of the structures that obey power law relations. Not all power law relations imply a fractal structure the way we define it here, however, all fractals will obey some kind of power law with regard to its dimension and measurement scale. [29].

CHAPTER 3

RENEWAL THEORY, POISSON AND NON-POISSON RENEWAL PROCESSES

3.1. Introduction

In this chapter I give a very brief account of what the concept of probability as it applies for a physicist from the point of view of computer experiments is. I make a short review of the renewal theory and renewal Poisson processes, then starting with the basic idea of a binomial process I make a connection with a diffusion model based on asymmetric walk, and then establish the connection between Binomial processes and Poisson processes. I then discuss the results of ordinary statistical mechanics that collision time distribution in a gas is of the exponential form. Finally I discuss renewal processes where the distribution function of the collision times prove to be a power law function instead of an exponential form. This model is used in the perturbation of renewal processes models in this thesis as explained in the forthcoming chapters which is the basic core subject of this dissertation.

3.2. Concept of Probability from an Experimental Framework

History of probability concepts dates back to ancient times. Indeed, archeologists found Dice made of particular hoof bones of the sheep called *astragolai* dating back to 6 millenia ago to the Neolithic period, as old as the first farming societies [32]. The Etruscan played with twelve faced dice 3 millenia ago. It is also well known that Roman Emperor Augustus who made many reforms in his reign used to play dice very often, as well as one of his successors, Emperor Claudius. In fact Claudius was so consumed with the game that he even wrote a book about it.

Roman goddess Fortuna was one of the most popular among the Romans and people built temples in her name, who was no one other than the Greek goddess Tyche, the goddess of chance. Although the concept of uncertainty has been appealing for the

18

people of all civilizations, it was not until Galileo Galilei, Blaise Pascal, Pierre de Fermat, and Abraham de Moivre, the mathematics of probability had started to develop.

Concept of probability is our attempt to ascertain the rules of uncertain situations. It is a measure of the likelihood of an event. The case of uncertainty where we know that we have to think in terms of probabilities may arise from the lacking knowledge on the system under consideration, or it might as well be an intrinsic built in probability that arises as the result of a measurement process as in the case of Quantum Mechanics. Regardless of the source of the uncertainty, the legitimate way to define the probabilities for a given situation is through observation. From the point of view of an observer, probability is nothing more than the frequency of occurrence of events in the very long time limit which emerges as this time of observation tends to infinity. This aspect defines its empirical side from the perspective of our experiments.

On the other hand, some of the properties of probabilities can be defined *a priori*, without regard to a certain experiment using the set theory. One of these laws is *the law of unions*, where we want to define the probability of occurrence of one of the two events A and B. If the probabilities of event A and B are P_A and P_B, respectively, the probability $P(A \cup B)$ of either event A or B takes place is denoted as

(3.1)
$$P(A \cup B) = P(A) + P(B) - P(A \cap B)$$

that is the sum of the probabilities of both events minus the probability that both events occur.

It also is obvious if we draw a dice and the result is 6, the next may or may not be 6, so the process is memoryless. If we take two dice and draw and get 6 from one of them, it does not effect the result of the other one, it could as well be 6 or not, what the first one reveals does not affect the second one at all, so we name such events with independent probabilities. For the occurrence of independent events the joint probability calculation is easy, it is simply a multiplication of the two probabilities. For dependent events however, the joint probability of the two events is given as the multiplication of

the probability of the first event and the conditional probability that the second event occurs provided the first one has occurred .

In this context we will discuss Bayes' theorem which is also known as Bayes' rule or Bayes' law. Bayes' Theorem connects conditional and marginal probability distributions of random variables. The probability of an event E occurring conditional to an event H is usually different from the probability that the event H occurring conditional to the event E occurring, but one can establish a connection. Bayes' theorem is the statement of these conditional probabilities.

Bayes' theorem expresses the connection between the conditional and marginal probabilities of stochastic events E and H as follows

$$(3.2) \qquad prob(E|H) = \frac{prob(H|E)prob(E)}{prob(H)}$$

where $prob(E|H)$ denotes the conditional probability that event E occurs on the condition that event H occurs, and sometimes referred to as *posterior probability*. The expressions $prob(E)$ and $prob(H)$ are sometimes referred to as *prior probabilities* or marginal probabilities of events E and H respectively implying that the probability does not take into account any information of the other.

By definition of the conditional probability that event E given event H is

$$(3.3) \qquad prob(E|H) = \frac{prob(E \cap H)}{prob(H)}$$

where $prob(H) \neq 0$ and similarly, the conditional probability of event H given event E is

$$(3.4) \qquad prob(H|E) = \frac{prob(E \cap H)}{prob(E)}$$

where $prob(E) \neq 0$, which then implies the following lemma sometimes called the product rule for probabilities

(3.5) $$prob(E|H)prob(H) = prob(E \cap H) = prob(H|E)prob(E)$$

which when divided by $prob(B)$ implies the Bayessian theorem that states

(3.6) $$prob(E|H) = \frac{prob(H|E)prob(E)}{prob(H)}$$

In a sense by its very definition, conditional probability concept implies the Bayessian theorem, and the definition of conditional probabilities and Bayessian theorem are the same thing.

In what follows we will make use of these very basic probability rules.

3.3. Renewal Theory

Development of Renewal Theory started as the need for it in Industrial Engineering sub-discipline Operations Research rose. Its basic tenet was related to probability problems connected to the failure and replacement of components, such as electric light bulbs although it could have been valves or any other standard component. The variable of interest will be the life time of the component which we will sometimes refer to as *the waiting time* or *the sojourn time*, and *the failure* of the component stands for the event that we are concerned with. The generalized form of renewal theory uses the same terms yet it might be related to some other physical system and/or event, what is important in this picture is that in a time line there are events stemming from point processes, and the time it takes between consecutive events will comprise the waiting times. If one makes a histogram of the waiting times, in a system with non-changing physical rules one could expect a well defined probability distribution function (p.d.f.) for the sequence of waiting times, independent of time interval we are concerned with, if the statistical system is assumed stationary. Since time can not be negative, the variable of interest τ will always be positive and the probability associated for it at any particular time will be positive definite. The waiting time distribution under these conditions is defined as [33]

21

$$(3.7) \qquad \psi(\tau) = \lim_{\Delta\tau \to 0} \frac{prob(\tau < t < \tau + \Delta t)}{\Delta t}$$

and that it has to be normalized as

$$(3.8) \qquad \int_0^\infty \psi(\tau)d\tau = 1$$

in a more general sense one could define the moments of the waiting time distribution as follows

$$(3.9) \qquad <\tau^n> = \int_0^\infty \psi(\tau)\tau^n d\tau$$

where the zeroth moment ($n = 0$) being equal to 1 is imposed by the normalization condition of probability, and the first moment (or the average, with $n = 1$) and higher order moments, like $n = 2$ being the variance etc. can take on any value depending on the details of the distribution, or the physical system generating this kind of statistics. We can also define a *cumulative function F* as

$$(3.10) \qquad F(t') = prob(\tau < t') = \int_0^{t'} \psi(\tau)d\tau$$

Which is basically the probability that the component has failed by the particular time t'. Based on this premise, one could as well define *the survival probability function,* $\Psi(t')$ which points to the probability that the component will *not* fail by the particular time t' as

$$(3.11) \qquad \Psi(t') = prob(\tau > t\prime) = 1 - F(t') = \int_{t'}^\infty \psi(\tau)d\tau$$

Note here at this point that $\Psi(0) = 1$ and $\Psi(\infty) = 0$. Also, from the above definition it should be obvious that

22

$$(3.12) \qquad \psi(\tau) = -\frac{d\Psi(\tau)}{dt} = -\dot{\Psi}(\tau)$$

One must also define the failure rate, which from now on we will simply refer to as the rate, of events, which could as well be time dependent, which then we choose to denote as $r(\tau)$, and define within an interval Δt, where in the limit this time interval tends to zero. Let us define it as the conditional probability that up to time τ, having satisfied the condition that the probability for the component does not fail is realized, i.e. the component has survived till time τ, upon which, it fails in a time interval between $[\tau, \tau + \Delta t]$. Using the notation of conditional probability this is written as

$$(3.13) \qquad r(\tau) = \lim_{\Delta t \to 0} \frac{prob(\tau < t \le \tau + \Delta t | t < \tau)}{\Delta t}$$

Explicitly said, the conditional probability of immediate failure after time $t = \tau$ within an incremental time interval of Δt, the event we denote by E, under the condition that the system survived till to the time $t = \tau$ with no collision, the event which we denote by H.Based on the Bayesian theorem, the expression for the conditional probability $prob(E|H)$, that event E occurs proviso the Hypothesis H occurs is given as [19]

$$(3.14) \qquad prob(E|H) = \frac{prob(E \cap H)}{prob(H)}$$

where $prob(H) \ne 0$. Remember that the event E occurs with a probability of $\psi(\tau)\Delta t$ which is also the intersection of the two events E and H, where event H is denoted by the probability $\Psi(\tau)$. This implies

$$(3.15) \qquad r(\tau) = \lim_{\Delta t \to 0+} \frac{prob(\tau < t \le \tau + \Delta t)}{\Delta t} \frac{1}{prob(t < \tau)} = \frac{\psi(\tau)}{\Psi(\tau)}$$

Basically the rate of the process at time τ is simply the fraction of the probability distribution function ψ (a probability density function) to the survival probability Ψ evaluated at the particular time τ. Of course we may take into account that this fraction

might as well be independent of particular time value τ, i.e., might have a constant value, as it is in the Poisson processes. Using Eq.(3.12)this means that the rate can be written in terms of survival probability and its derivative

$$(3.16) \qquad r(\tau) = \frac{\psi(\tau)}{\Psi(\tau)} = -\frac{\dot{\Psi}(\tau)}{\Psi(\tau)} = -\frac{d}{d\tau} \ln \Psi(\tau)$$

$$(3.17) \qquad \int_0^\tau r(t')dt' = -\ln \frac{\Psi(\tau)}{\Psi(0)}$$

remembering that at time $t = 0$ the survival probability is zero, we can write the survival probability in terms of the rate of failures as

$$(3.18) \qquad \Psi(\tau) = e^{-\int_0^\tau r(t')dt'}$$

and Eq.(3.12) implies

$$(3.19) \qquad \psi(\tau) = r(\tau)e^{-\int_0^\tau r(t')dt'}$$

in which sense we can see that the failure rate $r(t)$ is the only variable that determines the survival probability function $\Psi(\tau)$ and hence the sojourn time distribution, or (p.d.f.) the probability distribution function, $\psi(\tau)$. Let us note here that if the failure rate is a constant, $r(t) = r_0$, then the survival probability function of Eq.(3.18) reads

$$(3.20) \qquad \Psi(\tau) = e^{-r_0\tau}$$

and Eq.(3.19) implies

$$(3.21) \qquad \psi(\tau) = r_0 e^{-r_0\tau}$$

24

Let us note at this point that this requirement is a two way street, namely that, if we assume a waiting time distribution of the form of Eq.(3.21), using the definition on survival probability at Eq.(3.11) and Eq.(3.16) that if we assume a waiting time distribution of the form given by Eq.(3.21) we have to end up with a constant rate of $r(t) = r_0$. We can state this important fact simply that an exponential waiting time distribution $\psi(\tau)$ implies that the immediate failure rate of the component does not depend on the particular time we are concerned with, the rate $r(t) = r_0$ of failure is always constant regardless of the specific age of the system.

3.4. Poisson Processes and Poisson Distributions

Let us consider a point process where the arrivals in time of the particles which we might as well call the events have the following enlisted parameters:[38]

(i) *The condition of linearity.* The probability p_f that an event occurs in a time interval is proportional to the time interval itself, $p_f = \lambda \Delta t$.

(ii) *The condition of no memory.* The existence of an event, or of the lack of it for that matter, has no influence whatsoever on the arrival of the next event , or non arrival of it. Namely the rate of the process λ is constant.

(iii) *The instantaneous event condition.* Two distinct events can not occur at the same time. The occurrence of a single event happens at a single point in time, hence the name Point Process. The event is assumed to happen instantly in a flash of time.

The number of expected counts in a time t is simply $n_f = \lambda t$, implying that the average time $< \tau >$, between two successive events is $< \tau >= \frac{t}{n_f} = \frac{1}{\lambda}$. In a time interval of Δt, the probability of an event, a jump forward, or a count if you like is $p_f = \lambda \Delta t$, so the probability of staying in the same position, failure or no count in the same time interval is $1 - \lambda \Delta t$. If we consider a certain time t, divided by n as time time interval $\Delta t = \frac{t}{n}$, since we also have the condition of no memory the probability of no event in time t is the multiplication of those in successive incremental time intervals which leads us to the survival probability till time t

$$(3.22) \qquad\qquad \Psi(t) = \left(1 - \frac{\lambda t}{n}\right)^n = e^{-\lambda t}$$

Let us now consider the case where the system "survived" with no event for a time τ and then in the next time interval of $d\tau$, the probability of an event $p_f = \lambda d\tau$ is realized. Again using no memory condition this spells nothing but the probability that the waiting time will lie between $[\tau, \tau + d\tau]$

$$(3.23) \qquad\qquad p_s(\tau) = \psi(\tau) d\tau = \lambda e^{-\lambda \tau} d\tau$$

where $\psi(\tau)$ is the probability distribution function of the waiting times. But what one usually observes and measures is not always the waiting time distribution in laboratory conditions. In the laboratory, people usually count the number of particles detected within a prescribed time interval, which is not necessarily coincident with the natural time step Δt of the process. Since the time interval between the arrival of the particles might be very small, may be beyond the time resolution limit of the experimental apparatus, it would be more appropriate to measure the cumulative effects of the detected particles within a macroscopic time interval chosen as the bin size for time, rather than the exact times when they arrive. Then one may obtain the histogram of different number of occurrences per this time interval chosen and obtain a distribution of the number of arrivals. This is exactly what the experimental physics pioneers Rutherford Geiger and Bateman did in 1910 [37] [38]. when they observed the number of alpha particle emissions from a radioactive source. They have counted and recorded the number of alpha particles counted within every successive 7.5 seconds and plotted the histogram of the number of arrivals versus the number of particles within 7.5 seconds intervals,where the data they acquired displays results very close to a Poisson distribution [37],[38].

I will investigate the connection of this data which yields a Poisson distribution, to Poisson sequences in the section 3.8 and section 3.7.

3.5. Timid Walker : Asymmetric Random Walk

I include here a heuristic model to study the random emissions of particles from radioactive nuclei [36]. For this first I start with a model of a timid walker, who at each successive time interval takes a step forward with a unit length with a probability p_f, or stays at the current position of his with a probability $p_s = 1 - p_f$. After n trials, the average distance from the initial position would be $<x> = np_f$. The expected square of the path length reads

$$(3.24) \qquad <x^2> = \sum_{i=1}^{n} x_i^2 + \sum_{i \neq j} x_i x_j$$

The first sum reads np_f since the jump is of unit length. The second sum reads $n(n-1)p_f^2$ since both different jumps of index i and j must be forward with independent probabilities. The variance reads

$$(3.25) \qquad \sigma^2 = <x^2> - <x>^2 = np_f(1 - p_f)$$

So for the Binomial case of an Asymmetric timid walker, the average distance traveled after n trials (time intervals) is $<x> = np_f$ and the standard deviation about this expected value of the distance is $\sigma = \sqrt{np_f(1 - p_f)}$. Let us picture this as n events taking place in time steps of Δt, yielding a total time of $t = n\Delta t$. Let us make the connection with radioactive decay and say that the emitting of a radioactive particle or else it's arrival at the detector as the event where the timid walker takes a step forward. The time in this case is continuous, the probability of success increases as the time interval chosen as $p_f = \lambda \Delta t$ as time interval Δt goes to zero the probability p_f also tends to zero. And the probability of the random walker staying at its current position p_s tends to 1. In this case the standard deviation of the arrival of particles will be, $\sigma = \sqrt{np_f}$. Since $np_f = \lambda n \Delta t = \lambda t$, this implies that the standard deviation of the number of detected particles scales as $\sigma = \sqrt{\lambda t}$, which is nothing but the square root of the number of expected number of particles. Hence the fluctuations scales as the square root of the expected number of particles to be detected.

3.6. Fair Binomial Coin leading to a Gaussian distribution

Let us consider a process where there are two probabilities for each draw, we may name the events success and failure, or else collision and miss for the sake of clarity. Or to be even more specific, let us say this is a coin tossing process and the outcome may be heads or tails, and let us suppose that the coin is a fair coin and hence the probability of heads and tails is the same: 50%. Here we denote head as success and let us say it is denoted by the probability p_h, and tails as failure and let us denote it by p_t. We are interested in the probability that after n draws, we will have r heads. So we will have r events with probability p_h and also the remaining $n - r$ events have to come up with tails each of which will be realized with a probability p_t. If the events are independent and sequential we have to multiply the probabilities to obtain $p_h^r p_t^{n-r}$, but also take into account that out of n trials we may choose r successful draws in $C(n, r)$ ways, combinations of r of n. Hence the probability that we will have r successes among n events is

$$(3.26) \qquad p(n, r) = \frac{n!}{(n - r)!r!} p_h^r p_t^{n-r}$$

notice that this distribution takes into account that the coin may have been unfair in which case p_h and p_t would be different. Let us also note that the expected value of r, $< r >= np_r$, and also the standard deviation of r, $\sigma = \sqrt{np_r p_t}$ may be calculated from the Binomial distribution. Let us now consider a fair coin which is drawn 2m times, which we will let tend to infinity afterwards, and we are interested in the probability of the event that there will be $m + r$ successes, obviously here r is a measure of how diverted we are from the obvious most expected case where m events are expected to lead to heads and the remaining m events read tails. The Binomial distribution for this case where we are concerned with a fair coin implies

$$(3.27) \qquad p(2m, m + r) = \frac{(2m)!}{(m + r)!(m - r)!} \frac{1}{2^{2m}}$$

28

the use of Stirling's approximation $n! = \sqrt{2\pi}n^{n+\frac{1}{2}}e^{-n}$, where m is a very large number, where upon inserting the Stirling's approximated forms for all the factorials and considering that $m \ll r$ reads [34]

$$(3.28) \qquad p(2m, m+r) = \frac{1}{\sqrt{\pi m}} e^{-\frac{r^2}{m}}$$

this distribution is akin to the Gaussian distribution and for large means that the probability of finding cases away from the equality case decreases as the inverse exponential of the deviation r. Taking into account the standard deviation expression for the Binomial distribution above, for $2m$ draws we have, $\sigma = \sqrt{m/2}$ which then implies

$$(3.29) \qquad p(2m, m+r) = \frac{1}{\sqrt{2\pi\sigma^2}} e^{\frac{-r^2}{2\sigma^2}}$$

Which is nothing but the normal distribution. So, a Binomial approximation with a fair coin tends to the Gaussian distribution in the limit of infinitely many draws.

3.7. Unfair Binomial coin as a Poisson Process

It is merely logical to ask for the probability distribution of success, collision or heads if you like when the case under consideration is subject to the condition that the coin is extremely unfair. For the sake of simplicity, let us take this case as $p_h = \frac{\lambda}{n}$ as n tends to infinity, this probability becomes incremental if λ is a constant. We are looking for the probability distribution of the number of successes in n trials where the probability of success in each trial is λ/n.

$$(3.30) \qquad \lim_{n\to\infty} p(n, r) = \lim_{n\to\infty} C(n, r)p_h^r(1-p_h)^{n-r} = \lim_{n\to\infty} \frac{n!}{(n-r)!r!}(\frac{\lambda}{n})^r(1-\frac{\lambda}{n})^{n-r}$$

$$(3.31) \quad \lim_{n\to\infty} p(n, r) = (\frac{n}{n})(\frac{n-1}{n})(\frac{n-2}{n})\ldots(\frac{n-r+1}{n})(\frac{\lambda^r}{r!})(1-\frac{\lambda}{n})^n(1-\frac{\lambda}{n})^r = \frac{\lambda^r e^{-\lambda}}{r!}$$

Hence the probability distribution of r successes in a Binomial process where the probability of success for each trial tends to zero and the number of trials tends to infinity approaches the Poisson distribution in the limit. I will discuss the Poisson processes in

29

more detail in the next chapter because of two reasons, firstly it is observed in many occasions in Nature, and that the perturbation of the rate of Poisson processes forms the basis of part of the research results of this thesis.

3.8. Mean Collision Time in a gas as a Poisson Process

Let us discuss the concept of mean free time or the mean collision time in a gas of same molecules, cause we want to discuss the diffusion of particles in gases in a physical context. Let us suppose a molecule moving with velocity **v**. Let us assign a probability for this molecule to survive without collision till time t, and assign this probability of survival from collision as Ψ_s. The particle can not collide immediately at time $t = 0$ as the motion starts and must suffer a collision in very long time limit as $t \to \infty$, therefore we can immediately set the boundary conditions on this probability of survival from any collision as $\Psi_s(t = 0) = 1$ and $\Psi_s(t \to \infty) \to 0$. So now we know that it should not be a surprise if Ψ_s is a decreasing function of time. Let us also assign a probability of collision at time t in a time interval of $[t, t+dt]$, and denote it with $r\,dt$. This probability is proportional to the time interval dt we consider, and let us assume r to be constant, which is a reasonable assumption since any time could be taken as $t = 0$, the initial time, and there is no reason why we should think that any time is different than any other time, so some kind of uniformity assumed for the collision rate is a reasonable one.By this token, let us attempt at obtaining the form of the survival probability from collisions as a function of time. The survival probability form collisions at time $t + dt$ is nothing but the survival probability at time t and that a collision will not take place in the time interval $[t, t + dt]$.

(3.32)
$$\Psi_s(t + dt) = \Psi_s(t)\,(1 - r\,dt)$$

(3.33)
$$\frac{1}{\Psi_s(t)}\frac{d\Psi_s(t)}{dt} = -r$$

using the initial conditions

30

(3.34)
$$\Psi_s(t) = e^{-rt}$$

Now we can define the probability $\psi_c dt$ that after surviving for time t the particle makes a collision during the time $[t, t + dt]$.

(3.35)
$$\psi_c dt = \Psi_s(t) r dt = r e^{-rt} dt$$

the average time of collision τ_c would be

(3.36)
$$\tau_c = <t> = \int_0^\infty t \psi_c(t) dt = \frac{1}{r}$$

Then the time dependent probability of collision is [35]

(3.37)
$$\psi_c dt = \frac{e^{\frac{-t}{\tau_c}}}{\tau_c} dt$$

and the probability distribution function for the collision times will read

(3.38)
$$\psi_c = \frac{1}{\tau_c} e^{\frac{-t}{\tau_c}} = r_0 e^{-r_0 t}$$

where $r_0 = \frac{1}{\tau_c}$ is the rate of the stochastic collision events. Notice that this is an exponential distribution of the waiting times between collision events.

3.9. Numerical Brute Force Generation of Poisson Renewal Sequences of Events

Here we describe an algorithm we use to generate a renewal Poisson sequence. Running this algorithm is relatively slow in compared to a more enhanced version we will introduce later, but has the advantage of being valid for all amplitudes of a harmonic perturbation. So we may name it the brute force algorithm of Poisson event sequences.

Let us consider the interval $I = [0, 1]$. Let us imagine that at any time step, $i = 1, 2, ...$, we randomly draw a number of this interval with uniform probability. Let us

31

assume that at any time step the interval is divided into two intervals, $I_1^{(i)}$ and $I_2^{(i)}$. The interval $I_1^{(i)}$ ranges from 0 to $p_{(i)}$ and the interval $I_2^{(i)}$ from p_i to 1. Let us define

$$(3.39) \qquad\qquad\qquad\qquad q_i = 1 - p_i.$$

Let us assume that $q_i << 1$.

It is evident that p_i and q_i are the probabilities of drawing at time i a number in the interval $I_1^{(i)}$ and $I_2^{(i)}$, respectively. It is also evident that at any time i we will find with large probability a number of the interval $I_1^{(i)}$, as a consequence of the fact that $p_i >> q_i$. The probability of remaining in the interval $I_1^{(i)}$, up to n drawing is given by

$$(3.40) \qquad\qquad\qquad\qquad \Psi(n) = \prod_{i=1}^{n} p_i.$$

Using the properties of logarithm and the condition $q_i << 1$, we get

$$(3.41) \qquad\qquad\qquad\qquad ln\Psi(n) = -\sum_{i=1}^{n} q_i.$$

Let us explain now how to obtain the time series $\{\tau_i\}$. This time series is generated as follows. We make sure that $q_i << 1$. This condition implies that there is an extended persistence. It means that for a very large number of times we draw numbers from the interval I_1. Let us do the experiment, and let us call *collision* the drawing of a number from I_2. The time distance from a collision and the next is usually a very large integer time, denoted with the symbol τ_i, namely, τ_1 is the time duration prior to the the first collision, τ_2 is the time distance between the first collision and so on.

$$(3.42) \qquad\qquad\qquad \psi(n) = -\frac{d\Psi(n)}{dn} = \frac{d\,e^{nq_i}}{dn} = q_i e^{q_i n}$$

here n plays the role of discrete time and q_i apparently the role of rate of the Poisson process. Evidently the system is a renewal system with an exponential sojourn time distribution function. As one runs the system if the rate is dependent on the real time, this formula will tell us about how we can perturb the rate of Poisson process. However since this method is rather slow as much as it is simple, we have developed another

numerical method more complicated but much faster which will be explained in detail in the Appendix A to investigate the perturbation of Poisson renewal processes.

If the rate is being modulated real time, the projected values in discrete time can be plugged in this model. Basically what we are doing then is that for a sinusoidal perturbation of the rate, the time dependent rate can assume

$$(3.43) \qquad\qquad q(n) = q_0(1 + \epsilon \cos(\omega t))$$

The relevance of this form of a perturbation to a stochastic resonance model will be discussed in Chapter 6.

3.10. Neuron Firing as a Renewal Non-Poisson Process

In this section we will use a paradigmatic model of a stochastic process generating renewal non-Poisson distribution as discussed in [39]. We make the assumption that the archetypal neurons under consideration acts on events based on such a stochastic system, which, we will later prove that is consistent with already carried out experiments.

In this model, the neuron firing process is described by a sequence of times, at which neuron firings (or spikes) occur: $\{t_i\}$, $i = 0, 1, 2, \dots$. The time instant $t_0 = 0$ is the time of the first neuron firing occurrence. Denoting by $\tau_{i+1} = t_{i+1} - t_i$, $i = 0, 1, 2, \dots$, the inter-spike time distances, the neuron firing process is defined to be renewal if the times τ_i are mutually independent random variables [33]. With this assumption, the spikes generated by neuron firings are critical events whose occurrence is associated with a mechanism erasing memory of the past. A renewal process is uniquely defined by the PDF of inter-spike times τ_i: $\psi(\tau_i)$, which does not change with the index i, or, equivalently, by the statistical distribution of the number of spikes in a given time interval. The non-exponential pdf of Eq. (8.2) corresponds to a Non-Poisson distribution of the spikes. Another way of defining a renewal process is the local rate of event (spike) production $r(t)$. Roughly speaking, the local rate $r(t)$ is the expected number of spikes per time unit in a neighborhood of the time t. More rigorously, following Cox [33] and assuming that the last spike occurred at t_i, the local rate $r(t)$ is the (conditional) probability density that a spike occurs in an infinitesimal time interval $[t, t + dt]$, given that no spikes occurred

33

in the time interval $[t_i, t]$:

$$(3.44) \qquad r(t) = \lim_{dt \to 0} \frac{1}{dt} \Pr\{t < t_{i+1} \leq t + dt \mid t_{i+1} > t\}$$

Limiting ourselves to the time interval between the first two spikes: $[0, t_1]$, it is easy to prove that the rate $r(t)$ is given by [33]:

$$(3.45) \qquad r(t) = \frac{\psi(t)}{\Psi(t)} = -\frac{1}{\Psi(t)} \frac{d\Psi(t)}{dt}, \qquad 0 < t < t_1$$

being:

$$(3.46) \qquad \Psi(t) = \int_t^{\infty} \psi(s)ds = 1 - \int_0^t \psi(s)ds$$

the Survival Probability, *i.e.*, the probability that the spike occurrence time is larger than t. Clearly, it results: $\psi(t) = -d\Psi(t)/dt$. Once the rate function $r(t)$ is known, the Survival Probability is simply derived by solving Eq. (3.45) with respect to $\Psi(t)$ and imposing the initial condition $\Psi(0) = 1$:

$$(3.47) \qquad \Psi(t) = exp\left(-\int_0^t r(t')dt'\right).$$

The pdd of inter-spike times in a Poisson process is an exponential decay and the associated spike rate is constant in time: $r(t) = r_0$ [33].

Consequently, a natural way to realize a Non-Poisson process, and the relative non-exponential distribution of inter-spike time distances, is based on the assumption that the rate $r(t)$ of spike production changes in time. This is the case of Pareto-Nutting law, Eq. (8.2). In fact, in this case the Survival Probability is given by:

$$(3.48) \qquad \Psi(t) = \left(\frac{T_0}{t + T_0}\right)^{\mu_0 - 1}, \qquad 0 \leq t < t_1$$

and, substituting in Eq. (3.45) and limiting ourselves to the time interval $[0, t_1]$, we obtain the following expression:

$$(3.49) \qquad r(t) = \frac{r_0}{1 + r_1 t}, \qquad 0 \leq t < t_1$$

where

$$(3.50) \qquad \mu_0 = 1 + \frac{r_0}{r_1} \quad ; \quad T_0 = \frac{1}{r_1}$$

and

$$(3.51) \qquad r_0 = \frac{\mu_0 - 1}{T_0} \quad ; \quad r_1 = \frac{1}{T_0}.$$

The parameter r_0 has the physical meaning of the rate value immediately after the occurrence of a neuron firing, whereas $T_0 = 1/r_1$ determines the decay time of the rate function.

An alternative and much simpler way of deriving these relations would be to start with the basic general definition of waiting time distribution $\psi(t) = -\dot{\Psi}(t)$, and applying the Pareto-Nutting form of power law distribution, one can obtain the Survival probability distribution. From that point on, if we again use the general form of rate $r(t)$ in term of $\psi(t)$ and $\Psi(t)$, we can reach at the Eq.(3.49). Of course as soon as an event takes place the system will be switched to initial conditions and time will start ticking again to ensure that this is a renewal process. Hence the formulation is self consistent and in accordance with general principles of renewal theory.

Note that the prescription of Eq. (3.49)applies only to the first time interval between the first firing at time $t_0 = 0$ and the next one at time $t = t_1 = \tau_1$. To extend the rate function to the entire time axis, let us first introduce the following auxiliary function:

$$(3.52) \qquad f(t) = \frac{r_0}{1 + r_1 t}.$$

This corresponds to the rate function when no spike occurs up to the absolute time t. Due to the renewal assumption, the occurrence of a neuron firing erases the system's memory and the rate function jumps from the value $r(t_1) = f(t_1)$ to the "initial" value r_0. An example of behavior of the rate $r(t)$ is displayed in Fig. 1b, showing that the rate restarts from the value r_0 after each neuron firing, occurring at times t_1, t_2, t_3, etc... Consequently, in the time interval $[t_1, t_2]$ the rate function is written in the following way:

$$(3.53) \qquad r(t) = \frac{r_0}{1 + r_1(t - t_1)} = f(t - t_1), \qquad t_1 \leq t < t_2.$$
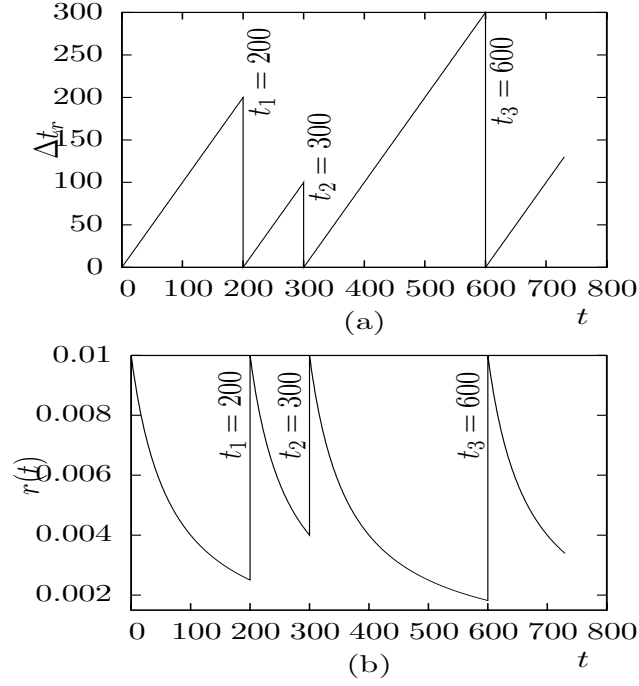
Figure 3.1.   An example of the time evolution of (a) the renewal time function Δt_r, Eq. (3.55), and (b) the rate function $r(t)$, Eq. (3.56). $r_0 = 0.01$, $r_1 = 0.015$.

For a given sequence of spike occurrence times $\{t_i\}$, this expression is easily generalized by applying suitable time shifts to the basic rate function $f(t)$:

$$(3.54) \qquad r(t) = f(t - t_i) = \frac{r_0}{1 + r_1(t - t_i)}, \qquad t_i \leq t < t_{i+1}.$$

Rigorously, the rate function has a formal dependence on the sequence $\{t_i\}$: $r(t, \{t_i\})$. However, at variance with the absolute time t, the dependence on the sequence $\{t_i\}$ is a kind of stochastic dependence, as the sequence of times is not known *a priori*, but it is a particular stochastic realization of the process, which is rigorously defined by the basic rate function $f(t)$ given in Eq. (3.52). In the following we will use the simple notation $r(t)$, as its mathematical and physical meaning is unambiguous. Further, in order to lighten the notation when considering the external perturbation, it is suitable to introduce the following *renewal time* function:

$$(3.55) \qquad \Delta t_r(t, \{t_i\}) = t - t_i \quad ; \quad t_i \leq t < t_{i+1}.$$

36

The renewal time Δt_r is a kind of random time, which is set to zero when a spike occurs and it increases linearly in the absolute time t from 0 to the values $\tau_{i+1} = t_{i+1} - t_i$, which are the random inter-spike time distances generated by the neuron set (see Fig. 1a).

Using the renewal time function, the rate function of Eq. (3.54) is rewritten in the following way:

$$(3.56) \qquad\qquad\qquad r(t) = \frac{r_0}{1 + r_1 \Delta t_r},$$

where the dependence of Δt_r on t and $\{t_i\}$ is left unindicated. From the computational point of view, Δt_r is simply the time measured from the last neuron firing.

Note that the renewal time function Δt_r is related to the internal dynamics of the system and its functional dependence on the time t is not the sign of an external forcing. This function describes the renewal character of the dynamics. On the contrary, the time dependence of one or both the parameters r_0 and r_1 in Eq. (3.56) would be the sign of an external perturbation.

3.11. Connection with Daly-Porporato Model

It is easy to show that our proposal to generate a non-Poisson firing process is exactly equivalent to the model recently proposed by Daly and Porporato [40]. These authors proposed the following equation of motion

$$(3.57) \qquad\qquad\qquad \frac{dx}{dt} = k - I(x, t),$$

where $x(t)$ is the state variable, k is a constant and $I(x, t)$ is a state-dependent Poisson process with rate

$$(3.58) \qquad\qquad\qquad r(x) = \frac{A}{(1 + x)}.$$

Let us imagine that at time $t = 0$ a firing event sets for the state variable the initial condition $x = 0$. The time evolution of the state variable up to the next firing event is given by

$$(3.59) \qquad\qquad\qquad x(t) = kt,$$

which has the effect of making $r(x)$ time dependent. By plugging Eq. (3.59) into Eq. (3.58), we obtain

(3.60)
$$r(t) = \frac{A}{1 + kt},$$

which is made exactly equivalent to Eq. (3.56) by setting $A = r_0$ and $k = r_1$.

As far as the perturbation of T_0 is concerned, in Section 8.4 we shall use an apparently different model, referred to as *dynamical model* [100].

Actually, it has been shown [95, 96] that the response of the dynamical model to weak perturbations is equivalent to the adoption of the model of a more elegant formulation given in Chapter 8.2, with the condition $\phi_1(t) = \phi_2(t)$ [39].

CHAPTER 4

DIFFUSION AND INTERMITTENCY

4.1. Diffusion as a Drunkards Walk

Having reached the distribution for the time dependent probability of collision times, now let us make some digression in attempting to analyze the diffusion problem as a drunkards walk, where we have the case as the successive displacements between the collisions are statistically independent. Let us consider only one of the 3 dimensions say x component, in an environment where effects of the external forces are negligibly small or better yet, do not exist at all. Let us denote the ith component of the displacement in the x direction with ξ_i, to denote that this displacement is arbitrary. The x component of the molecular position after n collisions would be

$$x_n = \sum_1^n \xi_i \tag{4.1}$$

The direction of motion being totally random we have $< x >$ since $< \xi_i >= 0$. For the dispersion though

$$< x_n^2 >= \sum_0^n < \xi_i^2 > + \underbrace{\sum_i^n \sum_j^n < \xi_i \xi_j >}_{i \neq j} \tag{4.2}$$

The rightmost term vanishes since based on statistical independence of successive displacements $< \xi_i \xi_j >=< \xi_i >< \xi_j >= 0$

$$< x_n^2 >= n < \xi^2 > \tag{4.3}$$

between the collisions the velocity v_x is constant so

$$\xi = v_x t \tag{4.4}$$

(4.5) $$< \xi^2 >=< v_x^2 >< t^2 >$$

let us note $v_x^2 = \frac{1}{3}v^2$ and let use the time dependent probability of collision, Equation.3.37 to obtain the dispersion of time [35]

(4.6) $$< t^2 >= \int_0^\infty t^2 \psi_c(t)dt = \int_0^\infty \frac{e^{\frac{-t}{\tau_c}}}{\tau_c} t^2 dt = 2\tau_c^2$$

and where $t = n\tau_c$,

(4.7) $$< x^2(t) >= \left(\frac{2}{3} < v^2 \tau_c > \right) t$$

so we can conclude that $< x^2(t) >\sim t$.

4.2. Diffusion Equation

Fick's first equation was derived by Adolf Fick in 1855, assuming steady flow, namely that the concentration of the diffusing particle dies not change with time, the flow is constant and is a result of some density gradient. Where p denotes density, x denotes the space coordinate in one dimension and J stands for the flux of the flow

(4.8) $$J = -D\frac{dp}{dx}$$

where D stands for the constant quantity called diffusion coefficient. Fick's Law, just like $F = ma$ defines a quantity , diffusion constant D, just like mass m, and hance it is a statement of a relation ship between some quantities. $D \geq 0$because a flow is always from a high concentration to a lower concentration gradient, to balance the gradient and to destroy the gradient. Taking a control volume in an fluid flow, where the fluid may be compressible or incompressible, whatever goes in must either change the concentration in the control volume or must go out, we can write the continuity equation

(4.9) $$\frac{\partial p}{\partial t} + \frac{\partial J}{\partial x} = 0$$

if we inset Fick's 1st law into the equation of continuity, we obtain Fick's second law

$$(4.10) \qquad \frac{\partial p(x, t)}{\partial t} = D \frac{\partial p(x, t)}{\partial x^2}$$

which is the classical diffusion equation. The solution to this equation is

$$(4.11) \qquad p(x, t) = \frac{1}{\sqrt{4\pi D t}} e^{-\frac{-x^2}{4Dt}}$$

Now let us notice that this solution to the diffusion equation satisfies the scaling form

$$(4.12) \qquad T(x, t) = \frac{\mathcal{A}}{t^\delta} f\left(\frac{x}{t^\delta}\right) \equiv \frac{1}{\sqrt{4\pi D}} \frac{1}{t^{0.5}} \exp\left(\frac{-1}{4D} \frac{x}{t^{0.5}}\right)$$

4.3. Intermittency in Nature

Osborne Reynolds discovered the basic physics concerning the investigation of basic fluid mechanics and a very important concept called *dynamic similarity*. Dynamic similarity states that, no matter what the size of or the velocity or size or the viscosity of the fluid in which the material is moving, the analysis of the flow depends rather strongly on one parameter called the Reynolds number. Reynolds number is just the ratio of inertial forces on the object to the viscous forces, and even though the individual parameters like the velocity and size of the object may be different, if the Reynolds numbers of the same shape objects are similar, the flow characteristics are predicted to be similar as well. This sets the fundamentals for the Aeronautical engineer to use models of an aircraft in an air tunnel and also the ship engineers to make experiments on their models of the original ships in a smaller scale in environments of similar Reynolds numbers.

The 1883 paper [41],[42] by Osborne Reynolds points out to the importance of what we now know as the Reynolds number and also he points out to another important observation of his, the flow regime of the water, he clearly defines two distinctive flow types, *laminar* and *turbulent*, though he used the terms *direct* and *sinuous* originally at that time. In laminar flow different streamlines do not mix, whereas in turbulent motion they do. It appeared that the transition between laminar and turbulent flow appeared to

depend on the dimensionless quantity which is named as the Reynolds number to honor Osborne Reynolds

(4.13)
$$R_n = \frac{\rho v r}{\nu}$$

where ρ is the density, v is the velocity, r radius of the tube and ν is the viscosity of the fluid. In his experiments, he observed the phenomena what we now refer to as *intermittence.* So actually in short there are three flow regimes, for low Reynolds numbers the flow tends to laminar flow in which the flow streams could be followed, in very high R values, the flow is all mixing and hence turbulent, but there is a range of R values where one would have long times of laminar flow and shorter times and turbulent flow, following each other successively and in a manner that there is no correlation between when one or the other appears.
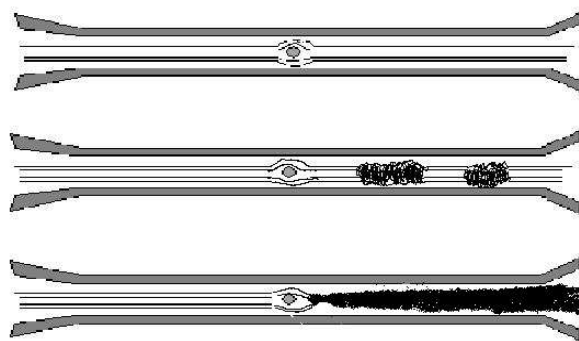
Figure 4.1.   The change of fluid flow regime from laminar to intermittent

to turbulent flow regimes as Reynolds number R_n increases.

Reynolds run another experiment in which he let two fluids of different color to flow in opposite directions in layers. What he observed was that as the velocity of the flows increases the interface becomes wavy, and then peaks formed and finally there appears transitions from laminar to turbulent flows. As a result he concludes that the transition from laminar to turbulent flow need not be a sudden transition. Even after so many years and although there has been great progress in explaining the nature of turbulence, the transition to turbulent flow is still far from being entirely understood as

of today. The intermittent behavior in fluid flow is observed in other configurations too. Having been convinced that the flow characteristics depend on a single parameter, namely Reynolds number R_n, Osborne Reynolds continued his experiments for investigation of the transitions between laminar and turbulent flow, using different tubes at different temperatures. He concluded the following after his experiments [42]

- The dependence of the transition to Reynolds number goes inversely proportional to the amplitude of the disturbance.
- There is a regime which we might call *"laminar"* with a Reynolds number $R_n <$ 1100 below which any disturbance will die out.
- There is a range of R_n values for which the eddies will appear suddenly,without a region of gradual transition.(This regime is named "the intermittent flow regime" by now).
- The disturbance would suddenly come through a certain length of the tube, whose appearance is rather like flashes
- We can also add the following observation today, there is no cross-correlation or auto-correlation between and amongst the time durations of the eddies and laminar flow in the intermittent regime [43]

With the air tunnel experiments performed on spherical objects in low and high Reynolds numbers [44], it is shown that the air drag on a ball reduces drastically when the system is in a turbulent regime, and that this regime comes with relatively low R_n values if the surface of the ball is even slightly scratched. This observation has led to the investigation of how a most efficient ball could be designed where the turbulence behind the ball can be triggered relatively easily reducing the air drag, which found its application in the production of baseball balls [45]. The appearance of turbulence and intermittency in fluid mechanics and magnetohydrodynamics is by no means limited to this generic example. Another case where transition to chaos via intermittency plays a major role in fluid dynamics in nature is Benard instabilities. This is a case where a thin sheet of fluid is heated from underneath and the heat transfer mechanism turns from conduction

where viscous forces are dominant over convection where dynamical forces are dominant due to the expansion of the fluid underneath based on the temperature difference. The flow characteristics of the fluid convection changes as the temperature and/or the overall shape and/or size of the fluid changes. When the temperature difference is relatively low and hence R_n is also low, the fluid viscosity wins and the fluid is transported through heat conduction. As R_n increases beyond a certain critical value R_{n_a} a state of stationary convection cells are formed.If R_n is increased through heat beyond yet another threshold R_{n_b} then a transition to chaos occurs. The experimental results tell us that the Fourier spectrum of the velocity shows peaks in the region where $R_{n_a} < R_n < R_{n_b}$ and a rather continuous power spectrum when $R_n > R_{n_b}$.

This kind of a chaotic behavior is important also because the interiors of the Earth is still a hot furnace due to ongoing nuclear reactions inside the Earth unlike other planets in our solar system, a fact which makes the plate tectonics of the Earth an active layer driven by the convection of the magma and the mantle. [46].

4.4. Manneville Map

P. Manneville came up with a map that models the behavior of the intermittent fluid flow properties mentioned above [47]. Although it actually came up to model the intermittency in fluid flow between laminar and turbulent flow, it is established as one of the three roots to chaos [43]. In this section we will discuss the properties of the Manneville map and its connection to our model of intermittency which basically is equivalent to the Manneville map. We will show why both models are equivalent, leading to the same results in terms of statistics and why it is used to model renewal processes. We will also discuss why revised Manneville map we use in our simulations and in connection to renewal processes will lead to power law distributions which are abundant in nature out of the realm of ordinary statistical mechanics which leads to exponential waiting time distributions. We will see where the perturbation of rate may have physical significance in Nature and how this perturbation may affect the related statistical properties of the physical system.
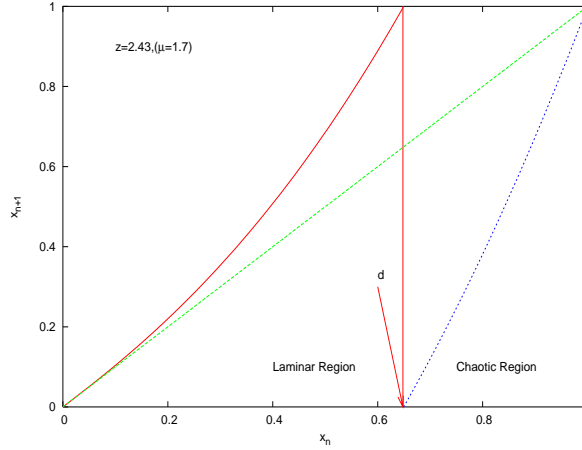
Figure 4.2. Manneville map sketch for $z = 2.43$, (a power index of $\mu = 1.7$)in a power law distribution for the waiting time distributions in the laminar region. The vertical line divides the laminar region on the left from the chaotic region on the right.

The Manneville map is given by [47] see Figure (4.4)

$$(4.14) \qquad\qquad x_{n+1} = \Phi(x_n) = x + x^z \, (mod\,1)$$

where $d(z)$ defines the dividing line between the laminar and the chaotic regions of the phase space as

$$(4.15) \qquad\qquad d + d^z = 1$$

or more rigorously

$$(4.16) \qquad\qquad x_{n+1} = x_n + x_n^z, \, (x < d)$$

$$(4.17) \qquad\qquad x_{n+1} = x_n + x_n^z - 1, \, (x > d)$$

where the laminar region is [0,d) and the chaotic region is (d,1]. The motion of the trajectory based on this map behaves in an intermittent manner, some steps will be taken in the laminar region, then eventually as x_{n+1} becomes larger than 1, the particle is injected in the chaotic region of the phase space, and then again it will be re-injected back into the laminar region in a deterministic yet unpredictable way, so that if we shrink

45
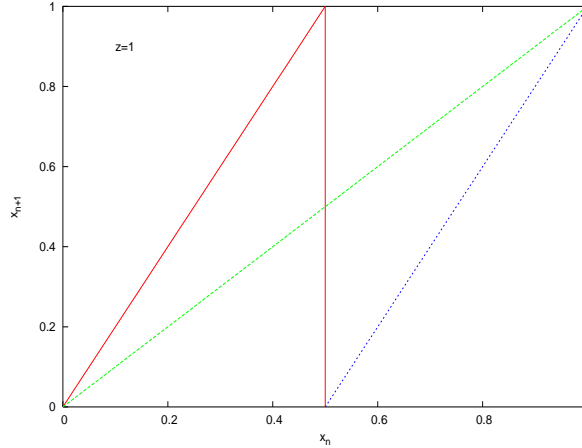
Figure 4.3.   Manneville map sketch for $z = 1$, leading to an exponential decay for the waiting time distributions on both sides. The map in this particular form is equivalent to Bernouilli Shift map.

the time spent in the Chaotic region to zero and consider only the time spent in the laminar region, which from now on we will refer to as the waiting time or the sojourn time, the lengths of the consecutive sojourn times are totaly uncorrelated. Yet this does not mean that we can not analyze the statistics of the Manneville Map. Here is an attempt to analyze the properties of the map.

As the particle leaves the laminar region for chaotic region, it spends a few steps in the chaotic region and then it will be re-injected back into the laminar region. The injection back process is uniform, independent of the particular value of the parameter z. In fact, if we record only position the particle under the directives of the Manneville map enters the Laminar region, we see that the distribution is uniform. Using this property we will work on a continuous time model of the Manneville map. But first with a little reasoning let us see what kind of a waiting time distribution the Manneville map will lead us to.

Let us start with the simplest case where $z = 1$ is used in the Manneville map. It is easy to see that, when $z = 1$, the model describes as that in Figure (4.4), is equivalent to Bernouilli Shift map used by Zaslavsky [48]

(4.18) $x_{n+1} = \Phi(x_n) = 2x_n, \, (mod \, 1)$

46

to prove the fundamental result that the Poincare return times are distributed as

(4.19)
$$P_R(t) \sim e^{-h_{KS}t}$$

or basically, the distribution of the Poincare recurrence times which in our case is nothing but the waiting time distribution follow an exponential distribution. In this expression h_{KS} denotes the Kolmogorov-Sinai(KS) entropy.

An argumentation is first started by Giesel and Thomae [49] and also discussed in Ref ([50]) to derive an analytical expression for the waiting time distribution in the laminar region. I extend this discussion and show its relevance for emphasizing the connection of Manneville map with our own Dynamical model for intermittency and their equivalence.

For the Manneville map, let us consider the case of a walker that has as his initial point of walk very close to the point $x_0 = 0$. If this is the case, the consecutive points will be very close especially as z becomes larger than 1, we can make the continuous time approximation that

(4.20)
$$x_{n+1} = x_n + x_n^z \rightarrow \frac{dx}{dt} = x^z$$

if we integrate to figure out the time t it takes for the particle to reach the position $x(t)$ starting from x_0,

(4.21)
$$\int_{x_0}^{x(t)} x^{-z}dx = \int_0^t dt$$

(4.22)
$$t = \frac{x(t)^{1-z} - x_0^{1-z}}{1-z}$$

the waiting $\tau(x_0)$ to reach the point $x(t)$ is simply

(4.23)
$$\tau(x_0, x(t)) \equiv \left(\frac{1}{x_0^{z-1}} - \frac{1}{x(t)^{z-1}} \right) \frac{1}{1-z}$$

47

if we want to know the time it takes to reach the border point where the particle exits from from the Laminar region all we have to do is to set $x(t) = d$.

$$(4.24) \qquad \tau(x_0, d) \equiv \left(\frac{1}{x_0^{z-1}} - \frac{1}{d^{z-1}} \right) \frac{1}{1-z}$$

$if\, x_0 \ll d$, we legitimately make the following approximation

$$(4.25) \qquad \tau(x_0) \sim \left(\frac{1}{x_0^{z-1}} \right) \frac{1}{1-z}$$

At this point if we define the injection probability distribution $p(x_0)$ and the waiting time distribution $\psi(t)$, their relation reads

$$(4.26) \qquad \psi(t)dt = p(x_0)dx_0$$

but the back injection probability is known to be uniform, and based on this equiprobability of beck-injection probability, the back-injection happens through a window of size $d(z)$ implies

$$(4.27) \qquad p(x_0)dx_0 = \frac{1}{d(z)} \left| \frac{dx_0}{d\tau} \right| d\tau$$

$$(4.28) \qquad \psi(t) = \frac{1}{d(z)} \left| \frac{dx_0}{dt} \right|$$

using Equation.(4.24)

$$(4.29) \qquad \psi(t) = d^{z-1} \left[1 + d^{z-1}(z-1)t \right]^{-\frac{z}{z-1}}$$

at this point let us set for the power of the expression in the paranthesis the following

$$(4.30) \qquad \mu_0 = \frac{z}{z-1}$$

implying

48

$$(4.31) \qquad z = \frac{\mu_0}{\mu_0 - 1}$$

and

$$(4.32) \qquad z - 1 = \frac{1}{\mu_0 - 1}$$

in this form the distribution of the waiting times can be written as

$$(4.33) \qquad \psi(\tau) = d^{\frac{1}{\mu_0-1}} \left[1 + \frac{d^{\frac{1}{\mu_0-1}}}{\mu_0 - 1} \tau \right]^{-\mu_0}$$

$$(4.34) \qquad \psi(\tau) = \frac{d^{\frac{1}{\mu_0-1}}}{\left[1 + \frac{d^{\frac{1}{\mu_0-1}}}{\mu_0-1} \tau \right]^{\mu_0}} = \frac{\frac{(\mu_0-1)d^{\frac{1}{\mu_0-1}}}{\mu_0-1}}{\left[1 + \frac{d^{\frac{1}{\mu_0-1}}}{\mu_0-1} \tau \right]^{\mu_0}}$$

$$(4.35) \qquad \psi(\tau) = (\mu_0 - 1) \frac{\frac{d^{\frac{1}{\mu_0-1}}}{\mu_0-1}}{\left(\frac{d^{\frac{1}{\mu_0-1}}}{\mu_0-1} \right)^{\mu_0} \left[\tau + \left(\frac{\mu_0-1}{d^{\frac{1}{\mu_0-1}}} \right) \right]^{\mu_0}}$$

at this point if we set

$$(4.36) \qquad T_0 = \frac{\mu_0 - 1}{d^{\frac{1}{\mu_0-1}}}$$

The waiting time distribution hence reads

$$(4.37) \qquad \psi(\tau) = (\mu_0 - 1) \frac{T_0^{\mu_0-1}}{(T_0 + \tau)^{\mu_0}}$$

which will give us a power law distribution for the probability distribution of the waiting times in the form of $\frac{1}{\tau^{\mu_0}}$ as $\tau > T_0$. For this reason we may refer to μ_0 as the power index and T_0 as the time it takes to make the transition to power law. Let us set in Equation.(4.36) the following

$$(4.38) \qquad \alpha_0 = d^{\frac{1}{\mu_0-1}}$$

which turns Equation.(4.36) into

$$(4.39) \qquad T_0 = \frac{\mu_0 - 1}{\alpha_0}$$

At this point, a legitimate question to ask is, how the system might be behaving if we set $z = 1$, for which case from the work of Zaslavsky Ref.([48]), that the Poincare return times which basically is nothing but the waiting time distribution behaves as an exponential distribution. Let us see if our result here will be consistent with what Zaslavsky has predicted for such systems with $z = 1$, or in other words, using Equation.(4.30) which corresponds to the waiting time distribution as $\mu_0 \to \infty$

$$(4.40) \qquad \lim_{\mu_0 \to \infty} \psi(\tau) = \lim_{\mu_0 \to \infty} \frac{\mu_0 - 1}{T_0} \left(\frac{T_0}{T_0 + \tau} \right)^{\mu_0}$$

$$(4.41) \qquad \lim_{\mu_0 \to \infty, z \to 1} \psi(\tau) = \lim_{\mu_0 \to \infty, z \to 1} \frac{\mu_0 - 1}{T_0} \left(1 - \frac{\tau}{T_0 + \tau} \right)^{\mu_0}$$

inserting Equation.(4.39)

$$(4.42) \qquad \lim_{\mu_0 \to \infty, z \to 1} \psi(\tau) = (\mu_0 - 1)(\frac{\alpha_0}{\mu_0 - 1}) \left(1 - \frac{\tau \alpha_0}{\mu_0 - 1 + \alpha_0 \tau} \right)^{\mu_0}$$

since

$$(4.43) \qquad \lim_{n \to \infty} \left[1 \pm \frac{x}{n} \right]^n \to e^{\pm x}$$

$$(4.44) \qquad \lim_{\mu_0 \to \infty, z \to 1} \psi(\tau) = \alpha_0 e^{-\alpha_0 \tau}$$

namely an exponential distribution in accordance with the prediction of Zaslavsky's analysis of the Poincare recurrence times. So Manneville map provides us with an adjustable tool to provide us a power law waiting time distribution of power index μ_0 or an exponential waiting time distribution of rate α_0 on demand, through the gauge of μ_0. For obvious reasons from now on we will refer to power law waiting time distributions as non-Poisson distributions, and exponential waiting time distributions as Poisson distributions.

Let us see the integration of the probability distribution over all possible values of the waiting times τ for the Poisson case.

$$(4.45) \qquad \int_0^\infty \psi(\tau)d\tau = \alpha_0 \int_0^\infty e^{-\alpha_0 \tau} d\tau = 1$$

Hence it is already normalized. If we do the same for the zeroth moment of τ for the non-Poisson waiting time distribution

$$(4.46) \qquad (\mu_0 - 1)T_0^{\mu_0-1} \int_0^\infty \frac{d\tau}{(T_0 + \tau)^{\mu_0}} = (\mu_0 - 1)T_0^{\mu_0-1} \int_{T_0}^\infty \frac{du}{(u)^{\mu_0}} = 1$$

So, both the non-Poisson and Poisson distributions have their zeroth moment equal to one, namely, they are already normalized in their present form.

In the Poisson case

$$(4.47) \qquad <\tau>_{Poisson} = \int_0^\infty \tau\psi(\tau)d\tau = \alpha_0 \int_0^\infty \tau e^{-\alpha_0 \tau} d\tau = \frac{1}{\alpha_0}$$

the first moment of the waiting time distribution the non-Poisson case reads, setting $u = T_0 + \tau$

$$(4.48) \qquad <\tau>_{non-Poisson} = (\mu_0 - 1)T_0^{\mu_0-1} \int_{T_0}^\infty \frac{u - T_0}{u^{\mu_0}} du$$

$$(4.49) \qquad <\tau>_{non-Poisson} = (\mu_0 - 1)(T_0^{\mu_0-1}) \left(\left[\frac{u^{2-\mu_0}}{2 - \mu_0} \right]_{T_0}^\infty - T_0 \left[\frac{u^{1-\mu_0}}{1 - \mu_0} \right]_{T_0}^\infty \right)$$

this quantity is finite only if $\mu_0 > 2$, remember that for the normalization condition to be satisfied, we already needed $\mu_0 > 1$.

$$(4.50) \qquad <\tau>_{non-Poisson} = \frac{T_0}{\mu_0 - 2}$$

So as a result for the first moment, average of the waiting times, we have $<\tau> = \frac{1}{\alpha_0}$ for the Poison case, and for the non-Poisson case $<\tau> = \frac{T_0}{\mu_0-1}$ for $2 < \mu_0$, and when $1 < \mu_0 < 2$, $<\tau> \to \infty$, basically as we proceed larger and larger values of τ will show up in this case that an average value is not defined for $1 < \mu_0 < 2$.

For the Poisson case, let us calculate the second moment $< \tau^2 >_{Poisson}$

(4.51) $$< \tau^2 >_{Poisson} = \int_0^\infty \tau^2 \psi(\tau) d\tau = \alpha_0 \int_0^\infty \tau^2 e^{-\alpha_0 \tau} d\tau$$

integrating by parts

(4.52) $$< \tau^2 >_{Poisson} = \frac{2}{\alpha_0} \underbrace{\int_0^\infty \tau e^{-\alpha_0 \tau} d\tau}_{\frac{1}{\alpha_0}} = \frac{2}{\alpha_0^2}$$

having reached the result for the second moment $< \tau^2 >_{Poisson} = \frac{2}{\alpha_0}$ and the average $< \tau >_{Poisson} = \frac{1}{\alpha_0}$, the variance and the standard deviation the for the Poisson case reads

(4.53) $$\sigma_{\tau,Poisson}^2 = < \tau^2 >_{Poisson} - < \tau >_{Poisson}^2 = \frac{1}{\alpha_0^2}$$

and

(4.54) $$\sigma_{\tau,Poisson} = \frac{1}{\alpha_0}$$

respectively.

Let us also investigate the second moment for the non-Poisson case.

(4.55) $$< \tau^2 >_{non-Poisson} = (\mu_0 - 1)T_0^{\mu_0-1} \int_0^\infty \frac{\tau^2}{(T_0 + \tau)^{\mu_0}} d\tau$$

setting again $u = T_0 + \tau$ as the new integration variable

(4.56)
$$< \tau^2 >_{non-Poisson} = (\mu_0 - 1)T_0^{\mu_0-1} \left([\frac{u^{3-\mu_0}}{3 - \mu_0}]_{T_0}^\infty - 2T_0[\frac{u^{2-\mu_0}}{2 - \mu_0}]_{T_0}^\infty + T_0^2[\frac{u^{1-\mu_0}}{1 - \mu_0}]_{T_0}^\infty \right)$$

obviously, this quantity will be finite only when $\mu_0 > 3$. Having satisfied the finiteness condition it leads to

(4.57) $$< \tau^2 >_{non-Poisson} = \frac{2T_0^2}{(2 - \mu_0)(3 - \mu_0)}$$

52

and the variance reads

$$(4.58)$$
$$\sigma_{\tau,non-Poisson} = <\tau^2>_{non-Poisson} - <\tau>^2_{non-Poisson} = \frac{2T_0^2}{(2-\mu_0)(3-\mu_0)} - \frac{T_0^2}{(\mu_0-2)^2}$$

$$(4.59) \qquad \sigma_{\tau,non-Poisson} = \frac{T_0^2(\mu_0-1)}{(2-\mu_0)(\mu_0-2)(3-\mu_0)}$$

So the standard deviation of the non-Poisson distribution is defined and finite only for $\mu_0 > 3$.

4.5. Dynamical Model for Poisson Renewal Processes using Modified Manneville Map

At this point we will introduce a dynamical model developed by our Non-Linear Science center at University of North Texas. The dynamic model in use in this section is inspired by the Manneville map [47], more recently modified [?] to reduce the time spent in the chaotic regime to only one time step, i.e., if we consider only the laminar sequence of times, this model will produce for us the renewal event sequences of the Manneville map.

Having established its advantages to model renewal systems, we will work on the effects internal or external parameters on this intermittency model, and finally with the aid of time series analysis methods based on entropic considerations we will establish connections with neuron systems.

Here we consider a particle moving in the positive direction in the interval , based on the non-linear equation

This model is based on a particle moving in the positive direction of the x-axis, within the interval $I \equiv [0,1]$, of size 1, defined by $x \in [0,1]$, with the following deterministic equation of motion

$$(4.60) \qquad \dot{x} = \alpha_0 x^z$$

where $1 \leq z$ and $1 \gg \alpha_0$. When the particle reaches the border point of $x = 1$, the particle is inserted back in the prescribed interval in a random way, to any point in the interval I with equal uniform probability as shown in the Figure.(4.5)
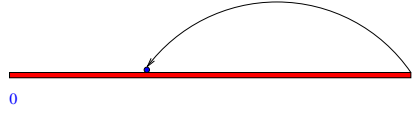
Figure 4.4.   Dynamical model for the particle driven by the Modified

Manneville Map non-linear equation. The particle is inserted back into the

interval randomly with uniform probability.

We will denote the time it takes to reach the border $x = 1$ from the initial point $x_0 = \xi$, by τ, where we use the symbol ξ to signify a random number in the interval $I \equiv [0, 1]$. Let us first investigate the case where we have $z = 1$. Then the equation reads

$$(4.61) \qquad \dot{x} = \alpha_0 x \to \int_{x_0}^{x(t)} \frac{dx}{x} = \int_0^t \alpha_0 \, dt$$

$$(4.62) \qquad \ln \frac{x(t)}{x_0} = \alpha_0 t$$

$$(4.63) \qquad x(t) = x_0 e^{\alpha_0 t}$$

let us remember that the initial position is a random number ξ and at the border the particle reaches $x(t) = 1$ within a sojourn time of τ [80]

$$(4.64) \qquad \xi = e^{-\alpha_0 \tau}$$

$$(4.65) \qquad \tau = \frac{-1}{\alpha_0} \ln (\xi)$$

This indeed is the simples way to drive Poisson sequence of waiting times in chronological order using a series of White Noise ξ_i.

For the waiting time distribution

$$(4.66) \qquad \psi(\tau) d\tau = p(\xi) d\xi$$

one has to remember that the back injection probability is constant and uniform implying $p(\xi) = 1$, hence

$$(4.67) \qquad \psi(\tau) = \left| \frac{d\xi}{d\tau} \right| = \alpha_0 e^{(-\alpha_0 \tau)}$$

Basically, the waiting time distribution for the dynamical model under investigation for the parameter $z = 1$ is a Poisson distribution. Remember that all the initial values x_0 are drawn from a set of random numbers with an equal probability in the interval $I \equiv [0, 1]$, hence the name white noise. Therefore the random numbers ξ_i and ξ_{i+1} are totally uncorrelated ensuring the renewal nature of the process under investigation. So, by this token, now we know that for $z = 1$, this system will produce waiting time distributions of renewal nature as Poisson renewal system should do, namely, an exponential distribution of the histogram of the renewal waiting times with no time auto-correlation in the chronological order. Note that this is the technique we use to create the unperturbed time series $\{t_i\}$, with the following criterion: $t_1 = \tau_1, t_2 = \tau_1 + \tau_2$, and so on. The numerical means of perturbing the Poisson sequences will be based on similar argumentation.

4.6. Dynamical Model for Non-Poisson Renewal Processes using the Modified Manneville Map

Let us now consider the case where we have $z \neq 1$.

$$(4.68) \qquad \frac{dx}{dt} = \alpha_0 x^z$$

$$(4.69) \qquad \int_{x_0}^{x(t)} \frac{dx}{dt} = \int_0^t \alpha_0 dt$$

$$(4.70) \qquad \frac{x^{-z+1}}{-z+1} \Big|_{x_0}^{x} = \alpha_0 t$$

55

$$(4.71) \qquad \frac{x^{1-z}}{1-z} - \frac{x_0^{1-z}}{1-z} = \alpha_0 t$$

when $x = 1$, the time $t = \tau$, and remembering that the initial value of the position $x_0 = \xi$ is drawn from a sample white noise randomly from the interval $I = [0, 1]$

$$(4.72) \qquad \tau = \frac{1}{\alpha_0(1-z)}(1 - \xi^{1-z})$$

This is the simplest means of obtaining the unperturbed renewal non-Poisson waiting times from a sequence of White Noise.

Again playing the same arguments as above that the back injection is uniform

$$(4.73) \qquad \psi(\tau)d\tau = \underbrace{p(\xi)}_{1} d\xi$$

with

$$(4.74) \qquad \xi = (1 - \tau\alpha_0(1-z))^{\frac{1}{1-z}}$$

and

$$(4.75) \qquad \psi(\tau) = \left| \frac{d\xi}{d\tau} \right| = \frac{\alpha_0}{(1 + \tau\alpha_0(z-1))^{\frac{z}{1-z}}}$$

set $\mu_0 = \frac{z}{z-1}$ implying that $z - 1 = \frac{1}{\mu_0 - 1}$

$$(4.76) \qquad \psi(\tau) = \frac{\alpha_0}{(\alpha_0(z-1))^{\mu_0} \left[\frac{1}{\alpha_0(z-1)+\tau} \right]^{\mu_0}}$$

and if we set

$$(4.77) \qquad T_0 = \frac{1}{\alpha_0(z-1)} = \frac{\mu_0 - 1}{\alpha_0}$$

this reads

$$(4.78) \qquad \psi(\tau) = (\mu_0 - 1)\frac{T_0^{\mu_0 - 1}}{(T_0 + \tau)^{\mu_0}}$$

A normalized power law distribution exactly in the same form as the Manneville map discussed earlier provides for us. We may name this model modified Manneville map, because it has all the benefits of the original Manneville map, but also the additional

56

advantage that in the modified case, the parameters T_0 and μ_0 might be adjusted independent of each other, which also means that, one can perturb one independent of the other. So modified form of the Manneville map gives us tools to play with the system parameters to adjust the transition time to power law T_0, which also serves as a time scale parameter of the system, or the power index μ_0 independently, which is possible to do in a physical system depending on what parameters are time dependent.

CHAPTER 5

FUNDAMENTAL CONCEPTS IN TIME SERIES ANALYSIS

5.1. Scaling Detection Methods in Time Series

A time series comprises of a series of data equally spaced in time as $\xi_1, \xi_2, \xi_3, \ldots, \xi_n$. One can establish a connection between a particular time series and a diffusion process. The Brownian particle we consider is assumed to undergo collisions and hence change its velocity with equal intervals that correspond to the time unit interval of time series Δt. In such a motion of the Brownian particle, the time series ξ_i might be assigned for the velocity components. For the sake of rigor, between the time interval $t = 0$ to $t = 1$, where we have assigned the time interval between the consecutive elements of the time series as the unit time interval $\Delta t = 1$, we have the velocity component as ξ_1 leading to a displacement of $x_1 = \xi_1 \Delta t = \xi_1$. Between the time interval $t = 1$ and $t = 2$, the velocity component assigned is ξ_2 leading to a displacement during this time interval of $x_2 = \xi_2$. If the particle starts motion at $x_0 = 0$ under the command of the velocity components given as the elements of the particular time series under consideration, at time t the particle will be at the position $x(t) = \sum_{i=1}^{t} \xi_i$, where t is a positive integer. Overall the above equation describes the position of the Brownian particle starting its motion at $t = 0$ at $x_0 = 0$. But one can not have spring with just a single blossom of a flower, for a statistical approach to a diffusion process we need an ensemble of identical particles starting with the same initial condition at $t = 0$ and $x_0 = 0$. However, a time series yields only a single realization whereas we need many realizations of Gibbs ensembles with identical initial conditions. To overcome this problem the technique of *overlapping windows* is introduced and defined as follows.

If we have a single realization as the time series of N discrete elements, $\xi_1, \xi_2, \xi_3, \ldots, \ldots, \xi_N$, different diffusion trajectories may be defined by taking consecutive elements in a window
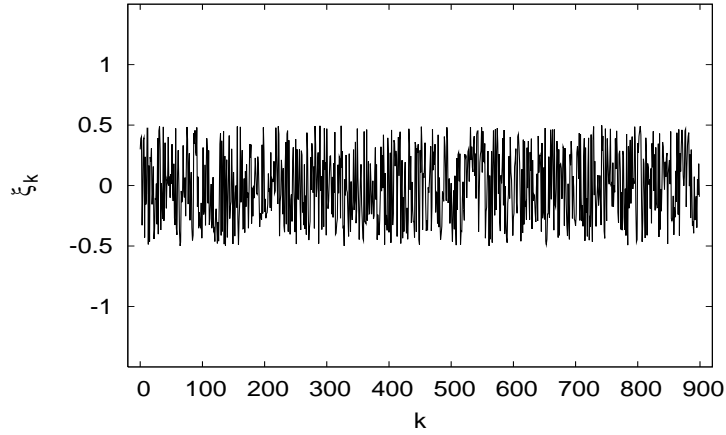
Figure 5.1.   Brownian White noise driving a diffusion process.
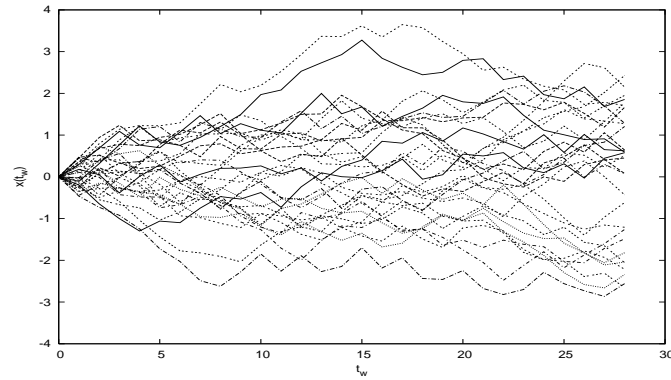
Figure 5.2.   Trajectories obtained from non-overlapping windows.

of size t_w. So for window of size $t_w = 3$, we will have 3 successive elements in every case as follows

$$x_1(3) = \xi_1 + \xi_2 + \xi_3;$$

$$x_2(3) = \xi_2 + \xi_3 + \xi_4;$$

$$x_3(3) = \xi_3 + \xi_4 + \xi_5;$$

$$\ldots\ldots\ldots$$

$$x_{N+1-t_w}(3) = \xi_{N-2} + \xi_{N-1} + \xi_N;$$

or in general

$$(5.1) \qquad\qquad x_\kappa(t = t_w) = \sum_{i=\kappa}^{\kappa+t_w} \xi_i$$

where $\kappa = 1, 2, 3, \ldots, N+1-t_w$. So, now we have $N+1-t_w$, trajectories representing diffusing particles all stating their motion at $t = 0$, $x_0 = 0$, and ending up at the points in space $x_i(t_w)$, $i = 1, 2, 3, \ldots, N + 1 - t_w$. The distribution of points $x_i(t_w)$ will define a distribution of Gibbs ensemble of particles at time $t = t_w$, so, we have a distribution of $N + 1 - t_w$ particles and clearly as $N \to \infty$, it will define a well fit distribution. By means of this method of *overlapping windows*, even if we have a single realization of a time series , we can define a set of Gibbs ensemble of particles to follow in which manner the distribution of the particles evolve in time as a function of the window size t_w. The method of overlapping windows for a time series of 900 elements and a windows size of 30 will yield 30 trajectories. A Brownian Noise of such properties with 900 elements is shown in figure (5.1) and the resulting trajectories with non-overlapping windows method is shown in figure (5.1). If we used overlapping windows method we would have $N + 1 - t_w = 871$ windows available, but with non-overlapping windows method we only have 30 trajectories. The superiority of the quality of the resulting statistics using overlapping windows method is obvious.

5.2. Standard Deviation Analysis for Scaling Inspection

The method is based on the presumption that a diffusion process does not need to scale as $\delta = 0.5$, for sub-diffusion or for super-diffusion processes this scaling coefficient could well be different ranging from $\delta = 0$ to $\delta = 1$ in the ballistic case. The diffusion equation may read

(5.2) $$p(x, t) = \frac{1}{t^\delta} exp(-x^2/4Dt^\delta)$$

namely it could still be a Gaussian distribution but the dependence of the variance on time may scale may be different from a normal diffusion process. For normal diffusion process we have already shown that $< x^2(t) > \sim t^{2H}$ where $H = 1/2$. For $< x(t) >= 0$ the variance coincides with the mean square displacement and $\sigma(t) \sim t^{2H}$ simply reduces to $< x^2(t) > \sim t^{2H}$. The correlation function of the time series that results in normal a Brownian motion is zero because the kind of noise that generates normal Brownian motion

is a white noise with no correlations. If $0 < H < 0.5$, the noise results in a fractional Brownian motion resulting in a sub-diffusion trajectory with anti-persistent properties meaning a negative correlation, whereas for $0.5 < H < 1$ the resulting trajectory shown persistent behavior therefore leading to a positive correlation and a diffusion with super-diffusion properties and the diffusion simply becomes a ballistic diffusion for the special case of $H = 1$.

Since with the use of *the method of overlapping windows* described in the former section, we can generate different trajectories for an ensemble of Gibbs particles derived from the time series under study, we can obtain the final positions of these particles for a window size of t_w with the notation used above as $x_i(t_w)$, there i stands for the ith particle. so now we have a distribution of $N + 1 - t_w$ particles each of which is considered to start the motion at the initial position $x_0 = 0$. In this regard one could as well think of the motion and the trajectories of these particles described here as the projection of a 3-dimensional diffusion process on one of the dimensions, say that of ink in water, where ink is injected in the water with a syringe and the point of injection is taken as the point of origin for the diffusion process. Now if want to consider the population variance of these diffusing particle trajectories by definition

$$(5.3) \qquad \sigma^2 = \sum_{i=1}^{N} (x_i - \bar{x})^2 Pr(x_i)$$

for N particles with an average position of $\bar{x}$ where $P(x_i)$ stands for the probability of x_i^{th} trajectory to occur. Here we do not have to consider the probabilities since we have the exact knowledge of the distribution for a time window of size t_w, the variance will read

$$(5.4) \qquad \sigma^2(t_w) = \frac{1}{N + 1 - t_w} \sum_{i=1}^{N+1-t_w} (x_i(t_w) - \bar{x}(t_w))^2$$

where the ensemble average value for the final positions for a time window of length t_w is defined as

$$(5.5) \qquad \bar{x}(t_w) = \frac{x_1(t_w) + x_2(t_w) + x_3(t_w) + \ldots + x_{N+1-t_w}(t_w)}{N + 1 - t_w}$$

Let us note however that we are not really obliged to use overlapping windows method, we could as well have used a non-overlapping windows method as well, for which the number of trajectories available to define diffusing particles with different indices will decrease significantly. With a time series data of size N, the non overlapping window method yields $(\frac{N}{t_w})$ distinct windows as trajectories where we have $N + 1 - t_w$ trajectories available using the overlapping windows method, and obviously, for $N \ll t_w$, the number of trajectories is significantly larger in the case of overlapping windows method. Since the statistics in the case of non-overlapping windows approach leads to weaker statistics, we prefer the overlapping windows method.

For the case where $\sigma(t_w) \sim t_w^\delta$, we will have $\ln(\sigma(t_w)) \sim \delta \ln(t_w)$. So on a log-log scale of the above mentioned variance versus time window size plot, the slope will define the scaling coefficient if it exits (provided of course that the standard deviation of the sequence is finite for the distribution under question.).

Here we can consider a simple case where we draw the elements of the time series from a power law distribution $\psi(\tau)$ defined as

$$\text{(5.6)} \qquad \psi(\tau) = (\mu_0 - 1)\frac{T_0^{\mu_0 - 1}}{(T_0 + \tau)^{\mu_0}}$$

with $1 < \mu_0 < 3$. Remember that the second moment for the case is not finite for this case. So if the time time series $\xi_1(t_w), \xi_2(t_w), \xi_3(t_w), \ldots, \xi_{N+1-t_w}(t_w)$ are drawn from a distribution satisfying the above mentioned power law distribution as, $\tau_1, \tau_2, \tau_3, \ldots, \tau_{N+1-t_w}$, we see that the second moment of the trajectories based on this time series as the discrete velocities will yield a second moment which is not finite. But there might as well be cases, in fact many power law cases in nature satisfy the condition mentioned above with $\mu_0 < 3$ will yield a variance which basically is not finite. Hence for such a time series, even the distribution may be satisfying the scaling condition with some form of the scaling function F and a scaling coefficient δ, but the second moment will be tending to infinity as the window size $t_w \to \infty$. Obviously, variance analysis will not work for the detection of a scaling coefficient even if the scaling condition might have been satisfied for the case of a power law distribution with $\mu_0 < 3$, where the process

will be named Levy walk or Levy flight depending on the particular value of μ_0 and the walking rule applied. We will work this case in more detail based on the Diffusion Entropy Analysis Method we introduce in the next section.

5.3. Diffusion Entropy Analysis

DE technique of analysis was born with the papers of Refs. [73, 74]. The connection between the DE method and the concept of algorithmic complexity is discussed in Ref. [51]. This technique rests on converting the time series $\{\tau_i\}$ into a diffusion process.. In principle, having available a Gibbs ensemble of time series, we should consider

$$(5.7) \qquad\qquad x(l) = \sum_{i=1}^{l} \tau_i.$$

Each system of the Gibbs ensemble can be considered as being a random walker that at time l occupies the position $x(l)$. Due to the fact that in the cases of practical interest we have available only one time series, we make the ergodic assumption and we generate a set of many random walkers walking for a time t by the method of mobile window [73, 74]. We consider a window of size l and shifting it along the sequence of fluctuations we get for the $t - th$ random walker the position

$$(5.8) \qquad\qquad x(l, t) = \sum_{i=t}^{t+l} \tau_i.$$

Note that the slope of the straight line obtained with log-log plot of $S(l)$ versus l must be

$$(5.9) \qquad\qquad \delta = \frac{1}{2}.$$

In the Gaussian case of the probability distribution function F the time dependence of $S(l)$ is the same as that of $log(< x^2(l) - < x(l) >^2)^{\frac{1}{2}}$. Therefore, in principle, we might also apply the method of analysis based on variance [67]. However, in the recent literature there are indications [76, 77] that the DE analysis always detects the correct scaling, which might be different from the scaling determined by means of the variance method. Thus, we use the DE method, even if the use of the variance method might lead to essentially identical results in the particular case of the probability distribution function

63

for the diffusion process F is a Gaussian, yet this function need not be Gaussian, it could as well be a Levy Function where the second moment of the distribution is not finite for instance. Therefore, DEA has the obvious advantage of detecting the correct scaling even when Second Moment Analysis fails.

Obviously for Levy walk and Levy Flight where we may have a power law index of $1 < \mu_0 < 3$, the Variance Analysis Method proves to be incapable of providing the correct scaling coefficient δ if the condition for scaling is satisfied by the time series under study. However the Diffusion Entropy Analysis Method provides for us a means of detecting the correct scaling for the probability distribution function $p(x, t)$ of a diffusion process with fractal scaling derived from a time series data. Since we know that we can detect the scaling coefficient δ for diffusion process generated by Fractional Brownian Motion by Variance Analysis and also from Diffusion Entropy analysis, as they must be identical for the case under study. However, for other cases the Variance analysis and Diffusion Entropy Analysis need not lead to the same result, so the Hurst Exponent H and scaling coefficient δ might lead to different results and we will discuss the particular cases shortly after the introduction of the method itself.

Let us start with the basic condition of scaling and assume for beginners that this condition is to be satisfied by the probability distribution function of the diffusion process generated by the time series under study, the condition is

(5.10)
$$p(x, t) = \frac{1}{t^\delta} F\left(\frac{x}{t^\delta}\right)$$

where δ denotes the scaling coefficient and the function F is not necessarily a Gaussian function.

Let us make the connection with the time series which we may denote as $\xi_1, \xi_2, \xi_3, \ldots, \xi_N$, to denote that this time series could as well be derived from some kind of Brownian White Noise, or from a Fractional Brownian Noise. However, let us keep in mind that this series could be derived from a renewal process with a power law distribution or with an exponential distribution, in which case the time series $\tau_1, \tau_2, \tau_3, \ldots, \tau_N$ might as well denote the sojourn times between the critical rare events of a renewal process. In any case,

64

from a single realization of a time series we can infer a diffusion process based on the overlapping windows method expressed in section (5.1). Based on the time series we have defined the trajectories of the ensemble of individual particles which will then yield us to the distribution of the particles for a window size of t_w.

As soon as we have the final points of the individual trajectories of the particles for a fixed time window size of size t_w, we have to develop a numerical method to evaluate the probability distribution function and the numerical method calls for a division of the x-axis with a given equal size Δ_x which might as well depend on the time window size t_w itself. And the cell size Δ_x must be determined such that the final distribution $p(x, t_w)$ will be a well defined distribution, not to result in a poor statistics or a fractured structure. Once we set the size of cells $(\Delta_x(t_w))_i$, we will count the number of trajectories that end up in this i^{th} cell, where i denotes the particular cell position, and we may say this number is $P(x_i, t_w)$. Notice that the number of trajectories that end up at the same cell increases with the cell size, so what really matters is the number density of the particles ending up in a particular cell, which has the advantage that even when with the time window size t_w we may need to use a different cell size, the number density of the diffusing particles in these cells is optimally independent of the cell size. The number density for the ith cell $n_i(t_w, x)$ is given as

$$(5.11) \qquad\qquad n_i(t_w, x) = \frac{P(x_i, t_w)}{(\Delta_x(t_w))_i}$$

So since this distribution must be normalized and the total number of trajectories is $N - t_w + 1$, the distribution function will be obtained by dividing the number of trajectories that end up in a particular cell by the total number of trajectories for a window size of t_w,

$$(5.12) \qquad\qquad p(x_i, t_w) = \frac{n_i(t_w, x)}{N - t_w + 1}$$

When we do the partitioning of the x-axis and then label the cells in order the count the number of particles in the cell, by defining a cell size of $\Delta_i(x, t_w)$, we may shift

to counting the number of particles in each cell and by means of dividing by the total number of particles $N - t_w + 1$, this method will give us a fair distribution function when the length of the time series $N \rightarrow \infty$, since by then we will have a large number of particles that will be diffusing.Since we have a finite number of particles and for a time window t_w tending to ∞ we still have a finite number of particles to consider, average position $\bar{x}$ and the variance σ^2 of our diffusing particles will be a well defined number. To determine the bin size which is the cell size for a window size of t_w, we can use a fraction of the standard deviation of the positions of these diffusing particles. I found it more adequate to use the cell size as one tenth of standard deviation. Using these prescriptions one can define a well defined number density of the particles in these cells and hence a well defined probability distribution function $p(x, t_w)$, which from now on will define as $p(x, t)$ can well be defined. Once we have the time evolution of the probability distribution function we can discuss how one can determine if the time evolution of this probability distribution function obeys a scaling relation or not. Let us start with the assumption that this scaling relation is satisfied *per se*, in which case if we end up in an inconsistency by means of *reductio ad absurdum* the scaling condition is not satisfied. But if we can reach a condition which is only satisfied if this scaling relation is satisfied, by the use of the condition as the test of existence we can check if the scaling condition is satisfied by the probability distribution function or not. So for beginners let us assume

$$(5.13) \qquad p(x, t) = \frac{1}{t^\delta} F \left(\frac{x}{t^\delta} \right)$$

is satisfied, where, F is not necessarily a Gaussian function of x,and δ is the scaling constant.

At this point, having obtained the probability distribution $p(x, t_w)$ of the diffusing particles, we can obtain the Shannon Entropy of this distribution, by definition

$$(5.14) \qquad S_{sh}(t) = - \int_{-\infty}^{\infty} p(x, t) \ln(p(x, t)) dx$$

since the time is discrete

$$(5.15) \qquad S_{sh}(t_w) = - \sum_{i=1} p(x_i, t_w) \ln(p(x_i, t_w))$$

summation over the indices of all the partitioning cells.Let us assume that the scaling condition is already satisfied by the probability distribution function, and that for large times t the simplifying condition that the continuous assumption is valid. So, substituting for the probability distribution function the scaling condition directly

$$(5.16) \qquad S_{sh}(t) = - \int_{-\infty}^{\infty} dx \frac{1}{t^{\delta}} F\left(\frac{x}{t^{\delta}}\right) \ln\left(\frac{1}{t^{\delta}} F\left(\frac{x}{t^{\delta}}\right)\right)$$

by changing the integration variable to $u = x/t^{\delta}$ it reads

$$(5.17) \qquad S_{sh}(t) = \delta \ln(t) \left(\int_{-\infty}^{\infty} du F(u)\right) - \int_{\infty}^{\infty} du F(u) \ln(F(u))$$

Since normalization of $p(x, t)$ implies the normalization of the function F, Shannon entropy of the pdf under the condition that it satisfies the scaling condition reads

$$(5.18) \qquad S_{sh}(t) = \delta \ln(t) + A$$

- Lemma : Notice that if we use the definition of Equation.(2.4), provided that the distribution is normalized (which it should by definition, it would yield the same scaling constant δ if it exists, regardless of the particular value of $\mathcal{A}$.)

so if we plot the Shannon entropy versus time graph in semi-log scale where the time axis t is plotted in logarithmic scale, provided the pdf satisfies the scaling condition, we will have a well defined slope which is equivalent to the scaling coefficient δ.In a diffusion process with a finite number of particles it will take some time for the process to reveal its scaling properties depending on the particular form of the function F, so the transition region in the Diffusion Entropy Analysis till a well defined scaling coefficient appears as the slope may also tell us something about the diffusion process itself as well.

67

It is important to notice that in the short time region, namely, in the region of windows with small length l, the continuous-time approximation of Eq. (33) is invalidated. Thus, A is not the values of $S(l)$ for $l = 1$. It is rather the intercept of the tangent to $S(l)$ in the large l region with the ordinate axis. However, for simplicity, we shall refer to A as the value of $S(l)$ at $l = 1$, which is, in fact, the time origin in the logarithmic representation.

Note that the entropy $S(l)$ is positive definite. However, in practice, its actual value depends on the size of the cells that we adopt to transform the continuous PDF into a set of probabilities p_i, with $p_i \equiv p(x_i, l)\Delta$, with Δ being the cell size. To properly determine the scaling δ, which is an asymptotic property, it is convenient to use cells of large size, and this might have the effect of making the entropy negative in the short-time region. That is why I usually use $S(t) - S(1)$ in DE versus time plots, as is customary since the first papers on DE appeared, and the scaling properties of the system emerges in the long time-asymptotics.

5.4. DEA with different walking rules

In this Section we follow the authors of Ref. [90] who adopted the method of Diffusion Entropy (DE) [73, 74, 97] to analyze the data produced by the Hodgkin-Huxley (HH) neuron model. The DE method rests on converting a time series into a diffusion process $x(t)$, and in evaluating the entropy of the resulting Probability Density Function (PDF) $p(x, t)$. When the diffusion process act as continuous in time and space in the long time limit, if the scaling condition is satisfied the time dependent entropy of the resulting diffusion process would read

$$(5.19) \qquad S(t) = A + \delta \ln(t),$$

where

$$(5.20) \qquad A = - \int_{-\infty}^{\infty} dz \, F(z) \ln\left(F(z)\right).$$

According to Ref. [73] the efficiency of this method of analysis depends on the walking rule adopted to generate the diffusion process $x(t)$. In the following, the sequence of

inter-spike times is converted into a diffusion process with the Asymmetric Jump Model (AJM) rule [73]. According to the authors of Ref. [73], the AJM walking rule is the most accurate one, and it leads to a fast convergence to the scaling condition. We have also noticed that AJM is a better indicator of real time effects of the perturbation than LJM (Long Jumps Model)

With AJM rule each inter-spike time τ is represented by a sequence of zeros, and then by a jump of constant length, say 1, in a fixed (positive) direction. The coordinate of the random walker $x(t)$ is then defined as the sum of jumps occurred until time t. Let us consider the case of a sequence of inter-spike times whose probability density satisfies the asymptotic behavior: $\psi(\tau) \sim 1/\tau^{\mu_0}$, namely, the asymptotic behavior of the prescription of Eq. (8.2). In this case, the relation between the (unperturbed) scaling δ_0 of the AJM rule and the power index μ_0 is given by [73]:

$$(5.21) \qquad \delta_0 = \begin{cases} \frac{1}{\mu_0 - 1}; & 2 < \mu_0 < 3 \\ \\ 0.5; & \mu_0 \geq 3 \end{cases}$$

Considering the unperturbed system, the transition from $\mu_0 < 3$ to $\mu_0 > 3$ corresponds to a transition where the scaling δ_0 is anomalous ($\delta_0 > 0.5$) to the scaling $\delta_0 = 0.5$ of ordinary diffusion. The Poisson condition corresponds to $\mu_0 = \infty$. However, for the Poisson scaling $\delta_0 = 0.5$ to show up it is enough to cross the border $\mu_0 = 3$. For simplicity, we define $\mu_0 < 3$ as the non-Poisson basin and $\mu_0 > 3$ as the Poisson basin. Thus, the adoption of the DE analysis allows us to establish whether the system is located in the Poisson or non-Poisson basin through the measurement of δ_0. Eq. (5.21) applies also in the perturbed case.

CHAPTER 6

STOCHASTIC RESONANCE

6.1. Stochastic Resonance Concept and Phenomena in Nature

Stochastic resonance was introduced for the first time in 1981 [52] to explain the periodic recurrence of ice ages which repeat with a periodicity of 10^5 years [53], upon the occurrence of which the global temperature has fallen by about $\Delta T = 10C$. Researchers first attempted to explain this phenomena by the weak periodic external signal due to the slow modulation of the Earths eccentricity that also has a period of 10^5 years. This change in the eccentricity appears to be modulating the total amount of Solar influx by only 0.1%, so how was it going to account for the considerable change in the global temperature change? But a climate model theory where a cooperative effect between the weak periodic signal and the intrinsic stochastic dynamics of the Solar energy influx also due to the changes in the Earth atmospheres turbulent dynamics makes the explanation plausible. Indeed a double well potential model which will be discussed below explains this effect resulting in the expected values of the parameters matching the data. This was the first physical phenomenon that the Stochastic Resonance found its first application indeed also it's name.

Since then the same principle has been applied in a wide variety of systems. Nowadays stochastic resonance is commonly invoked when noise and nonlinearity concur to determine an increase of order in the system response. SR-based techniques has been used to create a novel class of medical devices (such as vibrating insoles) for enhancing sensory and motor function in the elderly, patients with diabetic neuropathy, and patients with stroke. The idea found its application in medicine immediately but rather on a discovery basis first, for improving the mechanoreceptor functions of the sensory neurons by means of external noise in the form of a noisy electrical current [55]. The input signal must be stochastic (noisy) by nature, because otherwise it will give the nervous system an

opportunity to adapt just like it adapts to constant smell, noise, or the itching of new clothes etc [54], after a while a perfectly periodic signal will be ignored, so the signal to be transmitted must be intermixed with a stochastic component so that the neurons can not adapt [54]. note that,in the chapters on the perturbation of Poisson (Chapter 7) or non-Poisson systems (Chapter 8) rate by a periodic signal where we model the neurons with renewal systems, the stochastic character is already intrinsically involved in the system dynamics.

6.2. Basic Models: Double-Well Potential as a Model for SR

Let us consider a particle in the classical double well potential illustrated in Fig.(6.2). Let us assume the particle is under the effect of the forces due to the potential itself, $-\frac{dV(x)}{dx}$, a friction force $-\gamma v$, and a stochastic force, which I will denote by $\xi(t)$, which stands for the noise. The Langevin equation of motion for this system would be [56]

$$(6.1) \qquad m\frac{d^2x}{dt^2} = -\gamma\frac{dx}{dt} - \frac{V(x)}{dx} + \xi(t)$$

when we consider the case of strong friction $\gamma \ll 1$, Shmoluckovsky approximation implies, (if we also re-scale time as $t' = \gamma t$)

$$(6.2) \qquad \frac{dx}{dt'} = -\frac{dV(x)}{dx} + \xi(t'/\gamma)$$

note that rescaling the white noise time parameter is nothing but a white noise meaning

$$(6.3) \qquad < \xi(t) >= 0$$

$$(6.4) \qquad < \xi(t)\xi(t') = D\delta(t - t') >$$

where we obtain the noise due to the coupling of the system to a heat bath of temperature T in which case the noise intensity D is given as

$$(6.5) \qquad D = k_B T$$

71

in other words the bath temperature T determines the noise amplitude and by intuition also the transition rate of the particle between the wells too because if there were no noise, there would be no transition at all. Any transition is based on the kick of the white noise in this model since otherwise dissipative forces would win very fast for the particle to end up at the bottom of one of the wells.

What we are interested in this problem is only the transition between the wells due to the effect of this white noise, and not the intra-well motion of the particles.

Quoting Kramer's formula for the rate of the transition between the wells

(6.6)
$$r_0 = \frac{\sqrt{\frac{d^2 V(0)}{dx^2} \frac{d^2 V(c)}{dx^2}}}{2\pi} \exp -\frac{Q}{D}$$

where an average residence time or rather an average waiting time can be defined as

(6.7)
$$< \tau >= \frac{1}{r_0}$$

and now we can ask what if the potential is perturbed in such a way that when the potential is slightly lower than it's unperturbed value on one well it will be slightly higher than it's usual unperturbed value in the other well, and this asymmetric perturbation will be sinusoidally time dependent. One can intuitively say that if the period of the perturbation is such that when a particle completes its residence time in one of the wells, the potential barrier to be overcome in this well becomes lower so as to make the transition to the other well relatively easier, and when the transition is completed the same happens with the next well, there we may expect some kind of resonance between the perturbing signal and the resulting stochastic process. Namely if the period of perturbation is twice as large as the expected waiting time of the particle in one well, we may then talk about a resonance. Indeed such resonance exists where the signal becomes more consistent with the resulting stochastic series, and it is named "Stochastic Resonance" or SR.

6.3. Subthreshold Signal under the Effect of Noise as SR Model

One of the most essential models of stochastic resonance is a weak subthreshold signal being summed up with a noise, for the case of simplicity we can consider this
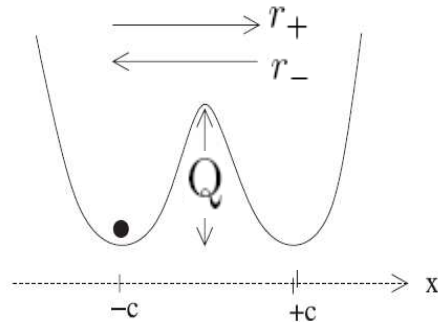
Figure 6.1.   Stochastic resonance modeled as particle in a bi-stable double well potential, transitions driven by an external stochastic noise and a weak sinusoidal oscillation of the potential.
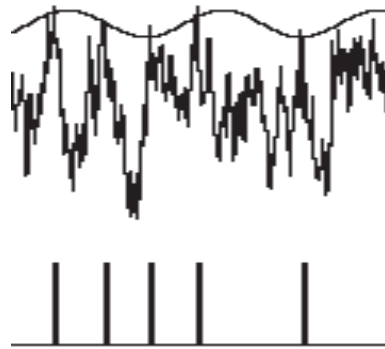
Figure 6.2.   Stochastic resonance modeled as a weak subthreshold signal plus a noise.

to be a white noise in this particular model, and when the total sum exceeds a definite predetermined threshold, an event will be recorded, for an illustration of the model see Fig.(6.3). So in this model it is obvious that if there is no noise at all there will be no events recorded. If on the other extreme the noise amplitude is very large this time there will be many events and the signal again will be lost. Intuitively one can see that for an intermediate range of noise values the signal might find a way for itself to be transmitted through the threshold, the crossings of the threshold by the weak signal will be enhanced by the noise present. Actually, noise in this model is obviously helping the signal to cross the barrier.

From Fig.(6.3) and the brute force method of obtaining the waiting times for Poisson renewal systems under the perturbation of rate discussed in Section(3.9) one can easily notice the connection between the two models. Actually the perturbation of rate acts like

73

a weak perturbation and there is already the same white noise in the process. The events are threshold crossings in both cases. It is more like the threshold is being modulated itself in the perturbation of Poisson processes whereas in SR the weak signal is being modulated, but one can be embedded in the other one. So the model similarity is almost at a degree of identity for the two phenomena modeled in this manner.

6.4. Signal to Noise Ratio as a function of rate

We are now interested in a more general form of information transmission through a random environment. For this we have to review some aspects of ordinary stochastic resonance. Here in this concise review, I aim to illustrate the basic aspects of the phenomena illustrated in Ref.[71].

Let us consider the ordinary master equation for a bi-stable system:

$$(6.8) \qquad \frac{dp_1}{dt} = -\frac{r_+}{2}p_1 + \frac{r_-}{2}p_2$$

where p_1 and p_2 are the probabilities of finding the particle in the first well or the second one respectively. The transmission rate from the first well to the second one is denoted with r_+ and the reverse as r_-.

$$(6.9) \qquad \frac{dp_2}{dt} = -\frac{r_-}{2}p_2 + \frac{r_+}{2}p_1$$

Now let us imagine that the transition rates are perturbed simple harmonically

$$(6.10) \qquad r_\pm(t) = r_0(1 \pm \epsilon \cos(\omega t))$$

Let us set

$$(6.11) \qquad \Pi = p_1 - p_2$$

where we have considered a two state system with the variable $\xi_{1,2} = \pm 1$, and hence to transmit a signal

$$(6.12) \qquad \Pi = <\xi> = p_1\xi_1 + p_2\xi_2 = p_1 - p_2$$

74

so Π is in a way the mean value of the signal. The signal we are trying to transmit through this stochastic system obviously is $S = \cos(\omega t)$. If $<\xi(t)>$ oscillates as S, we can transmit the signal. Making use of $\Pi = p_1 - p_2$ and $p_1 + p_2 = 1$, we can substitute for $p_1 = \frac{1+\Pi}{2}$ and $p_2 = \frac{1-\Pi}{2}$ to get

$$(6.13) \qquad\qquad \frac{d\Pi}{dt} = r_0 \Pi - \epsilon r_0 \cos(\omega t)$$

$$(6.14) \qquad\qquad \Pi = -\epsilon r_0 \int_0^t e^{-r_0(t-t')} \cos(\omega t') dt'$$

it is in the form of

$$(6.15) \qquad\qquad \Pi(t) = <\xi(t)> = \kappa \int_0^t \Phi_\xi(t-t') E(t') dt'$$

is the Green-Kubo theory concludes where

$$(6.16) \qquad\qquad \Phi_\xi(t-t') = r_0 e^{-r_0(t-t')}$$

$$(6.17) \qquad\qquad E(t) = \cos(\omega t)$$

and $\kappa = \epsilon$, so in conclusion, the traditional linear response theory holds true. Taking the integral it reads

$$(6.18) \qquad\qquad \Pi(t) = -\frac{\epsilon}{2} r_0 e^{-r_0 t} \left[\frac{e^{(r_0+i\omega)t}}{r_0 + i\omega} + \frac{e^{(r_0-i\omega)t}}{r_0 - i\omega} \right]$$

as $t \to \infty$ becomes

$$(6.19) \qquad\qquad \Pi(t) = \epsilon \frac{r_0^2 \cos(\omega t) + \omega r_0^2 \sin(\omega t)}{r_0^2 + \omega^2} = -\Sigma \cos(\omega t - \phi)$$

where $\phi = \arctan(\frac{\omega}{r_0})$ and $\cos(\phi) = \frac{r_0}{\sqrt{r_0^2 + \omega^2}}$, thus we have

$$(6.20) \qquad\qquad \Sigma = \frac{\epsilon r_0^2}{r_0^2 + \omega^2} \frac{1}{\cos(\phi)}$$

75

$$(6.21) \qquad\qquad \Sigma = \frac{\epsilon r_0}{\sqrt{r_0^2 + \omega^2}}$$

The Signal to Noise ratio is

$$(6.22) \qquad\qquad \frac{S}{D} = \frac{\Sigma}{D} = \frac{\epsilon r_0}{\sqrt{r_0^2 + \omega^2}} \frac{1}{D}$$

In the ordinary case of stochastic resonance, Arrhenious property reads.

$$(6.23) \qquad\qquad r_0 = A e^{-\frac{Q}{D}}$$

assuming for simplicity that A=1,Q=1,

$$(6.24) \qquad\qquad D = \frac{1}{In(\frac{1}{r_0})}$$

$$(6.25) \qquad\qquad \frac{S}{D} = \frac{\epsilon r_0}{\sqrt{r_0^2 + \omega^2}} In(\frac{1}{r_0})$$

If we plot the Signal to Noise ratio $\frac{S}{D}$ as a function of the rate r_0 we see that depending on the period of the perturbation T, there is a definite value of r_0 that the Signal to Noise ratio will yield a maximum value, which we refer to as resonance synchronization that maximizes the Signal transmission.

Gammaitoni et. al. [71] has calculated the expected power spectral density for the series of events obtained for the case of stochastic resonance and they found out that a peak corresponding to a time of half of the period perturbation displays a major maximum as shown in Figure(6.4). This frequency ν_0 corresponds to a value of time that corresponds to the expected waiting time in the double well. The next peak comes at $3\nu_0$ and then at $5\nu_0$. So we can see a series of peaks for the fundamental harmonics and the higher harmonics decreasing in amplitude very fast, but they are there. The details of the power spectrum depends on the characteristics of the noise used, for simplicity
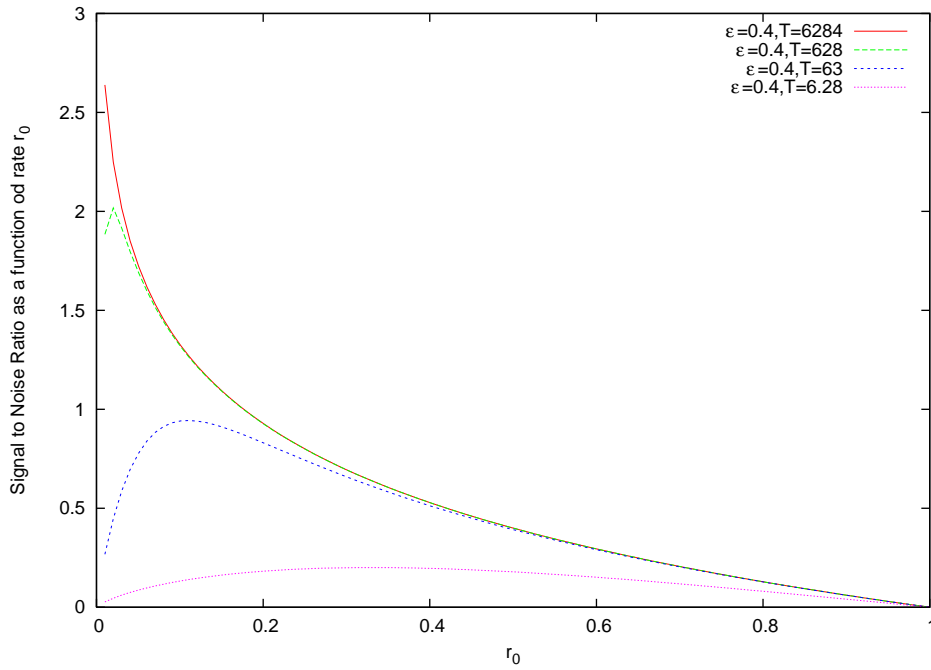
Figure 6.3. The Signal to Noise ratio as a function of the rate r_0 for $\epsilon=0.4$ and various values of ω.
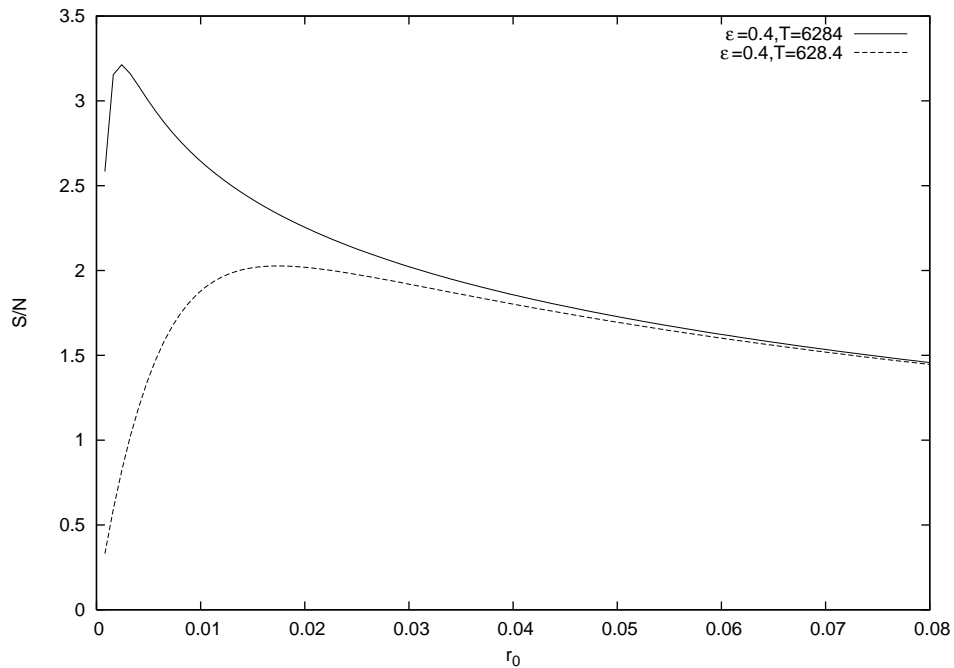
Figure 6.4. The Signal to Noise ratio as a function of the rate r_0 for $\epsilon=0.4$, $T = 6284$ & $T = 628.4$.

we have used here a white noise, but one could as well use brown noise or pink noise or for that matter any colored noise and the particular details of the power spectrum might as well be modified by the details of the noise utilized in SR. What is important to
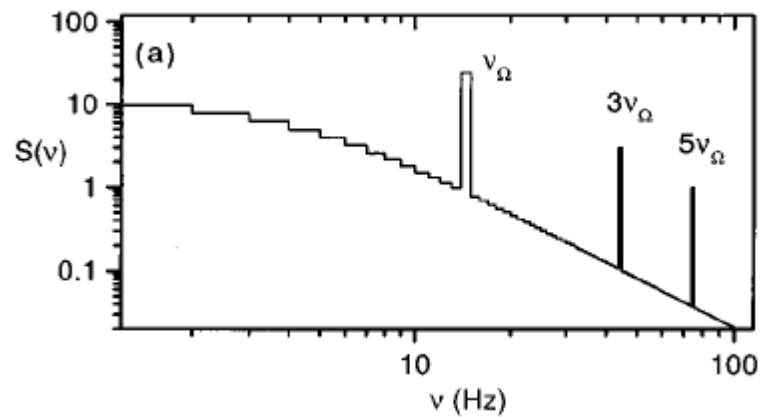
Figure 6.5. Typical power spectrum calculated for an SR model displays peaks at certain frequencies.

notice is that SR power spectrum displays peaks at definite values of the frequency axis. This observation indeed also comes along when we check the FFT power spectrum for the perturbation of Poisson as well as the non-Poisson renewal processes as pictured in Chapter.7 and Chapter.8.

For the models of Poisson or non-Poisson renewal processes we can not change the value of the noise. This is especially obvious for the Brute force model of the Poisson perturbation model. Instead the parameters that can be modified are the signal amplitude and the period of perturbation. This makes sense because what really mattes is the relative ratio of the signal amplitude to that of the noise amplitude. The interplay between these two variables and the frequency of the perturbation completes our analogy with the SR model. So here we can take a look at the results and implications of SR model in neuroscience.

6.5. SR in Neuroscience

There is no general systematic known way for finding the waiting time distributions for threshold crossings for all cases of a double potential (where the system is asymmetric, the potential minima are different etc) [71]. However, Papoulis [58] had calculated the distribution for symmetric bistable distribution of the form

$$(6.26) \qquad \psi(\tau) = \frac{1}{\tau_c} e^{-\frac{\tau}{\tau_c}}$$

78

basically a Poisson distribution.

One thing we don't really know for sure. Do neurons obey Poisson statistics or do they obey non-Poisson statistics. As mentioned in Chapter 8 there is support for both claims. So then let us take a look at the early experiments.
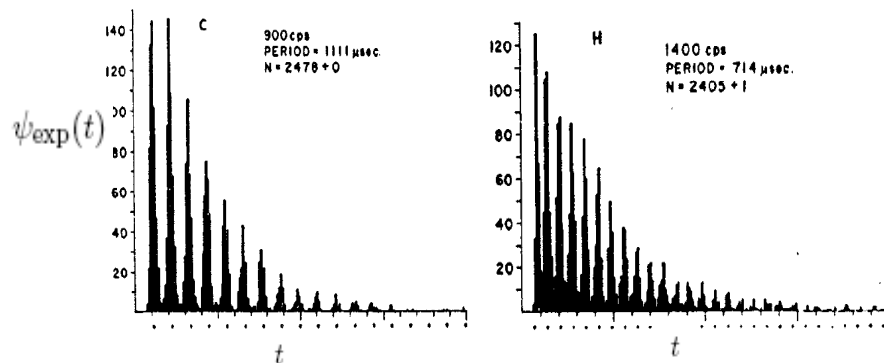
Figure 6.6.   Waiting time distributions obtained under the effect of stimulant perturbation from neurons of makaque monkeys.

The predictions of this model can be compared to already carried out experiments on makaque monkeys sensory neurons under the effect of periodic perturbation of the amplitude of the stimulant. Figure 6.5 displays these results. The decay of the sojourn time distribution peak is essential an exponential function for both cases. One can compare these results to that of [104],who performed a more a more recent experiment. The results all display an exponential decay of maxima and a bunching of the waiting times following the period of perturbation.

The general predictions od SR are consistent with data under the perturbation of the stimulant. But as we will show they are also consistent with the predictions of Perturbed renewal processes as we we have already shown the similarity with the Poisson perturbed cases, we will also prove in Chapter 8 that non-Poisson systems may also provide similar experimental results under the effect of perturbation..

CHAPTER 7

PERTURBATION OF POISSON PROCESSES

7.1. Introduction

In this Chapter I discuss the connection of Stochastic Resonance phenomena [66] mentioned earlier in Chapter 6 with Poisson processes under periodic perturbation [80]. I also refer to former results obtained at UNT CNS concerning seasonality and detrending algorithms [62, 63] where the case of underlying seasonality is summed with external noise which is not correlated to the seasonality itself. In this Chapter, I show how a Poisson process under perturbation can act as a model where the fluctuations are correlated to noise itself.

In the literature of complexity there are many cases where the statistical features of the time series under study are characterized by evident periodicity. One of the most important cases is given by meteorological phenomena such as the temporal distribution of rain fall events [59]. Such phenomena are indeed characterized by several processes, each mainly affected by a given time scale of periodicity, such as the diurnal cycle or the seasonality. An even more impressive case of climatological interest, is given by the global surface warming [60]. In this particular case, the periodic component based on the solar cycle, whereas the systematic temperature increase might be human made. In this, and other cases of the same kind, a question of great interest is related to whether the statistics of fluctuations are related to the regular trend, either periodic or systematic. A better understanding of this question should help the search of a proper model for this important environmental issue.

There are other meteorologic issues, where the phenomenon of interest is the periodic signal itself, as in the case of chirps produced by sprites [61]. Another interesting case is given by seasonal effects on sociological processes [62, 63]. Based on the results of these earlier works we know that the superposition of a seasonal component and uncorrelated

noise can be detected by means of de-trending methods. In a given data the effect of hidden seasonal effects can be detected by means of diffusion entropy analysis regardless of the noise amplitude being small or large in compared to the signal, Direct Assessment of DEA on the data reveals the effect of periodic component as shown in the Fig(7.1) and Fig(7.1). The scaling is determined in a longer time span for relatively low noise, but nevertheless it is correctly determined, and for even much stronger noise case the seasonal effect is also determined by the DEA method on the artificial data as well as the correct scaling.
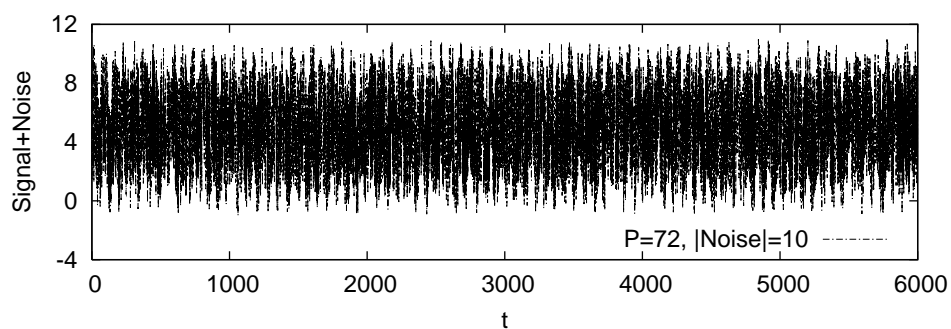
Figure 7.1.   Seasonal component in the form of a sinusoidal function of period $P = 72$ superposed with a white noise of amplitude 10 times larger than the signal itself.

The data of babies born to teen age mothers in the state of Texas, show a slow modulation, due to seasonal effects, and a systematic increase, probably due to immigration. In other cases, the periodicity might be characterized by fluctuating frequencies, these fluctuations being the complex phenomenon to understand [64]. The work of Yang *et al.* [90] discusses the fluctuation versus periodicity issue with the Hodgkin-Huxley neuron model, thereby suggesting a possible connection with the stochastic resonance of neurons studied years ago by Longtin, Bulsara and Moss [66].

When the time series to analyze are characterized by periodicity, it is only natural to make the assumption that the signal consists of a mere superposition of fluctuations and a sinusoidal trend [67, 68] and de-trending techniques of ever increasing efficiency have been proposed in the last few years [69, 70]. However, the possibility that a correlation exists between the periodic trend and the fluctuations cannot be ruled out. By correlation
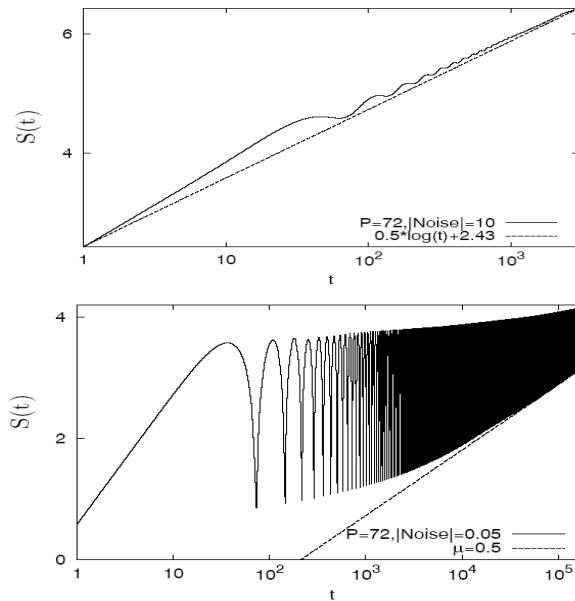
Figure 7.2. Direct assessment of DEA on the seasonal effect plus uncorrelated white noise. (top) The noise amplitude is 10 times larger.(bottom) The noise amplitude is 0.05 times that of the noise. For both cases DEA detects the correct scaling of $\delta = 0.5$, as well as the effect stemming from the existence of seasonality.

between trend and fluctuations what is meant is the possibility that the response of a physical system to an external forcing is not only given by a regular trend, but it involves also the statistics of the fluctuations about the average. The discussions in this chapter focuses on the case where an external perturbation, assumed to be periodic, not only creates a trend, but also establishes a correlation between fluctuation about the trend and periodicity. Our aim is to establish a detection technique that might reveal this correlation if it exists, and to realize this goal we work on artificial sequences that are theoretically proved to be characterized by a strong fluctuation-periodicity correlation. These artificial sequences are generated by a dynamic model, which is closely related to the subject of stochastic resonance [71]. The main conclusion of this research is that after removing the trend from the time series, it is convenient to analyze the modulus of the de-trended fluctuations rather than their real values, which can be either positive or negative. The statistical analysis of the real values might give the misleading impression that no fluctuation-periodicity correlation exists.

The outline of this paper is as follows. In Section 7.2 we illustrate the method that we adopt to create fluctuation-periodicity correlation. We devote a special attention to establishing the condition ensuring a strong correlation between fluctuation and periodicity. In Section 7.3 we discuss how to reproduce the periodic clusters of the real data [60, 62, 63], and in a special condition we solve this problem with an analytical treatment. In Section 7.6 and 7.7, using the artificial sequences, created with the algorithm of Section 7.2, we establish a procedure to make two methods of statistical analysis, the Diffusion Entropy (DE) [73, 74] and Correlation Function (CF), sensitive to the fluctuation-periodicity correlation. In Section 7.8 we draw some final conclusions.

7.2. A Model Generating Correlation between Periodicity and Fluctuation

This section is devoted to illustrating the method I use to produce fluctuation-periodicity correlation. This method is inspired by the well known dynamical system of a particle in a double-well potential, driven by white noise and an external periodic forcing, which is nothing but the paradigmatic model of stochastic resonance [71]. However, the approach I follow here does not directly use the double-well potential to generate the sojourn time probability distribution, and can be easily extended to the case when the unperturbed system is not of Poisson nature [72], a case which I discuss in the next Chapter. For simplicity's sake, in this Chapter I limit the discussion to the case of the unperturbed system being an ordinary Poisson process. I use this method to create a time series that is qualitatively similar to those examined in Refs.[62, 63, 73]. The authors of those papers studied time series, whose data points represent the number of babies born to teen-age mothers in the State of Texas. Thus the values of time series are positive integer numbers, and the intensity of these numbers, although erratic, exhibit a clear periodic trend that, to a first approximation, can be assumed to be of a sinusoidal form[73]. These papers do not address the issue of a possible intrinsic correlation between fluctuation and an inherent periodic trend, and are based on the implicit assumption of a mere superposition of a periodic trend and a complex signal. The model I propose in this

section makes it possible to establish fluctuation-trend correlation, and consequently, to discuss to what extent complexity might emerge from this correlation.

7.3. Perturbation-Induced Memory

The system under consideration is of renewal nature since the initial condition ξ of Eq.(4.64) is totally independent of the earlier initial conditions, so that the sojourn time τ is independent of the earlier sojourn times as well. Consequently, the time series $\{\tau_i\}$ and $\{t_i\}$ are memoryless, and the order of the times τ_i adopted to produce the time series $\{t_i\}$ is not important. This model spells a totaly memoryless stochastic system.

We now show that an external perturbation turns the sequence $\{\tau_i\}$ into a sequence with memory. This means that, as we shall see, the sequence of times τ_i, plotted according to the order they are produced, reflects and preserves in its inherent nature the time dependence of the external perturbation even when the effect of the perturbation is not obvious. Let us assume that, as a consequence of an external perturbation, the transition rate q, becomes time dependent with the form

$$(7.1) \qquad\qquad q(t) = q_0(1 + \epsilon \cos(\omega t)).$$

Note that this expression coincides with the Taylor expansion, for $\epsilon \rightarrow 0$, of the rate of escape of a particle over a time dependent barrier, under the influence of a white noise [79]:

$$(7.2) \qquad\qquad q(t) = Q_0 \; e^{-k(1+\eta \cos \omega t)} = q_0 e^{-\epsilon \cos \omega t}$$

where $q_0 = Q_0 e^{-k}$ and $\epsilon = k\eta$. We use this expression to derive the results of Fig. (7.5), which, in turn, will serve the purpose of proving the equivalence of this model with the stochastic resonance model of Refs. [66] and [79].

I proceed as in the earlier subsection: replace Eq. (4.60) with (where for the Poisson case we set the power to $z = 1$)

$$(7.3) \qquad\qquad \dot{y} = q(t)y$$

and subsequently Eq. (4.64) with

(7.4)
$$\xi = e^{-\left(\int_{t'}^{t'+\tau} q(t'')\,dt''\right)}.$$

With the uniform back injection assumption, we get

(7.5)
$$\psi(\tau|t') = \left|\frac{d\xi}{d\tau}\right| = q(t'+\tau)\,e^{-\left(\int_{t'}^{t'+\tau} q(t'')\,dt''\right)}.$$

and, as a consequence,

(7.6)
$$\psi(\tau|t') = q_0\,e^{-q_0\tau}\left(1 + \epsilon\cos(\omega(t'+\tau))\right)e^{-\left(\frac{q_0\epsilon}{\omega}\right)\left(\sin(\omega(t'+\tau)) - \sin(\omega t')\right)}.$$

The function $\psi(\tau|t')$ is the conditional probability that the system sojourns within the interval I for a time τ, given the fact that the earlier period of sojourn ends exactly at time $t = t'$. We see that the probability for the system to sojourn in the interval I for a time τ is not independent of the earlier times. In fact, this probability depends on t', which signals the end of an earlier sojourn time, depending, in turn, on the cumulative of the earlier sojourn times.

It is convenient at this point to define the key parameter

(7.7)
$$R = \frac{q_0}{\omega}.$$

Note that $T_\omega = 2\pi/\omega$ is the time period of the harmonic perturbation. In Eq. (7.1) and that $T_0 = 1/q_0$ is the mean sojourn time in the absence of perturbation. Thus, we express the parameter R in the following form

(7.8)
$$R = \frac{1}{2\pi}\frac{T_\omega}{T_0}.$$

Consequently the parameter R allows one to estimate the measure of the number of sojourn times in one period of the perturbation, if $2 > 1$, and, conversely, the number of time periods in the mean sojourn time T_0, if $2\pi R < 1$.

Consider the limiting case of:

(7.9) $$R >> 1$$

the time period T_ω of the perturbation is very large with respect to the mean sojourn time T_0 and the change of $q(t')$ is negligible on the time scale T_0 itself (slow perturbation). In this case we derive an analytical expression for the moments of the conditional distribution density $\psi(\tau|t')$:

(7.10) $$< \tau^n(t') >= \int_0^\infty d\tau \; \tau^n \; \psi(\tau|t')$$

The maximum contribution to this integral comes approximately from the interval between $\tau = 0$ and $\tau = \frac{1}{q_0}$. In this interval, given the limiting condition (7.9), the inequality $\omega\tau << 1$ applies. As a consequence, we are allowed to expand the sines and the cosines with respect to $\omega\tau$, henceforth creating an expression via first-order contraction of the form $\psi(\tau|t')$, which can be used explicitly to compute the moments $< \tau^n(t') >$. It is straightforward to obtain the following results

(7.11) $$< \tau(t') >= \frac{1}{q(t')} - \frac{2\epsilon\omega q_0 \sin(\omega t')}{q^3(t')},$$

(7.12) $$< \tau^2(t') >= \frac{2}{q^2(t')} - \frac{6\epsilon\omega q_0 \sin(\omega t')}{q^4(t')}$$

and

(7.13) $$\sigma^2(t') \equiv < \tau^2(t') > - < \tau(t') >^2 = \frac{1}{q^2(t')} - \frac{2\epsilon\omega q_0 \sin(\omega t')}{q(t')^4} - \frac{4\epsilon^2 q_0^2 \sin^2(\omega t')}{q(t')^6}.$$

notice that for $R \to \infty$,

(7.14) $$< \tau(t') >= \frac{1}{q(t')}$$

and

(7.15) $$\sigma^2(t') = \frac{1}{q^2(t')}.$$

Therefore, the distribution of sojourn times at time t' is an exponential distribution with the local rate $q(t')$. This is a case where the mean value $< \tau(t') >$ and the fluctuation

intensity $\sigma(t')$ are strongly correlated. Notice here that the dynamic model we use forces us to interpret the values τ_i as times. However, in this Chapter this model is essentially used as a method to generate correlation between fluctuation and periodicity, so as to address the interesting issue of how to reveal this correlation with some techniques of statistical analysis. For this reason, in Section 7.5 and Section 7.6 I analyze the time series $\{\tau_i\}$ with the ordinary correlation function method and DEA, where this time series is used as a paradigmatic case of correlation between fluctuations and seasonality, where fluctuations not necessarily have the meaning of times. The interesting question of how to use a dynamic model of the same kind with the values τ_i getting a sociological or environmental meaning is beyond the purpose of my discussion at this point.

7.4. Histogram and Chronological Order of Sojourn Times

This section is devoted to comparing the conventional Sojourn Time Histogram (STH), to the Time Series $\{\tau_i\}$ in Chronological Order (TSCO). The (STH) is the histogram based on dividing the τ-axis into bins of size $d\tau = 1$,and in counting how many sojourn times τ_i are located in a given bin between τ and $\tau + d\tau$. We use the STH to define the waiting time distribution density $\psi_{exp}(t)$, where the subscript exp denotes that this waiting time distribution is obtained from a numerical experiment. The TSCO reveals the clustering effects produced by the time dependent perturbation. These clustering effect becomes larger with the increase of R. In fact, in this case, the clustering effect is due to the time lengths being proportional to $1/q(t')$.

The STH can also produce clustering effects, in conditions that require a numerical treatment. The clustering effect becomes ostensible when we depart from the use of Eq.(7.1) where $R >> 1$. First of all let me discuss how to theoretically derive $\psi_{exp}(t)$ under the condition $R >> 1$. I denote by $\psi_s(t)$ the analytical expression for $\psi_{exp}(t)$.

(7.16) $$\psi_s(t) = \int \Pi(q) q e^{-qt} dq,$$

Here $\Pi(q)$ is the distribution of the transition rates, given by:

$$(7.17) \qquad \Pi(q) \propto |\frac{1}{\dot{q}}|$$

By using Eq. (7.1) and the normalization condition, one can easily obtain:

$$(7.18) \qquad \Pi(q) = \frac{1}{\pi \sqrt{(\epsilon q_0)^2 - (q - q_0)^2}}$$

Note that $\Pi(q)$ is defined between $q_{min} = q_0(1 - \epsilon)$ and $q_{max} = q_0(1 + \epsilon)$. The effective distribution of sojourn times is obtained by substituting this expression into Eq. (7.16), thereby yielding:

$$(7.19) \qquad \psi_s(t) = q_0 e^{-q_0 t}(I_0(q_0 \epsilon t) - \epsilon I_1(q_0 \epsilon t)),$$

where $I_0(t)$ and $I_1(t)$ denote the modified Bessel functions of order zero and one, respectively. Note that for Eq.(7.19) to hold true, the condition $R >> 1$ is not enough. It is necessary to assign suitably small values to ϵ as well. In fact, the expression given in Eq. (7.16) is reasonable only if the perturbation is slow, *i.e.*, it does not change on the scale of the mean sojourn time T_0. The time scale of change of the transition rate can be estimated by means of the following quantity:

$$(7.20) \qquad \frac{|\dot{q}(t)|}{q(t)} = \frac{\epsilon \omega |sin(\omega t)|}{1 + \epsilon cos(\omega t)}$$

In order to satisfy the slow perturbation approximation, this quantity must be always very much smaller than q_0. On the other hand, with $\epsilon = 1$, this quantity diverges periodically, thereby breaking the assumption of slow perturbation.

In the set of Figs.(7.4), the STH is displayed in some different conditions. In all cases the unperturbed exponential waiting time distribution is reported for comparison. We note first of all that these figures illustrate the change of $\psi_{exp}(t)$ with increasing R, while keeping fixed the perturbation intensity ($\epsilon = 0.4$). From panels (a) and (b) it is evident that in the range of small R an oscillating pattern emerges as R decreases. The panels (c) and (d) show that, although no sign of this pattern is left at large values of R, as R increases, the decay of $\psi_{exp}(t)$ becomes slower than the decay $\psi(t)$, the unperturbed STH, and $\psi_{exp}(t)$ tends to coincide with the slow-perturbation theoretical prediction of
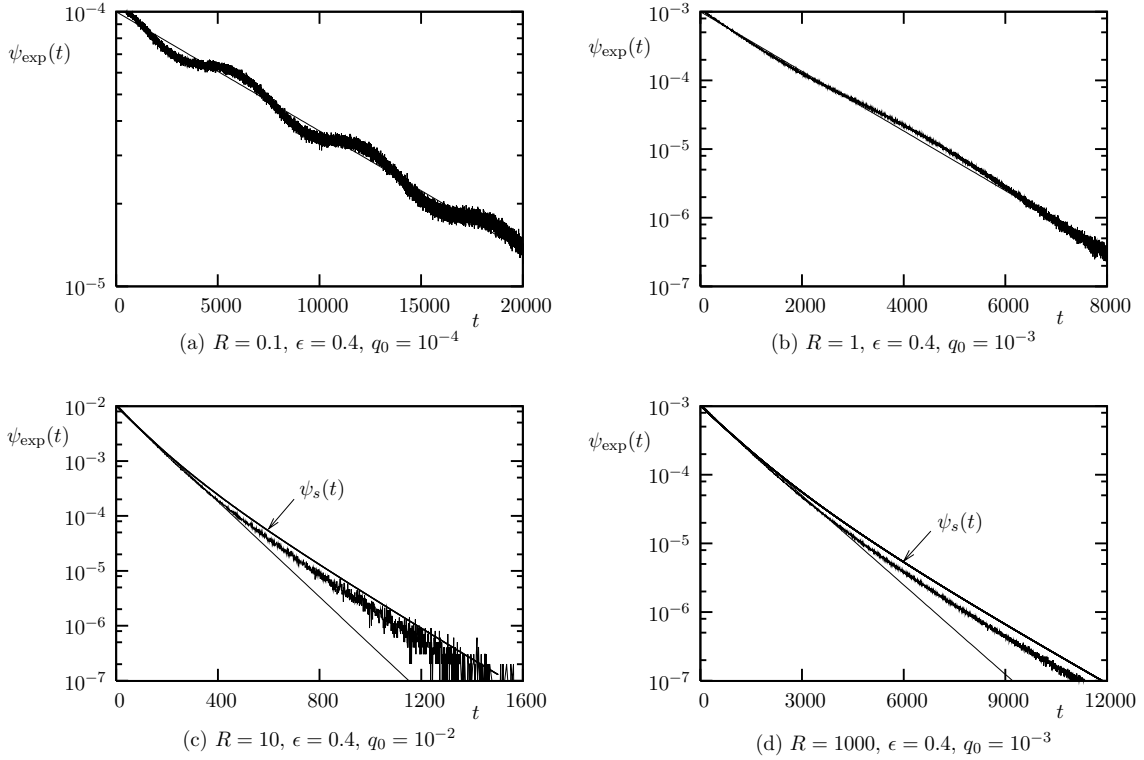
Figure 7.3. $\psi_{exp}(t)$ for different values of R with $\epsilon = 0.4$. (a) R=0.1 (b) R=1 (c) R=10 (d) R=1000. The continuous straight line is the unperturbed exponential waiting time distribution. The arrow of (c) and (d) indicate the theoretical prediction of Eq.(7.19).

Eq.(7.19). According to the estimates of numerical simulation the agreement between $\psi_{\exp}(t)$ and $\psi_s(t)$, improves as ϵ decreases and/or as R increases.

To establish a rigorous connection with the subject of stochastic resonance [66],[79], I discuss the results illustrated in Fig.(7.4) and Fig.(7.5).

Fig.(7.4) illustrates $\psi_{exp}(t)$ with a very small R. This means a condition where the oscillations around the unperturbed exponential waiting time distribution are even more pronounced than in Fig.(7.4) a . In fact we consider $R = 0.01$ rather than $R = 0.1$. Note that we set the value $\omega = 0.001$. Thus, according to $T_\omega = 2\pi\omega$, we have $T_\omega = 6284$, which corresponds to the period of the oscillations of Fig.(7.4). Note that these fast oscillations have an extremely small intensity and also that, in a coarse grained representation, the time evolution of $\psi_{exp}(t)$ would be qualitatively similar to the exponential waiting time distribution of Eq.(7.1). In Fig.(7.5), we consider the choice of

89
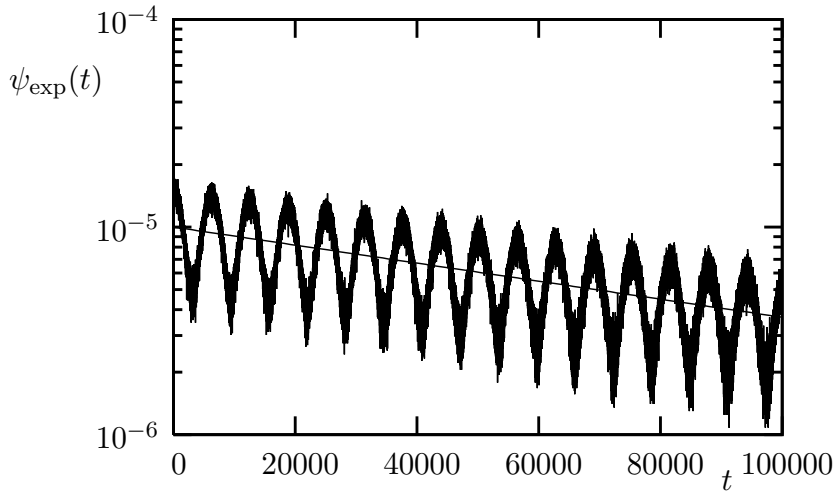
Figure 7.4. $\psi_{exp}(t)$ as a function of t. $\epsilon = 1, q_0 = 0.00001, T_\omega = 6284, \omega = 0.001, R = 0.01$.
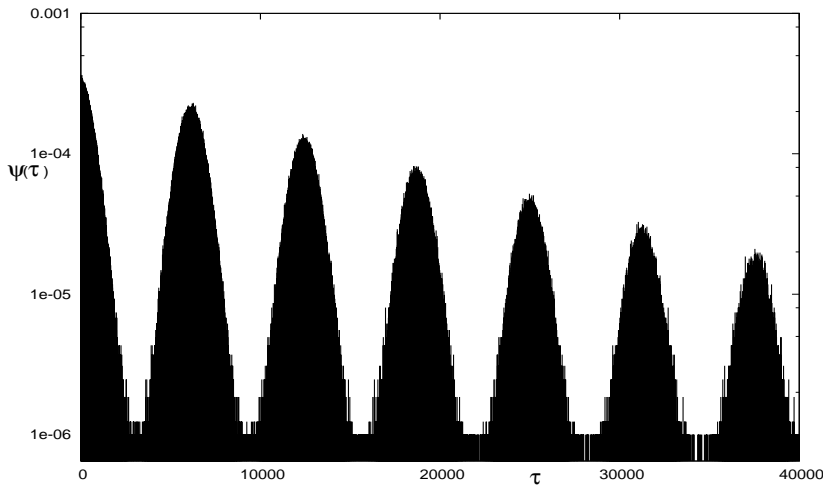
Figure 7.5. $\psi_{exp}(t)$ for $q(t)$ of Eqn.(7.2) with $k = 5$, $Q_0 = 0.0005$, $\eta = 0.99$, $T_\omega = 6284, R = 0.02$

Eq.(7.2) with $R = 0.02$. We see that with R of the same order of magnitude as that of Fig.(4) an impressively large clustering effect appears. This is the physical condition considered in Ref.[79]. In the following sections, which illustrate the main result of this Chapter, we make the statistical analysis of the time series $\{\tau_i\}$ in the case where $R >> 1$, with the choice of Eq. (7.1), in a condition that is far from the stochastic resonance condition of Ref.[79].

Let us discuss now the TSCO, with the help of Fig.(7.4) and Fig(7.4). It appears that the TSCO reveals a tendency contrary to the STH picture. Fig.(7.4) a illustrates the TSCO of the Poisson process with no perturbation, and no cluster, and Fig.(7.4)

90

b illustrate a case under perturbation. In fact, in Fig.(7.4)b, $q_0 = 0.1$ and $\omega = 10^{-3}$ and consequently the time period in the time scale of this chronological order is $T q_0 = 2\pi R \sim 628$, which indeed corresponds to the time period of the quasi-periodic bunching of the sojourn times in chronological order.

(a) no perturbation ($\epsilon = 0$), $q_0 = 10^{-3}$ (b) $R = 100$, $\epsilon = 0.4$, $q_0 = 0.1$
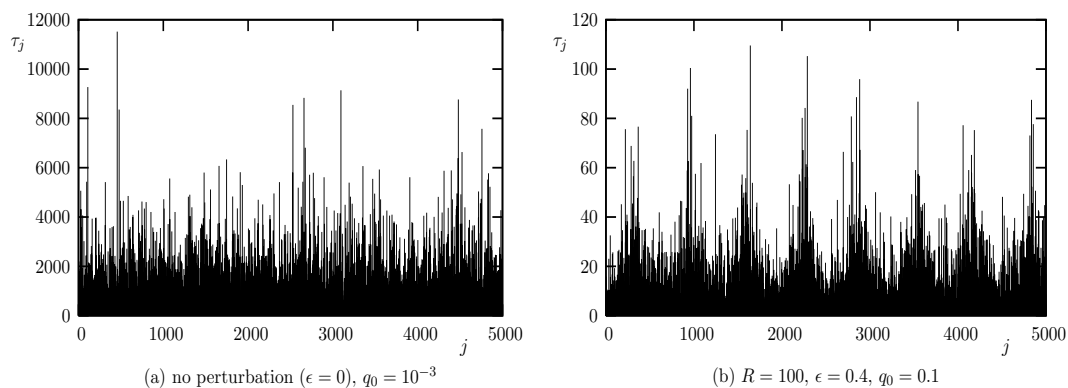
Figure 7.6.   Sojourn times in chronological order, according to the choice of Eq.(7.1). (a). The parameter values are $\epsilon = 0$, No perturbation, $q_0 = 0.001$; (b)$\epsilon = 0.4$, $q_0 = 0.1$, $\omega = 0.001$

(a) $R = 10$, $\epsilon = 1$, $q_0 = 0.01$ (b) $R = 100$, $\epsilon = 1$, $q_0 = 0.1$
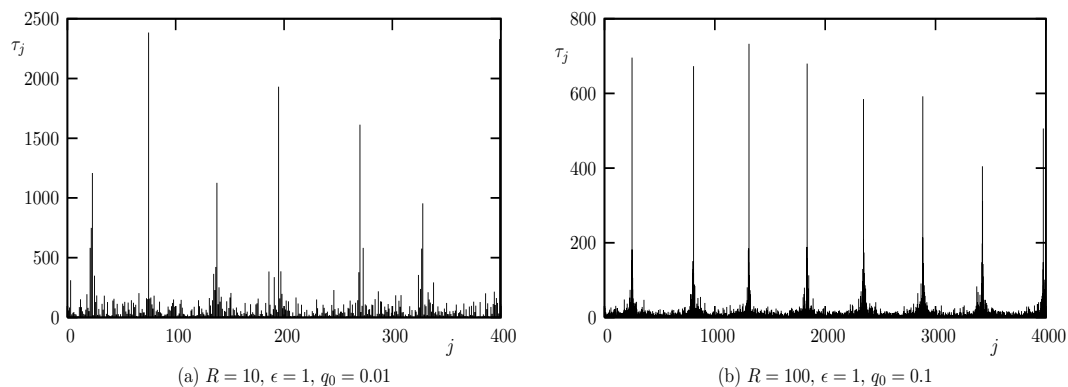
Figure 7.7.   Sojourn times in chronological order, according to the choice of Eq(7.1), $\epsilon = 1$ (a) $q_0 = 0.01$, $\omega = 0.001$, $R = 10$ (b) $q_0 = 0.1$, $\omega = 0.0001$, $R = 100$.

In this case the change of the transition rate $q(t)$ is quite slow and the sojourn times are mainly affected by the local value of $q(t)$. Consequently, the regions with a smaller rate q corresponds to those with longer sojourn times and vice versa. In general, given a value of ϵ, the clustering effect in the TSCO increases with increasing R. At small values of R the clustering patterns in the TSCO tend to disappear. Conversely, for large values

of R the effect of the external perturbation becomes significant and almost perfectly periodic clusters arise. The relative width of such clusters becomes smaller and smaller for larger and larger values of R. In the set of Figs.(7.4) we show a clustering effect in a condition far from the slow-perturbation condition ($\epsilon = 1$). Evidently, also in this case the clustering effect increases with R, as in the earlier case. Notice that, in this case, there is a further effect generated by the extremal value $\epsilon = 1$. In this case the transition rate $q(t)$ goes to zero periodically. As a consequence, if R is very large, the cluster size reduces to a single waiting time, whose magnitude is very much larger than the typical scale of the other sojourn times, which is given by $T_0 = 1/q_0$. Obviously, in the close neighborhood of these spikes the slow perturbation assumption fails.

7.5. DEA on a Sequence of Data under the influence of an Oscillating Perturbation

Let us now consider the DE in action when the Poisson system is significantly affected by an external cyclic perturbation with time period T. Let us make now the assumption that fluctuation and periodicity are not correlated, as in the theoretical work of Ref. [51]. Let us illustrate here a heuristic theory that has the merit of yielding a qualitatively satisfactory explanation of these earlier results. Let us imagine that there are no fluctuations about the periodic trend, in which case the entropy $S(t)$ does not remain constant. The DE method [73, 74, 51] rests on the use of a mobile window of length l, moving along the trajectory of imaginary diffusing particle. This window determines a diffusion trajectory of length l, which makes the random walker move by the quantity $\Delta(t, l) = x(l + t) - x(t)$. Due to the selection of different values for t, the quantity $\Delta(t, l)$ spreads around a mean value, thereby broadening the resulting distribution, and making the entropy increase. In a sense, this entropy increase is determined by the uncertainty on the initial conditions. The trend is a deterministic function, for instance, a harmonic oscillation. However, changing t, corresponds to a phase change, and the bunch of trajectory of diffusion created by moving the window of length l along the sequence, is equivalent to creating a diffusion process with a deterministic walker, whose initial conditions are selected randomly.

Thus, $S(l)$ increases with the window size l. However, for windows of length $l = nT$, with $n = 1, 2, ...$, the length of the path traveled by the lth walker, vanishes, namely, $\delta(l, nT) = 0$, regardless of the particular value of l. This means that $S(l) = A$, namely, the entropy $S(l)$ recovers the initial small value, after reaching its maximum value at $l = T(n+1)/2$, which is the middle point between two consecutive minima.

Let us now imagine that the signal is the sum of a periodic trend and an uncorrelated, and stationary, fluctuation , a white noise . As a consequence, $S(l)$, is not forced to recover the initial value A at $l = nT$. The values of $S(l)$ in these points are determined by the uncorrelated fluctuations, and lie on the straight line $B(L) = A + 0.5L$.
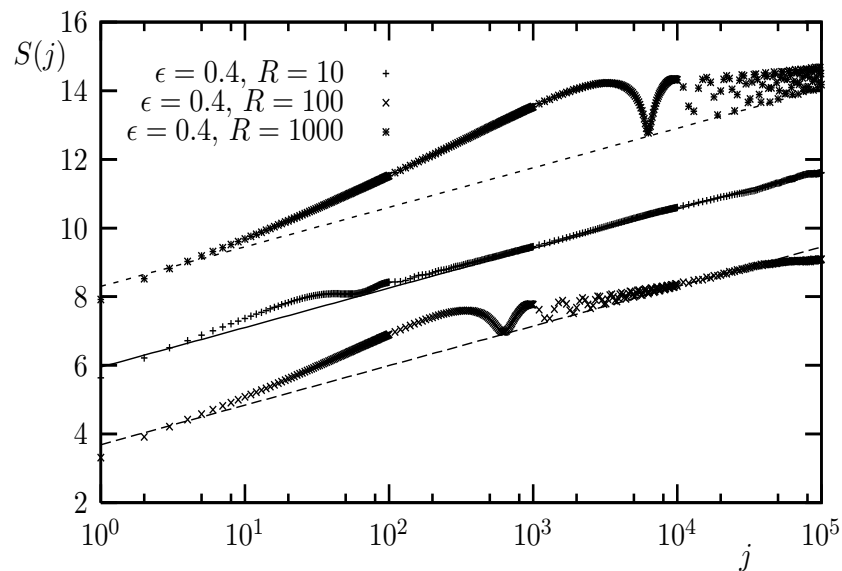
Figure 7.8.   Diffusion entropy $S(j)$ as a function of j, with j denoting the chronological order.

As shown by Fig.(7.5), the Poisson sequences under perturbation produced with a moderate value of ϵ and a value of R large enough, are qualitatively similar to those obtained in the earlier work [51]. Consequently, the DE behavior is expected to be similar. How about the case when we perform the de-trending? This is a very interesting question, given the big interest by many groups to look for the most efficient de-trending techniques [62, 63, 61, 67, 68]. On the basis of the theory developed in this Section, after de-trending, the resulting fluctuation will have a vanishing mean value, but the variance will still have a periodic dependence on time, with time period T. On the basis

of an earlier work on the DEA method [74], we argue that converting the resulting time series, with both positive and negative fluctuations, into a new time series whose values are given by the moduli of the time series with vanishing mean values, might be beneficial. Let us note also that the authors of Ref.[74] proved that the adoption of an asymmetric walking rule leads to a faster attainment of the scaling, a fact that also suggests a larger sensitivity to the real nature of the process under discussion. Note that the time series produced by the modulus prescription looks like the original perturbed Poisson process. Under these conditions, one may expect that the analysis, after de-trending will yield the same resonant-like effects as the DE method applied to the original time series. As a matter of fact, in Section 7.7 I show that this prediction turns out to be correct.

7.6. Correlation Function

This section shows the Correlation Function (CF) method in action with regard to Poisson process under the effect of perturbation. We work with the time series $\{\tau_i\}$ derived with the method described in Section 7.2. In the statistical analysis of this Chapter we consider two kinds of CF. The first is given by

$$(7.21) \qquad\qquad C(j) \equiv \overline{(\tau_i - \overline{\tau})(\tau_{i+j} - \overline{\tau})}.$$

The meaning of the bar is that we are taking a time average. As in the case of DE method, we consider a window of size j, we move this window along the sequence by assigning to i all possible values. Due to the harmonic nature of the perturbation, the process is stationary and consequently also the time mean value of τ_i, denoted by $\overline{\tau}$ is very well defined. Thus, this first kind of correlation function is a legitimate prescription. We also define a second prescription, given by

$$(7.22) \qquad\qquad \tilde{C}(j) \equiv \overline{(\tau_n - \tau_a(t_i'))(\tau_{i+j} - \tau_a(t_{i+j}'))},$$

where $\tau_a(t') = < \tau(t') >$ given by Eq.(7.11) and $t_i' = \tau_1 + ... + \tau_i$, i.e., the sum of the first n sojourn times. This second form of correlation function is based on the concept of a local de-trending, and, to a first sight, might be judged to be more appropriate than the

94

prescription of Eq.(7.21). Actually, we shall find that this latter form of CF is insensitive to the fluctuation-periodicity correlation, while the former form is not.

7.7. Discussion on the Numerical Experiments

Fig. 8 shows the results produced by the DE method applied to the artificial time series $\{\tau_i\}$ for different values of the parameter R. We see that the diffusion entropy becomes more and more sensitive to the perturbation periodicity with the increase of the time period $2\pi R$. However, the relative minima of all three curves lie on the straight line with the slope $\delta = 0.5$, a property, shared, according to the remarks of the earlier subsection, also by the case where no periodicity-fluctuation correlation exists.
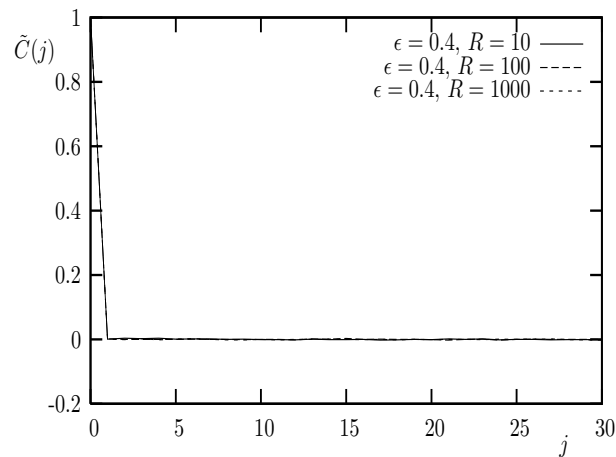
Figure 7.9.   Correlation function $\tilde{C}(j)$ of Eq.(7.22) as a function of j.

At the same time, Fig.(7.7) shows that the CF of Eq.(7.22) is insensitive to the fluctuation-periodicity correlation as well.

This result may seem somewhat disappointing because it would imply that the perturbation-induced memory is invisible to both the CF and the DE method. Let us now address the problem of examining through the DE method the de-trended sequence. This means that we have to replace τ_i with $\tau_i - <\tau(t_i') >$, where $t_i' = \tau_1 + ... + \tau_i$. Note that the average here is not a time average but an ensemble average which is calculable through means that are already expressed.

95
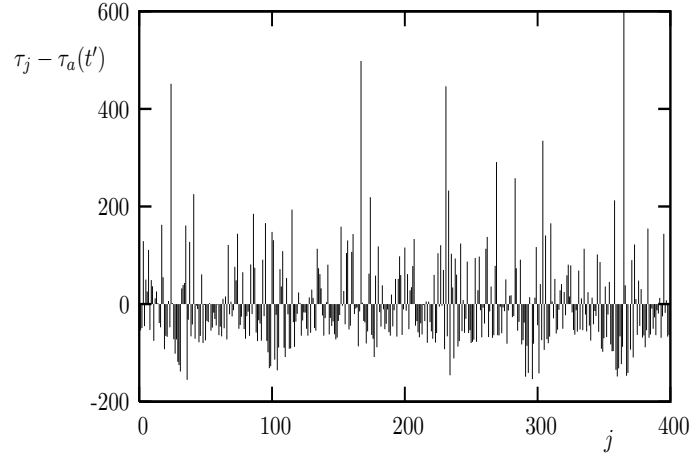
Figure 7.10. The fluctuations $\tau_j - < \tau(t') >$ in chronological order. The value $< \tau(t') >$ is given by Eq.(7.11),and the time t' is a function of j, determined by the prescription $t' = \tau_1 + ..\tau_j$.

In Fig.(7.7) we plot the de-trended sequence. Let us apply the DE method to this de-trended sequence. The result is illustrated by Fig.(7.7)a. We see that there is no sign of the fluctuation-periodicity correlation.
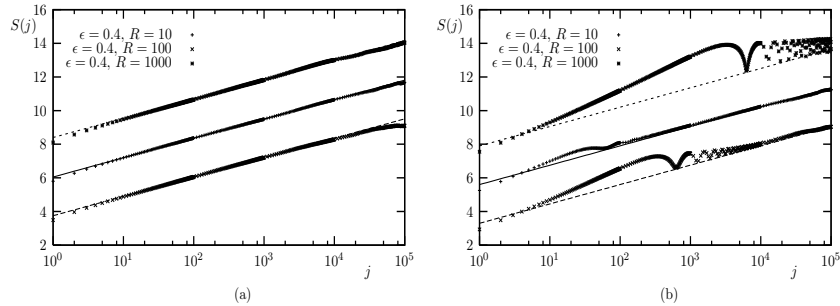
Figure 7.11. Diffusion entropy of the de-trended sequence,as a function of j. We use the choice of Eq.(7.1) with $\epsilon = 0.4$. (a) We derive the diffusion process from the sequence $\{\tau_i - < \tau(t') >\}$; (b) We derive the diffusion process from the sequence $|\{\tau_i - < \tau(t')\} > |$. From the bottom to the top the three curves refer to $q_0 = 0.1$, $T_\omega = 6284$,$\omega = 0.001$,$R = 100$; $q_0 = 0.01$,$T_\omega = 6284$, $\omega = 0.001$, $R = 10$;$q_0 = 0.001$, $T_\omega = 6283185$, $\omega = 0.000001$, $R = 1000$.

We consider several values of R, so that the three curves there plotted,the one with $q_0 = 0.1$ and $R = 100$, refers to the same physical condition as that of Fig.(7.4)b, with a strong perturbation-induced re-ordering effect. In spite of this significant time

96

re-ordering effect, this curve yields a straight line with $\delta = 0.5$, a property shared by the other two curves.

We are in a position to check a conjecture earlier made, on the benefits stemming from using random walker always jumping in the same direction. Let us consider the sequence $\{|\tau_i - <\tau(t_i')>|\}$, namely, the sequence of moduli of the de-trended time. We apply the DE method to the resulting sequence, and we find the result plotted in Fig.7.7b. The similarity between Fig.7.7b and Fig.7.5 is remarkable. This is because of the reason that the adoption of the absolute values of the fluctuation around the mean waiting time produces a signal similar to the original sequence, as a consequence of the fact that the variance $\sigma(t)$ has the same periodicity as the trend $<\tau(t)>$. As in the case of Fig.(7.5), the sensitivity to periodicity becomes larger with the increase of R. How about the Correlation Function (CF) method? Let us apply the prescription of Eq. (7.22).
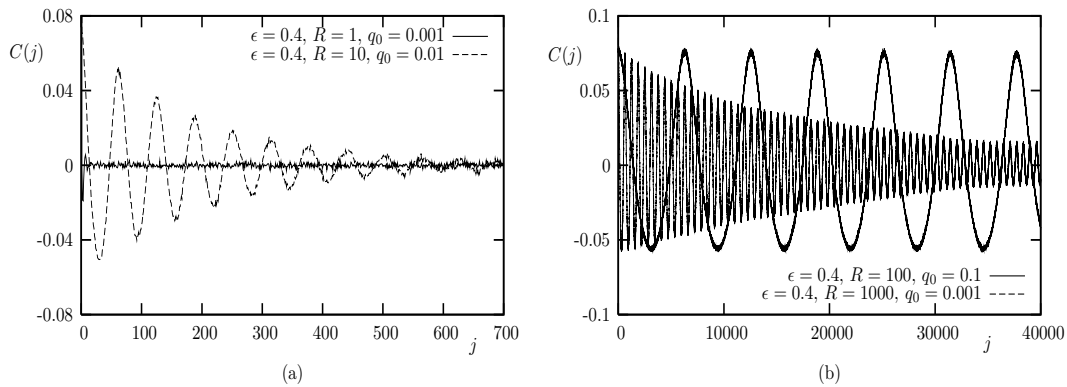
Figure 7.12.   Correlation function of the waiting times in chronological order, for (a)$R = 1, q_0 = 0.001$ and $R = 10$, $q_0 = 0.01$. (b) $R = 100, q_0 = 0.1$ and $R = 1000, q_0 = 0.001$.

In Fig.(7.7) we illustrate the results of this analysis. We show that this correlation function acts as a reliable indicator of the perturbation-induced memory of the sequence. In fact the oscillation period is of the order of $2\pi R$, and, even more important, the decay of the amplitude of these oscillations become slower and slower with the increase of R.

I want to also take a note about the Fourier Transform Power Spectrum of the chronological order of the waiting times for the Poisson perturbation using Fast Fourier

97

Transform algorithm of Origin 6.1 program. In the plot of Fig(7.7) it is obvious that there is a peak in the fundamental frequency of $f = 1/2\pi R$. And then there are higher harmonics too, which is one of the signatures of Stochastic Resonance. Recall that I have demonstrated the similarity of the physical picture of this Chapter to physical picture explained in the Chapter on Stochastic Resonance (Chapter 6).
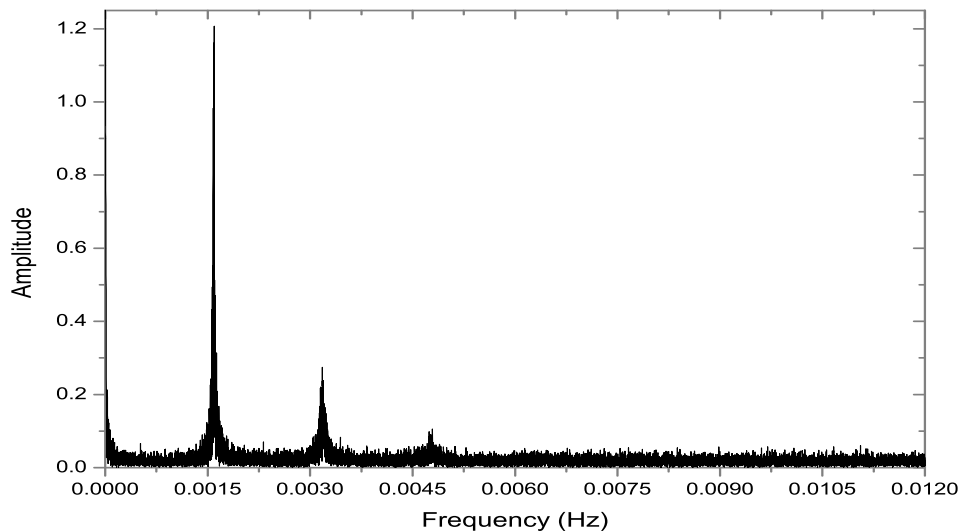
Figure 7.13.   The FFT power spectrum of the perturbation of Poisson renewal rate process with $\epsilon = 0.4$, $T = 6284$, $R = 100$.

We also ran FFT for a band pass filter, of the chronological order. As a result in the Figure(7.7) we see that when we detect a signal by means of a band pass filter, what we see is that although we perturb the rate with a perfectly periodic rate in the chronological order, the chronological order on the other hand is not perfectly periodic for all time, the period from a bunch to the next one increases or decreases from time to time as a result of stochastic character of the renewal process under consideration.

7.8. Concluding Remarks

Our main motivation has been the implementation of an algorithm that generates time series with a significant correlation between fluctuation and periodicity. We have adopted a picture based on a Poisson process, with a rate perturbed by an external harmonic disturbance.
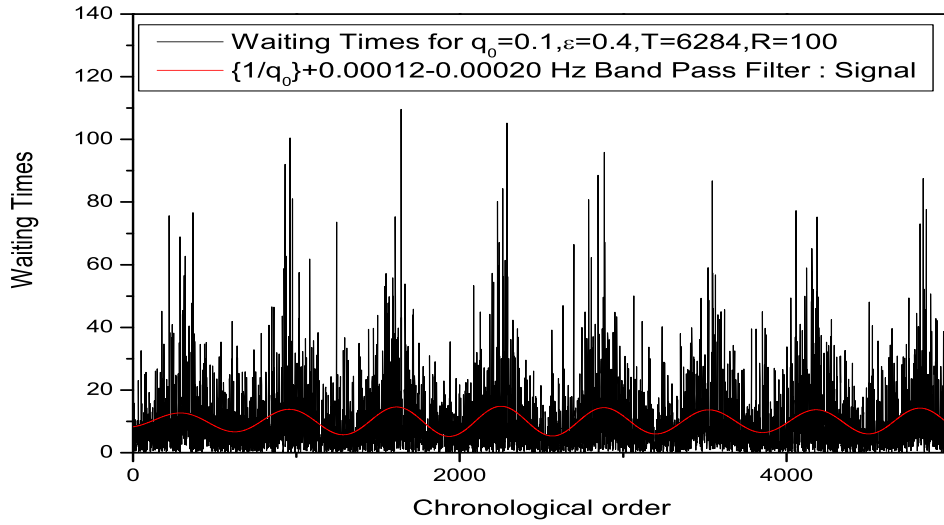
Figure 7.14.   The Band-Pass filter of the perturbation of Poisson renewal rate process with $\epsilon = 0.4$, $T = 6284$, $R = 100$ in chronological order.

We have seen that an external perturbation has the effect of turning a memoryless sequence into a sequence with memory. This is closely connected to the subject of stochastic resonance [66, 79], and Fig.(7.4) and Fig.(7.5) are clear signatures of this connection. With the help of these artificial sequences we have found that the adoption of a de-trending process would not be enough to detect the fluctuation-periodicity correlation. In fact, the adoption of the CF method would fail to find evidence for the residual variance periodicity after de-trending. This is so, because the CF method is successful to detect memory only if it is applied in the form of Eq. (7.21)). After de-trending, the difference between the prescription of Eq. (7.22) and of Eq. (7.21) is annihilated, and the CF method is expected to perceive only the local Poisson condition.The main conclusion of this Chapter is, therefore, that the most convenient method to find fluctuation-periodicity correlation is that after de-trending, the resulting sequence has to be properly processed. This means that the moduli of the de-trended fluctuations have to be considered. We establish the modulated-rate Poisson renewal process as a paradigmatic model for a system where fluctuations are directly related to the seasonality of the system underneath itself.

CHAPTER 8

PERTURBATION OF NON-POISSON RENEWAL PROCESSES

8.1. Introduction

In this Chapter I discuss the effects of linear and non-linear perturbations on a non-Poisson system [39], which also acts as the extension of the case where the system is merely a Poisson system [80]. I show using time series analysis techniques that under the effect of a non-linear perturbation a non-Poisson system may as well respond in just the same way as a Poisson system would, with an exponential cascade. Therefore, I show that exponential cascade does not set a proof for a system being Poisson in nature.

The response of a statistical system of neuro-physiological interest to an external perturbation is a problem of fundamental importance in physics, insofar as the perturbation is a probe, the response to which brings information on the physical nature of the system under study. The remarkable work done by Moss and coworkers [78, 79] is a seminal work that triggered much interest.These authors investigated the effect of an external harmonic perturbation on the dynamics of a neuron firing process, finding as main effect that of reordering the firings (or spikes) generated by the neuron dynamics. As a consequence, the histogram of inter-spike time distances becomes a sequel of equally spaced peaks, whose intensity decays with an exponential envelope. The time period of the peaks is equal to the period of the external harmonic perturbation. I refer to this property as *exponential cascade*. The exponential cascade has been recently derived from the perturbation of a Poisson process both linear and non-linear[80], which is mentioned in Fig(7.5), thereby suggesting that the experimental results of Refs. [78] and [79] may be an indication that neurons obey Poisson statistics. This is a quite intuitive result, as the unperturbed Poisson process is characterized by an exponential decay in the Probability Density Function (PDF) of the inter-spike time distances.

At this point I want to refer to a data obtained from an experiment that was carried out by R.M.Siegel [104] in 1990, where the data is used by both papers of [78, 79]. The experiment is performed as follows. Primary visual cortex of a cat is exposed to a periodical excitation by an external light source with a period we denote by T_ω cyclically, and the plot is obtained by normalizing the abscissa as $\frac{\tau}{T_\omega}$. The vertical axis is the result of the average of 26 different values of T_ω (Vertical axis $\psi(\frac{\tau}{T_\omega})$ is not normalized), and in all occasions it appears that the peaks of the waiting time distribution lies on an exponential decay curve. To be rigorous, Siegel fits the maxima to the function $y(x) = 2.2 * 0.51^{-x}$, in which case is easy to show that it is consistent with the choice of

$$(8.1) \qquad\qquad y(x) = \rho_1 e^{-\rho_0 x}.$$

which itself obeys an exponential cascade. The fact that the values of ρ_1 and ρ_0 are different will prove to be consistent with our assumption of archetypal neuron model obeying a non-Poisson statistics in the unperturbed case, which under the effect of a non-linear perturbation will respond in the form an exponential cascade. With Fig(7.5) we have already shown that exponential cascade may be obtained from Poisson statistics and here we show that non-Poisson neurons may as well result in the same type of behavior under certain conditions.

The exponential cascade of Refs. [78, 79] has been produced by the numerical and theoretical work of other authors. The work of Ref. [81] devotes a large attention to the reset issue involved by the so called integrate-fire model [82]. The more recent work of Ref. [83] contains remarkably interesting analytical expressions for the inter-spike time distances in the presence of harmonic perturbation.

It is interesting to notice that results appreciably similar to those of the pioneering work of Moss and co-workers [78, 79] have been found [84] using the model of Fitzhugh-Nagumo [85]. The authors of Ref. [84] made a numerical calculation and found that the envelope of the peaks in the inter-spike times histogram is indistinguishable from an exponential function.

Another model widely used to model firing neurons is the Hodgkin-Huxley neural model [86], which has been the subject of some recent studies aiming at establishing the response of this model to a harmonic perturbation [87, 88, 89, 90]. Although a controversy exists on whether or not a stochastic gain is obtained, the papers of Refs. [87, 88, 89] seem to recover the exponential cascade of Moss and coworkers [78, 79], which in turn is shown to be compatible with the assumption of Poisson statistics. The authors of Refs. [90], on the contrary, reveal the emergence of an anomalous scaling.

Finally, we want to mention the work of Reibold, Just, Becker and Benner [91] who recovered the exponential cascade of the leading work of Moss and co-workers [78, 79] from a theoretical picture adopting an intermittent map, which definitely departs from the Poisson condition.

According to some neuro-physiologists neurons are renewal [92] and Non-Poisson processes [93], *i.e.*, the inter-spike time distances are mutually independent random variables with non-exponential PDF and the statistical distribution of the number of events in a given time interval is a Non-Poisson distribution.

How is it possible therefore that real experiments, and theoretical models as well, some of which based on Non-Poisson dynamics, may systematically end up in the exponential cascade of the pioneering work of Moss and coworkers? The answer to this question should be related to the way the unperturbed Non-Poisson statistics interacts with the external perturbation.

The main aim of this Chapter is to shed light into this intriguing issue by making the assumption, supported by the results of Refs. [92, 93], that the statistics of inter-spike time distances are satisfactorily described, in the unperturbed state, by a renewal Non-Poisson random process [33]. We note that, if experimental data of unperturbed neuron firings are available, this assumption can be also checked by means of a statistical analysis based on the aging properties of renewal processes [94].

We make the assumption that the inter-spike time distances generated by the unperturbed neuron firing process are distributed according to the following class of Pareto-Nutting power-law PDFs:

$$(8.2) \qquad \psi(\tau) = (\mu_0 - 1)\frac{T_0^{\mu_0 - 1}}{(\tau + T_0)^{\mu_0}},$$

with

$$(8.3) \qquad 2 < \mu_0 < \infty \quad ; \quad T_0 > 0.$$

In this range of parameters the mean time is finite and given by:

$$(8.4) \qquad \langle \tau \rangle = \frac{T_0}{(\mu_0 - 2)}$$

In the next sections we will introduce two different models generating sequences of inter-spike time distances according to the PDF of Eq. (8.2). Both models also satisfy the renewal condition for the sequences of inter-spike time distances.

The choice of Eq. (8.2) is done to yield in the asymptotic time limit the inverse power law $1/\tau^{\mu_0}$, while making the inter-spike time distance distribution $\psi(\tau)$ fulfill the normalization condition, without introducing any short-time truncation. The time scale T_0 has the important role of defining the extension of the region of transition from the short-time condition, with no unphysical divergence, to the long-time limit, where the inverse power law appears. The power index μ_0 signals the specificity of the cooperative properties that establish the complex nature of the process.

According to this picture, the parameters μ_0 and T_0 afford complete information about the unperturbed system dynamics, and it is a reasonable assumption that the effect of an external perturbing field is that of turning either T_0 or μ_0, or both, into time dependent parameters $T(t)$ and $\mu(t)$. For simplicity's sake we shall not consider the case where both parameters are perturbed simultaneously.

We are adopting the same theoretical perspective as that of the earlier works of [94, 72, 95, 96]: it is possible to predict the effect of external perturbation on the process under study only on the basis of the probability density $\psi(\tau)$, under the key

assumption that the process is renewal. In Refs. [72, 95, 96] the assumption was made that the external perturbation affects T_0, but the question of the form acquired by the inter-spike time PDF was not addressed. In this Chapter, we shall study also the effect of perturbing μ_0. We shall prove that in this second case a form of genuine transition from Non-Poisson to Poisson statistics may be realized, while the perturbation of T_0 generates only a form of apparent transition to Poisson statistics, insofar as the system does not lose its Non-Poisson nature. To make this conclusion more convincing, following the authors of Refs. [90, 80], we use Diffusion Entropy (DE) analysis [73, 74, 97] to reveal the anomalous scaling that is a signature of the hidden Non-Poisson nature of the system under study.

We also find the surprising result that, for given T_0, there exists an intermediate range of the perturbation time scale T_ω where some kind of cooperation between perturbation and system's dynamics emerges and generates an unexpected form of complexity. We reach this conclusion using the DE analysis.

In conclusion, this Chapter is devoted to studying non-Poisson processes in non-homogeneous conditions, being the time inhomogeneity a direct consequence of the external perturbation [95, 96]. Consequently, this is a significant extension of the earlier work of Ref. [80], which was limited to studying Poisson processes being made non-homogeneous by an external perturbation [98, 99].

The structure of this Chapter is as follows. In Section 3.10 we have already illustrated the model we will use here for the perturbation of μ_0. That model is equivalent to the model proposed by Daly and Porporato [40]. In Section 8.3 we discuss theoretically and numerically the effects of an harmonic perturbation on μ_0. We devote Section 8.4 to illustrate the model that we adopt to perturb the parameter T_0, This model is based on the theoretical procedure of Refs. [72, 95, 96] to obtain the unperturbed renewal waiting times. We illustrate the effects of the perturbation of rate by means of numerical simulations details of which are explained in the Appendix. In Section 8.5 we make a concise review of DE method of analysis and we show this method in action to assess if the transition from Non-Poisson to Poisson regime is a genuine property or some

hidden non-Poisson properties are still present in the perturbed system. We also use DE to illustrate the emergence of an unexpected form of complexity generated by the cooperation of harmonic perturbation and unperturbed non-Poisson dynamics. In the last Section we shall summarize the important results of this Chapter. Furthermore, we devote the Appendix to illustrate the details of the algorithm used in Section 8.4.

8.2. Numerical Structure

One of the numerical algorithms used for generating power-law renewal distributed waiting times is the one proposed in Chapter 3.

Consequently, the more general mathematical prescription for an external perturbation can be written in the following general form:

$$(8.5) \qquad\qquad r(t) = \frac{r_0 \phi_0(t)}{1 + r_1 \phi_1(t) \Delta t_r}.$$

In this formulation, the renewal character of the rate function $r(t)$ is again included in Δt_r, which is affected by the occurrence of a neuron firing (see Fig.8.3a). On the contrary, the functions $\phi_0(t)$ and $\phi_1(t)$ describe the effect of external forcing, which are not affected by the internal critical events (neuron firings or spikes). In analogy with the unperturbed parameters μ_0 and T_0 in Eq. (3.50), it is possible to write similar expressions for the perturbed power index $\mu(t)$ and the perturbed time scale $T(t)$:

$$(8.6) \qquad \mu(t) = 1 + \frac{r_0 \phi_0(t)}{r_1 \phi_1(t)} = 1 + (\mu_0 - 1)\frac{\phi_0(t)}{\phi_1(t)} \quad ; \quad T(t) = \frac{1}{r_1 \phi_1(t)} = \frac{T_0}{\phi_1(t)}.$$

We see immediately that the condition $\phi_0(t) = \phi_1(t)$ has the effect of leaving the power index μ_0 unchanged, while affecting the time scale T_0. Making $\phi_0(t)$ time dependent while keeping $\phi_1(t) = 1$, and thus time independent, has the effect of perturbing μ_0, while leaving T_0 unchanged.

A numerical algorithm, discrete in time, was used to generate the sequences of random times $\{t_i\}$ corresponding to the rate $r(t)$ of Eq. (8.5). This algorithm is based on an iterative procedure derived by the Cox definition of the rate of spike production. In fact, considering the interval $[t_i, t_{i+1}]$ and Eq. (3.44), the quantity $p(t) = r(t)dt$ is the probability of a spike occurrence in the infinitesimal interval $[t, t + dt]$, given that no

spikes occurred in the interval $[t_i, t]$. In the implementation of a numerical scheme, the time step dt cannot be infinitesimal, but it is necessarily a finite quantity. In order to get a good approximation of the continuous-time model described by the rate given in Eq. (8.5), the time step dt must be chosen in such a way that (a) $p_n = r(n \cdot dt + t_i) \, dt \ll 1$ for whatever value of $t = n \cdot dt + t_i$ larger than t_i and (b) dt is much less than all the relevant time scales.

The resulting stochastic process, discrete in time, can be interpreted as a two-state random process and the quantity p_n as the probability of getting a jump at the discrete time n. The occurrence of a neuron firing corresponds to a jump between the two states and the residence time in each state defines the inter-spike time distance. Note that, if p_n is not very small, the two-state random process, discrete in time, is not a good approximation of the original model given in Eq. (8.5), even if $p_n < 1$ (*e.g.*, $p_n \sim 0.5$). This is true also when condition (a) is satisfied, but condition (b) is not. Considering the unperturbed rate $r(t)$ of Eq. (3.56) and choosing $dt = 1$, from the conditions (a) and (b) follow:

$$(8.7) \qquad\qquad r_0 \ll 1 \quad ; \quad r_1 \ll 1,$$

implying that the internal times $1/r_0$ and $T_0 = 1/r_1$ are much larger than the time-step dt. These are the only two conditions required in the unperturbed case ($\phi_0 \equiv \phi_1 \equiv 1$), but they must be completed with other ones involving the time scales of the external perturbation, included in the functions $\phi_0(t)$ and $\phi_1(t)$ of Eq. (8.5).

The practical implementation of the numerical algorithm is as follows. First of all, condition (a) being satisfied, the interval $I = [0, 1]$ can be divided into two portions, one ranging from 0 to p_n, called interval P_n, and one from p_n to 1, called interval Q_n. Let us assume that a spike occurred at time t_i. Then, in order to find the next time t_{i+1}, we must follow the following iterative procedure:

- $n = 0$: draw a random number ξ_0, uniformly distributed in $I = [0, 1]$. If it is in the interval P_0 ($\xi_0 \leq p_0 = r(t_i) \, dt$), then a jump occurs and it results $t_{i+1} = t_i + dt$

or, equivalently, $\tau_{i+1} = dt$. If it is in the interval Q_0 ($\xi_0 > p_0 = r(t_i)\ dt$), then it is known that $t_{i+1} > t_i + dt$ and the next step ($n \geq 1$) must be carried out;

- $n \geq 1$: it is known from the previous step $n-1$ that $t_{i+1} > t_i + n \cdot dt$. Then, a random number ξ_n, uniform in $[0,1]$, must be drawn and compared with:

(8.8)

$$p_n = r(t_i + n \cdot dt)\ dt = \Pr\{t_i + n \cdot dt < t_{i+1} \leq t_i + n \cdot dt + dt \mid t_{i+1} > t_i + n \cdot dt\}$$

as given by the Cox definition, Eq. (3.44). As before, if ξ_n is in P_n ($\xi_n \leq p_n$), then $t_{i+1} = t_i + (n+1) \cdot dt$ and $\tau_{i+1} = (n+1) \cdot dt$, otherwise, it is in Q_n ($\xi_n > p_n$), and the iteration must be repeated for $n+1$, given the known condition: $t_{i+1} > t_i + (n+1) \cdot dt$;

Note that the iteration stops when the condition $\xi_n \leq p_n$ is satisfied for the first time. The resulting computed time t_{i+1} is an approximated value with maximum error dt.

If we consider the unperturbed rate, Eq. (3.56), with $r_1 = 0$, we get the Poisson case, $r(t) = r_0$, which is approximated by a two-state random process with a constant jump probability: $p_n = r_0\ dt = r_0$ ($dt = 1$). As known, the PDF of inter-spike times is an exponential function with decay rate r_0.

In the unperturbed Poisson case, this model is exactly equivalent to a stochastic generalization of the Leaky Integrate-and-Fire (LIF) model of Ref. [82]:

(8.9)
$$\frac{d}{dt}x = S - \gamma x(t) + \eta(t),$$

when $S = 0$. Here, x denotes the neuron potential, γx the leakage and $\eta(t)$ a stochastic force. Our model becomes Non-Poisson by setting $r_1 > 0$ in Eq. (3.56). This Non-Poisson condition could be reproduced by the users of the LIF model by assuming that, after resetting, the threshold potential, rather than remaining fixed, increases linearly as a function of time.

8.3. Perturbation of the Power Index μ_0

In this Section we limit ourselves to discussing the perturbation of r_0, which, as proved by Eqs. (3.50,8.6), is equivalent to perturbing the power index μ_0, while leaving the time

scale T_0 unchanged. This is the straight generalization of the way of perturbing a Poisson process [80]. In fact, in the Poisson case $r_1 = 0$, so that both μ_0 and T_0 become infinite. The constant rate $r(t) = r_0$, being an inverse time scale, becomes now the only basic parameter of the unperturbed renewal system.

The perturbation of a Poisson process introduced in [80] is given by:

$$(8.10) \qquad\qquad r_p(t) = r_0 \exp\left[\epsilon \cos\left(\frac{2\pi}{T_\omega}t\right)\right],$$

where $r_p(t)$ denotes the perturbed Poisson rate, *i.e.*, the perturbation of r_0, and T_ω is the perturbation period.

A well-known example of Poisson process is generated by a symmetric double-well potential [101]. In this case, the critical events are given by the jumps from one well to the other one and the residence times in a given well correspond to the inter-spike time distances. The unperturbed Poisson rate of event production is given by the following escape rate:

$$(8.11) \qquad\qquad r_0 = A exp(-Q/D),$$

where A is a constant depending on the frequency of the processes of molecular collision, Q is the potential barrier and D the white noise intensity. As a consequence, the expression in Eq. (8.10) coincides with the rate of escape of a particle over a time dependent barrier $Q(t)$, under the action of a white noise. This model was adopted by the authors of Refs. [78, 79] to reproduce the experimental exponential cascade. Without referring to the original model, the authors of Ref. [80] showed that a Poisson process with the rate prescription given in Eq. (8.10) gives these same results. Consequently, the behavior of the inter-spike time distances is independent of the particular model and depends only on the effect of the perturbation on the rate $r_p(t)$.

It is straightforward to generalize the perturbation of the Poisson rate of Eq. (8.10) by considering it as a limit, for $r_1 \to 0$, of the Non-Poisson rate given by Eq. (3.56),

with $r_p(t)$ replacing r_0. This is equivalent to perturbing the parameter r_0 itself:

$$(8.12) \qquad r(t) = \frac{r_p(t)}{1 + r_1 \Delta t_r} = \frac{r_0 \exp\left[\epsilon \cos(\frac{2\pi}{T_\omega} t)\right]}{1 + r_1 \Delta t_r},$$

and, as earlier mentioned, to perturbing the power index μ_0. In fact, comparing with Eq. (8.5) it results $\phi_0(t) = \exp\left[\epsilon \cos(\frac{2\pi}{T_\omega} t)\right]$ and $\phi_1(t) = 1$ so that, from Eq. (8.6), we can write an expression for the power index, changing in time, associated with the rate given in Eq. (8.12):

$$(8.13) \qquad \mu(t) = 1 + \frac{r_p(t)}{r_1} = 1 + [\mu_0 - 1] \exp\left[\epsilon \cos(\frac{2\pi}{T_\omega} t)\right],$$

being μ_0 given by Eq. (3.50). We refer to this perturbation process as *non-linear perturbation* of μ_0.

We define the *linear perturbation* of μ_0 as follows:

$$(8.14) \qquad r(t) = \frac{r_0(1 + \epsilon \cos(\frac{2\pi t}{T_\omega}))}{1 + r_1 \Delta t_r} \quad ; \quad \epsilon < 1$$

which implies for the power index:

$$(8.15) \qquad \mu(t) = \mu_0 + (\mu_0 - 1)\epsilon \cos(\frac{2\pi t}{T_\omega}) \quad ; \quad \epsilon < 1.$$

Note that if we adopt the Arrhenius-like picture of Eq. (8.11) and then we set in Eq. (8.10) the condition $\epsilon \ll 1$, the non-linear model becomes equivalent to the linear model. In fact, in this case the linear perturbation of μ_0 is derived from the non-linear perturbation by a simple Taylor expansion of the exponential function in Eq. (8.12), with respect to the parameter ϵ, when $\epsilon \ll 1$. If we adopt Eq. (8.14) with $\epsilon < 1$ without fitting the condition $\epsilon \ll 1$, we realize a condition that cannot be derived from the Arrhenius-like model, and thus from the non-linear model. In conclusion, the linear and non-linear model are different models for the neuron firing processes. However, it was observed from numerical simulations that these two models are significantly different only in the range $\epsilon \lesssim 1$.

Both the non-linear perturbation of Eqs. (8.12) and (8.13) and the linear perturbation of Eqs. (8.14) and (8.15) are determined by four parameters: the intensity ϵ and the period T_ω of the perturbation, the power index μ_0 and the time scale T_0 of the unperturbed

system. Note that we are considering a Non-Poisson condition with $\mu_0 > 2$, a condition ensuring that the mean value of τ exists, is finite, and it is given by

$$(8.16) \qquad \langle \tau \rangle = \frac{T_0}{\mu_0 - 2} = \frac{1}{r_0 - r_1}.$$

Therefore, following Ref. [80], we define the following dimensionless parameter:

$$(8.17) \qquad R = \frac{T_\omega}{\langle \tau \rangle}.$$

When $R \ll 1$, the perturbation is faster than the production of firing events, thereby producing what we define as *fast perturbation*, linear or non-linear. The opposite limit, $R \gg 1$, defines *slow perturbation*, linear or non-linear. Note that, as said in Section 3.10, we must supplement the conditions of Eq. (8.7) with the following one

$$(8.18) \qquad \frac{dt}{T_\omega} = \frac{1}{T_\omega} \ll 1,$$

associated with the time scale T_ω of the external perturbation.

In the case of non-linear perturbation of μ_0, the fast condition allows us to define the effective power index μ_{eff} as follows:

$$(8.19) \qquad \mu_{eff} = 1 + [\mu_0 - 1] \left\langle \exp \left[\epsilon \cos(\frac{2\pi}{T_\omega} t) \right] \right\rangle,$$

where $\langle ... \rangle$ indicates an average over one perturbation period T_ω. This average value is well-defined only in the range of fast perturbation ($R \ll 1$). In fact, when the condition $R \ll 1$ applies, the perturbation makes $\mu(t)$ execute many oscillations before reaching the time regime where $\psi(\tau)$ reveals its inverse power law nature. It is easy to prove that the average value μ_{eff} is independent of the perturbation period T_ω, but increases rapidly with the perturbation strength ϵ.

In Fig.(8.3) the numerical evaluation of μ_{eff} as a function of ϵ and for two different values of μ_0 is reported. As the limit $\mu_0 = \infty$ is associated with a genuine Poisson process, it is expected that very large values of μ_{eff} could generate a behavior of Poisson kind in the perturbed system. The threshold $\mu_{eff} = 3$ has to do with the Diffusion Entropy and will be explained in Section 8.5.
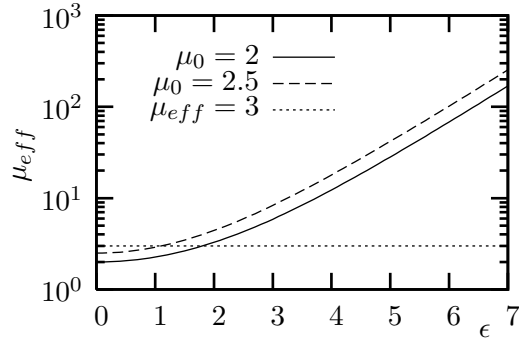
Figure 8.1. μ_{eff} vs. ϵ as given by the numerical evaluation of Eq. (8.19) for $\mu_0 = 2$, 2.5. The horizontal dotted line indicates the threshold $\mu_{eff} = 3$.

Conversely, it is also easy to see that the linear perturbation of μ_0, given by Eqs. (8.14) and (8.15), does not affect the effective power index, i.e., $\mu_{eff} = \mu_0$. In Section 8.5 we shall discuss in more detail the consequences of this behavior on the scaling properties detected by the DE analysis.
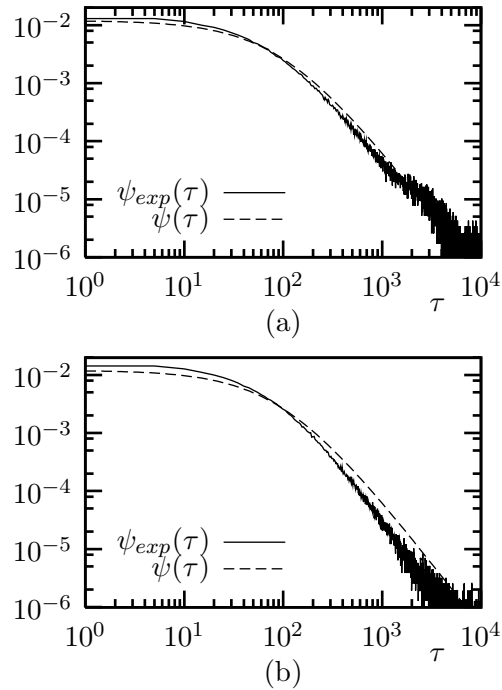
Figure 8.2. Slow linear perturbation of μ_0, Eq. (8.14). Comparison of the perturbed histograms of the inter-spike times, $\psi_{exp}(\tau)$, with the unperturbed ones, $\psi(\tau)$. $\mu_0 = 2.2$, $T_0 = 100$, $\epsilon = 0.6$ (a) $T_\omega = 5 \cdot 10^3$ $(R = 10)$; (b) $T_\omega = 5 \cdot 10^6$ $(R = 10^4)$.

111

Fig(8.3) and Fig(8.3) display the main results obtained from the application of the numerical algorithm introduced in Section 3.10 to the rate function of Eqs. (8.12) and (8.14).

Fig(8.3) and Fig(8.3) refer to the linear perturbation of μ_0, Eq. (8.14), with perturbation strength $\epsilon = 0.6$, and Fig.(8.3) is generated by the non-linear perturbation of μ_0, Eq. (8.12),with strength $\epsilon = 7$.
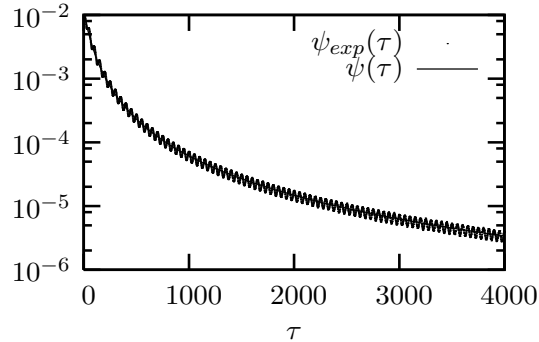
Figure 8.3.   Fast linear perturbation of μ_0, Eq. (8.14). Comparison of the perturbed histogram of inter-spike times (oscillating pattern $\psi_{exp}(\tau)$) with the unperturbed one. $T_0 = 100$, $T_w = 50$, $\mu_0 = 2.2$, $R = 0.1$, $\epsilon = 0.6$.
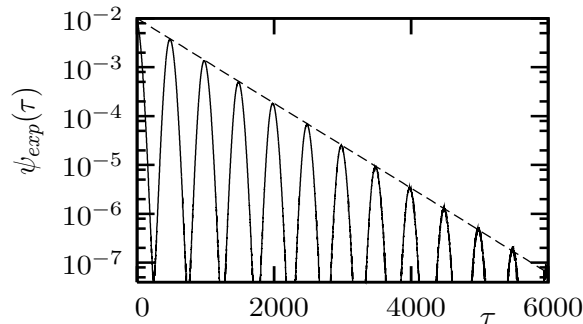

Figure 8.4.   Fast non-linear perturbation of μ_0, Eq. (8.12). Histogram of inter-spike times. $T_0 = 10^5$, $T_w = 500$ ($R = 10^{-3}$), $\mu_0 = 2.2$, $\epsilon = 7$. The dashed line is the exponential envelope of the maxima.

The probability density of inter-spike time distances is only weakly affected by making perturbation very slow, namely, $R \gg 1$, as shown by the histograms reported in Fig.(8.3). In Fig(8.3) a fast perturbation with the same strength ϵ of Fig.(8.3) is shown. In this case the fast perturbation produces more significant effects, as weak oscillations appears

in the histogram. However, we notice that the weak oscillations of Fig.(8.3) do not affect the inverse power law nature of $\psi(\tau)$, insofar as the histogram is clearly the addition of a genuinely power-law decay and of a pattern of weak and fast oscillations, with time period T_ω. In conclusion, the histogram averaged over the time T_ω results in a power-law decay with index μ_0.

It is important to compare Fig.(8.3) to Fig.(8.3). This comparison makes it possible for us to become acquainted with the main result of this Chapter. In Fig.(8.3) the result of a numerical simulation with a strong non-linear perturbation of μ_0 ($\epsilon = 7$) is shown. In agreement with the heuristic reasoning of Fig.(8.3), it is easy to see that, when we move from the weak linear perturbation of Fig.(8.3) ($\epsilon = 0.6$) to the strong non-linear perturbation of Fig.(8.3) ($\epsilon = 7$), both fast, we see that the non-exponential (power-law) average over the fast oscillation turns into the exponential cascade, a property shared by the perturbed Poisson system of the earlier work of Ref. [80]. This is shown in Fig.(8.3) by the exponential envelope of the maxima. As earlier mentioned, this is the reason why, to a first sight, the result of Fig.(8.3), and the experimental results of [78, 79] as well, can be interpreted as the consequence of the harmonic perturbation of a Poisson process [80].

In summary, our numerical simulations showed that, with increasing the coupling strength ϵ, the power-law decay emerges at a larger and larger time scale and the exponential cascade becomes more extended in time. On the other hand, the long inter-spike times are rare, and in the histograms realized with sequences of finite size, the statistical errors of the long-time tails are so large as to make virtually invisible the presence of an inverse power law behavior. This explains the lack of a significant deviation from the exponential behavior in Fig.(8.3) and the surprising qualitative similarity between the theoretical distribution of Fig.(8.3) and the experimental distribution of Fig. 1a of Ref. [78]. Note that in Fig. 1a of Ref. [78] the exponential regime extends to five perturbation cycles and that, due to the special choice of parameters adopted, in Fig.(8.3) is even more extended. As far as Fig.(8.3) is concerned, the origin of the exponential behavior

rests on the fact, accounted for by Eq. (8.19), that the perturbation creates an effective μ_{eff} of the order of 200.

In conclusion, the numerical results illustrated in this Section show that a Non-Poisson system under the influence of a strong and fast perturbation of μ_0 may produce the exponential cascade of Refs. [78, 79].

8.4. Perturbation of the Time Scale T_0

As pointed out in Section 3.10, the model of Eq. (8.5) can be applied to study the effect of perturbing T_0, while leaving μ_0 unchanged, by simply imposing $\phi_0(t) = \phi_1(t)$. However, mainly for reasons of computational convenience, we decided to use the dynamic model of Ref. [100] instead. Further, as already said in Section 3.10, the model of Ref. [100], in the range of small ϵ, yields results equivalent to the model of Eq. (8.5) [95, 96], which is also essentially equivalent to the model recently proposed by Daly and Porporato [40].

To make this article as self-contained as possible, let us review the dynamic model of Ref. [100]. Let us consider the equation of motion:

$$(8.20) \qquad \frac{dy}{dt} = \alpha_0 y^z, \qquad z \geq 1,$$

with y being a coordinate defined in the interval $I = [0, 1]$. This is a particle undergoing both regular motion and random jumps. The particle moves within the interval I with the dynamic prescription of Eq. (8.20). When it reaches the border $y = 1$, is injected back to a new initial random value within the interval I with uniform distribution. It is easy to prove [100] that this model yields the inter-spike time distribution of Eq. (8.2) with

$$(8.21) \qquad \mu_0 = \frac{z}{z-1} \quad ; \quad T_0 = \frac{1}{\alpha_0 (z-1)}$$

and

$$(8.22) \qquad z = \frac{\mu_0}{\mu_0 - 1} \quad ; \quad \alpha_0 = \frac{\mu_0 - 1}{T_0}.$$

114

Note that, in the unperturbed case, this model is exactly equivalent to the unperturbed rate function of Eq. (3.56). By comparing Eqs. (8.21) and (3.50) we get the following relationships between the parameters:

$$(8.23) \qquad\qquad r_0 = \alpha_0 \quad ; \quad r_1 = \alpha_0 (z - 1).$$

The second equality in Eq. (8.21) shows that, when the power index z is kept constant, T_0 depends only on α_0, thereby making it evident why the perturbation of the time scale T_0 is realized by replacing Eq. (8.20) with the following equation:

$$(8.24) \qquad\qquad \frac{dy}{dt} = \alpha(t)y^z.$$

It is possible to derive a general solution for this perturbed model, which shows how the external perturbation affects the systems by essentially introducing a form of memory in the renewal dynamics. To derive this solution, let us suppose that at time t_i a firing event occurs. This means that we randomly select a given initial condition $y(t_i) = \xi_i$, ξ_i being a random variable uniformly distributed in the interval $I = [0, 1]$. Then, $y(t)$ evolves according to Eq. (8.24) from the initial time t_i till to the moment when the particle reaches the border $y(t_{i+1}) = 1$:

$$(8.25) \qquad\qquad \int_{\xi_i}^{1} \frac{dy}{y^z} = \int_{t_i}^{t_{i+1}} \alpha(t')dt',$$

which then yields

$$(8.26) \qquad\qquad \frac{1 - \xi_i^{1-z}}{1 - z} = \int_{t_i}^{t_{i+1}} \alpha(t')dt'.$$

and

$$(8.27) \qquad\qquad \xi_i = \left[1 - (1 - z) \int_{t^i}^{t_{i+1}} \alpha(t')dt' \right]^{\frac{1}{1-z}}.$$

This last expression defines the relation between the uniform random variable ξ_i and the random inter-spike time τ_{i+1} or, equivalently, between ξ_i and the time t_{i+1} of occurrence of the first firing event following that occurred at time t_i. We can exploit the relationship between ξ_i, t_i and t_{i+1}, given in Eq. (8.27), to derive an expression for the conditional

probability $\psi(t_{i+1}|t_i)$ that an event occurs at time t_{i+1} given the condition that the previous event occurs at time t_i:

$$(8.28) \qquad\qquad \psi(t_{i+1}|t_i)dt_{i+1} = u(\xi_i)d\xi_i,$$

where $u(\xi_i)$ is the uniform distribution in the interval I, describing the random back-injection mechanism. Thus, we derive:

$$(8.29) \qquad \psi(t_{i+1}|t_i) = \alpha(t_{i+1}) \left[1 + (z-1) \int_{t_i}^{t_{i+1}} \alpha(t')dt' \right]^{\frac{1}{1-z}-1}.$$

By expressing the result in terms of μ_0, using Eq. (8.21), and of the inter-spike time $\tau_{i+1} = t_{i+1} - t_i$, we obtain

$$(8.30) \qquad\qquad \psi(\tau_{i+1}|t_i) = \frac{\alpha(t_i + \tau_{i+1})}{\left[1 + \frac{1}{\mu_0-1} \int_{t_i}^{t_i+\tau_{i+1}} \alpha(t')dt' \right]^{\mu_0}}.$$

The dependence on t_i is due to the important fact that the dynamic rule is changing as a function of time as a consequence of the external perturbation. We see that, as an effect of perturbation, the independence of the earlier jumps is lost. In fact, now the shape of $\psi(\tau_{i+1}|t_i)$ depends on the fact that the earlier jump occurs at t_i. Since the earlier jump depends on the jump before it, and so on, we find the surprising effect that an external perturbation undermines the renewal nature of the process and establishes, so to speak, an infinitely extended memory.

Let us make the following assumption [72]:

$$(8.31) \qquad\qquad \alpha(t) = \alpha_0 \left[1 + \epsilon \cos \left(\frac{2\pi}{T_\omega} t \right) \right].$$

As a consequence of this assumption it is possible to derive an analytical expression from Eq. (8.30):

$$(8.32) \qquad\qquad \psi(\tau_{i+1}|t_i) = \frac{\mu_0 - 1}{T_0} \frac{A(\tau_{i+1} + t_i)}{\left(1 + \frac{\tau_{i+1}}{T_0} + \frac{\epsilon}{2\pi} \frac{T_\omega}{T_0} G(\tau_{i+1}, t_i) \right)^{\mu_0}};$$

$$(8.33) \qquad\qquad A(\tau_{i+1} + t_i) = 1 + \epsilon \cos \left(\frac{2\pi}{T_\omega} (\tau_{i+1} + t_i) \right);$$

116

$$\text{(8.34)} \qquad G(\tau_{i+1}, t_i) = \sin\left(\frac{2\pi}{T_\omega}(\tau_{i+1} + t_i)\right) - \sin\left(\frac{2\pi}{T_\omega}t_i\right).$$

It is evident that the very large times τ_{i+1} cannot be significantly affected by the external perturbation, due to its periodic nature and to the fact that the perturbation strength ϵ cannot exceed the maximum value of 1. The numerical results of this Section confirm this expectation. An additional confirmation is given by the statistical analysis of Section 8.5.

As proved in Appendix A, this model generates a numerical algorithm drawing a random number only in association with the occurrence of a firing event. On the contrary, in the algorithm of Section 3.10 the draw of a random number is done at each time step and, consequently, the algorithm is much more time consuming.

(a)

(b)

Figure 8.5.　　Linear perturbation of T_0, Eqs. (8.24) and (8.31). Comparison of the perturbed histograms of inter-spike times, $\psi_{exp}(\tau)$, with the unperturbed ones, $\psi(\tau)$. $T_0 = 42.85174$, $\mu_0 = 2.4285174$, $\epsilon = 0.8$ (a) $T_\omega = 50$ ($R = 0.5$, fast perturbation), (b) $T_\omega = 10^5$ ($R = 10^3$, slow perturbation).

Figure 8.6. Fast linear perturbation of T_0, Eqs. (8.24) and (8.31). Histogram and exponential envelope of the maxima (dashed line) in the range of short inter-spike times. $T_0 = 10^4$, $T_\omega = 500$, $\mu_0 = 2.2$, $R = 0.01$, $\epsilon = 0.99$.
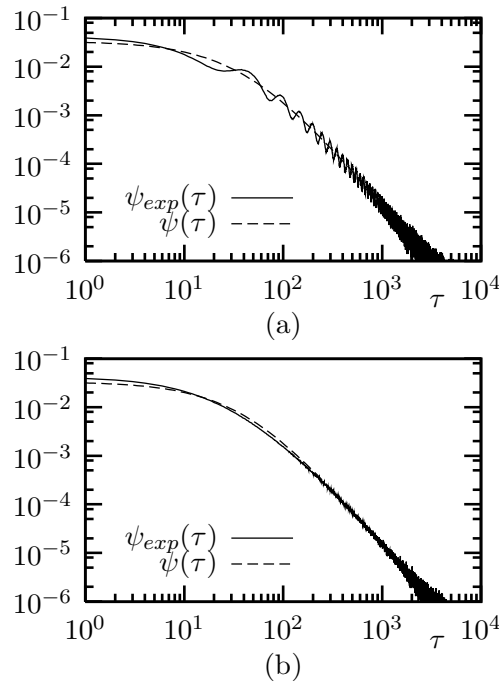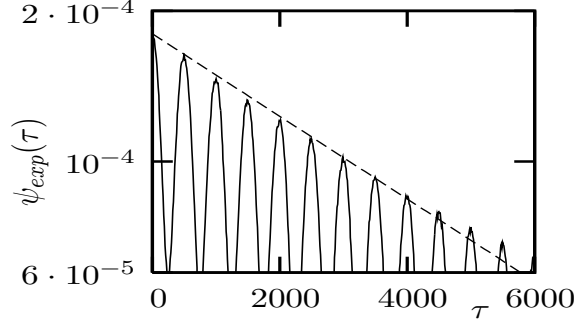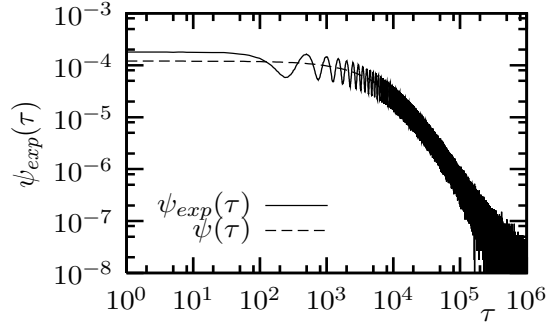

Figure 8.7. Fast linear perturbation of T_0, Eqs. (8.24) and (8.31). Comparison of the perturbed histogram of inter-spike times, $\psi_{exp}(\tau)$, with the unperturbed one, $\psi(\tau)$. $T_0 = 10^4$, $T_\omega = 500$, $\mu_0 = 2.2$, $R = 0.01$, $\epsilon = 0.99$.

We devote Figs.(8.4) and Fig.(8.4) to the illustration of the corresponding results. In Fig.(8.4) we explore the case $\epsilon = 0.8$ for both fast ($R = 0.5$) and slow ($R = 10^3$) perturbation. In this range of parameters, the perturbed system shows behaviors similar to those revealed in the case of the linear perturbation of the power index μ_0, Eq. (8.14). In particular, we observe that the effect of the perturbation is the emergence of small oscillations in the probability density, and they become more evident as R decreases.

We devote Figs.(8.4) and Fig.(8.4) to illustrating a condition corresponding to fast perturbation, $R = 0.01$, and to a value of ϵ close to the maximum ($\epsilon = 0.99$). An important remark must be made on the qualitative similarity between Fig.(8.4)and Fig.(8.3),

both showing the exponential cascade effect. Fig.(8.3) refer to the condition of non-linear perturbation of μ_0 described by Eq. (8.12), whereas the result of Fig.(8.4) was obtained by using the linear perturbation of T_0 introduced in this Section, although with a relatively strong coupling strength $\epsilon = 0.99$.

Figs.(8.4) and Fig.(8.4) show the same histogram at two different scales of the inter-spike times. The inter-spike time distribution in the range of short times ($\tau < T_0$) is displayed in Fig.(8.4), showing, as earlier remarked, an exponential cascade similar to that of Fig.(8.3) Fig.(8.4) shows the same histogram on a more extended range of inter-spike times, including times larger than T_0.

This allows to see that, for inter-spike times larger than T_0, the unperturbed histogram is essentially recovered, apart from the fast oscillations around a distinctly inverse power law behavior with the unperturbed power index $\mu_0 = 2.2$. We see that the transition from the former to the latter regime occurs at a time of the same order as T_0, thereby confirming our earlier observation that in the long-time regime the non-Poisson system recovers its original complexity, albeit partly blurred by fast oscillations making less accurate the evaluation of μ_0.

We are now in a position to argue that the non-linear perturbation of μ_0 behind Fig.(8.3) has more dramatic effects than the linear perturbation of T_0 introduced in this Section (Fig.(8.4) and Fig.(8.4)).

In next Section 8.5 we show how our guess is supported by the analysis of Diffusion Entropy.

8.5. DEA as applied to Non-Poisson Renewal Processes under Perturbation

Let us denote with δ the perturbed scaling, If $\delta > 0.5$ the system lives in the non-Poisson basin. The transition from $\delta > 0.5$ to $\delta = 0.5$ corresponds to a transition from the non-Poisson to the Poisson basin. Our guess is that the perturbed scaling δ is related to the effective power index μ_{eff} of Eq. (8.19) (at least, in the fast perturbation case). In Fig.(8.3) the threshold $\mu_{eff} = 3$ is reported to indicate the transition of the function $\mu_{eff}(\epsilon)$ from the non-Poisson to the Poisson basin. From this heuristic sketch,

a transition is expected in the range $1 < \epsilon < 2$. Actually, our numerical simulations showed that larger values of ϵ are needed to get reliable results (see Fig.(8.3)).

(a)

(b)

Figure 8.8. Slow linear perturbation of μ_0, Eq. (8.14). Diffusion Entropy (same parameters as Fig.(8.3)). $\mu_0 = 2.2$, $T_0 = 100$, $\epsilon = 0.6$, $\delta_0 \simeq 0.83$. (a) $T_\omega = 5 \cdot 10^3$ ($R = 10$); (b) $T_\omega = 5 \cdot 10^6$ ($R = 10^4$).

Figure 8.9. Fast linear perturbation of μ_0, Eq. (8.14). Diffusion Entropy (same parameters as Fig.(8.3)) . $T_0 = 100$, $T_\omega = 50$, $R = 0.1$, $\mu_0 = 2.2$, $\epsilon = 0.6$, $\delta_0 \simeq 0.83$.

In Fig.(8.5)-Fig.(8.5) we show the DE analysis at work. Figs.(8.5) and (8.5) illustrate the DE analysis applied to the case of linear perturbation of μ_0, as described by Eq.
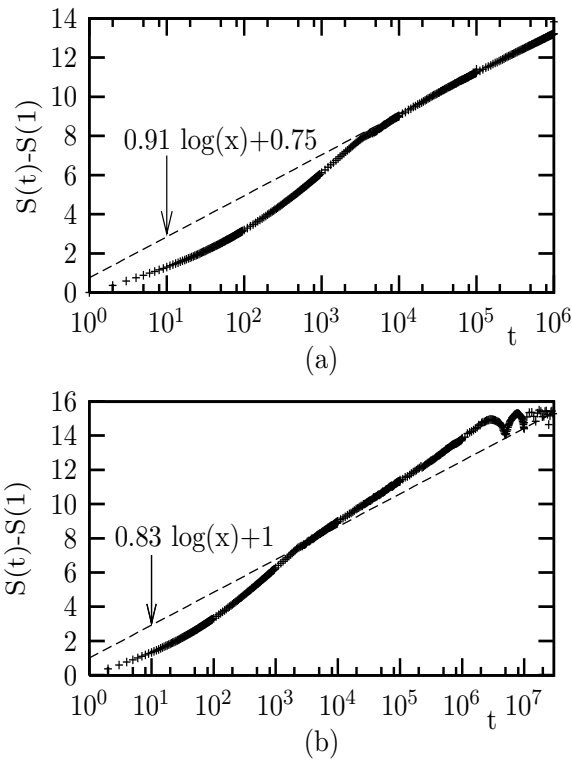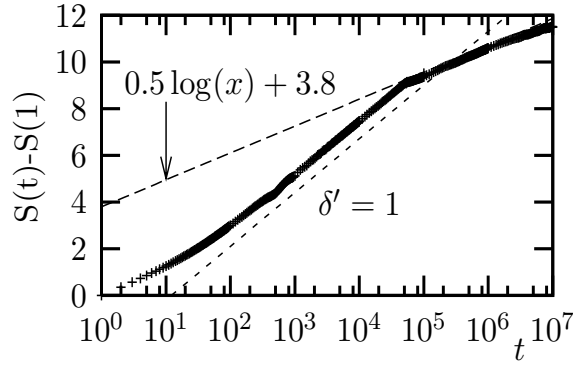
Figure 8.10. Fast non-linear perturbation of μ_0, Eq. (8.12). Diffusion Entropy (same parameters as Fig.(8.3)). $\mu_0 = 2.2$, $T_0 = 10^5$, $\epsilon = 7$, $T_\omega = 500$ ($R = 10^{-3}$), $\delta_0 \simeq 0.83$.

(a)

(b)

Figure 8.11. Linear perturbation of T_0, Eqs. (8.24) and (8.31). Diffusion entropy (same parameters as Fig.(8.4)). $T_0 = 42.85174$, $\mu_0 = 2.4285174$, $\epsilon = 0.8$, $\delta_0 = 0.7$. (a) $T_\omega = 50$ ($R = 0.5$, fast perturbation), (b) $T_\omega = 10^5$ ($R = 10^3$, slow perturbation).

(8.14), Fig.(8.5) illustrates the DE analysis applied to the case of non-linear perturbation of μ_0, according to the prescription of Eq. (8.12), and, finally, Figs.(8.5) and (8.5) show the DE analysis in action in the case of perturbation on the time scale T_0.
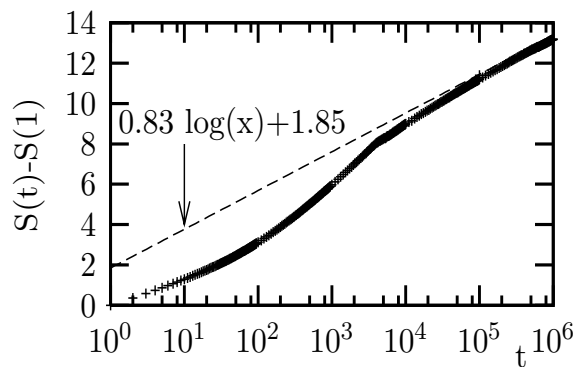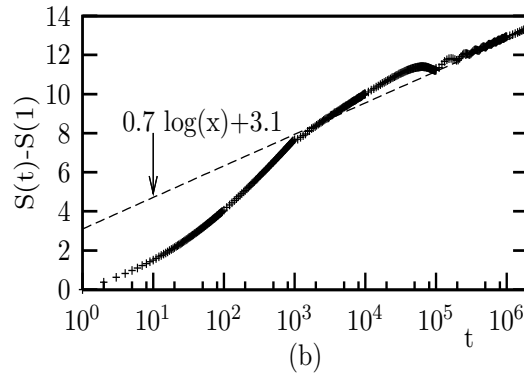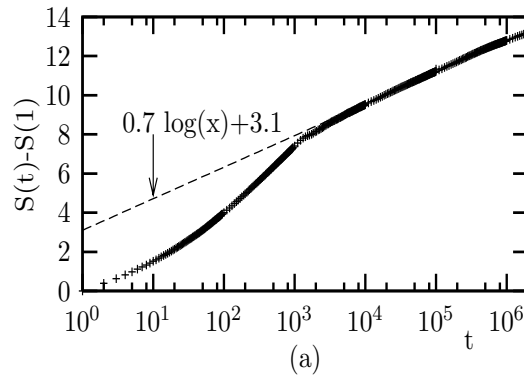
121
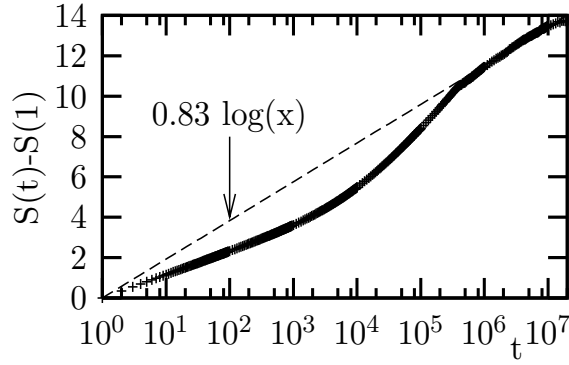
Figure 8.12.   Fast linear perturbation of T_0, Eqs. (8.24) and (8.31). Diffusion entropy (same parameters as Fig.(8.4)). $T_0 = 10^4$, $T_\omega = 500$, $R = 0.01$, $\mu_0 = 2.2$, $\epsilon = 0.99$, $\delta_0 \simeq 0.83$.

Figs.(8.5) and (8.5) correspond to the inter-spike time distributions of Figs.(8.3) and (8.3), respectively. Fig.(8.5) shows the DE analysis applied to two distinct sequences, simulating the effect of two slow ($R > 1$) linear perturbations of μ_0. We recall that, in this range of parameters, the probability density does not show significant oscillating behavior (see Fig.(8.3)). By comparing panels (a) and (b) of Fig. 9 and Fig. 10, it is possible to see that, at variance with the probability density, a clear oscillating pattern emerges in the DE curve only in the case of very slow linear perturbation, $R = 10^4$ (Fig. 9b). Fig. 9a illustrates the case where the linear perturbation is moderately slow, namely, in between the fast condition of Fig. 10 and the very slow perturbation of Fig. 9b.

Let us discuss the scaling detected by means of the DE analysis. First of all, let us notice that, according to the rule of Eq. (5.21), the power index $\mu_0 = 2.2$, shared by both Fig. 9 and Fig. 10, is expected to yield $\delta_0 \simeq 0.83$. We see that moving from the fast perturbation of Fig.(8.5) ($R = 0.1$) to the intermediate perturbation of Fig.(8.5)a ($R = 10$), does not produce any significant sign of oscillating behavior so that in both cases a neat asymptotic scaling δ appears. In the fast perturbation case (Fig.(8.5)) this scaling coincides with the unperturbed scaling $\delta_0 \simeq 0.83$, while in the intermediate case of Fig.(8.5)a the scaling gets the value $\delta = 0.91$, significantly larger than δ_0. In the case of very slow perturbation of Fig.(8.5)b the unperturbed scaling δ_0 appears again, although as the slope of the straight line on which the relative minima of $S(t)$ are located.

122

Let us explain this interesting result. In the case of fast linear perturbation of Fig.(8.5), the time dependent power index $\mu(t)$ of Eq.(8.15) oscillates many times within the time scale $\langle\tau\rangle$, so that the DE analysis perceives only its time average μ_{eff}, which, for the linear model of Eq. (8.14), is identical to μ_0, thereby yielding the unperturbed scaling δ_0. In the case of very slow perturbation of Fig. 9b we have to recall that the DE analysis rests on converting a single sequence into many diffusion trajectories using the mobile window method. When the length of the mobile window is equal to nT_ω, the influence of external perturbation is annihilated. This is the same explanation as that used in Ref. [80] and in the references to DE analysis therein. As a consequence, the relative minima of $S(t)$, represented in the linear-log representation, lie on the straight line, whose slope corresponds to the unperturbed scaling δ_0.

In the intermediate condition R=10 ($T_\omega = 10\langle\tau\rangle$), displayed in Fig.(8.5)a, the scaling changes to the value $\delta = 0.91$, significantly larger than the unperturbed scaling $\delta_0 = 0.83$. This result suggests the emergence of a form of complexity which is the consequence of the joint action of non-Poisson statistics and harmonic perturbation. This is not the linear superposition of two independent contributions, so that we can argue that, in this intermediate condition, linear perturbation and non-Poisson dynamics cooperate to create a new condition of complexity.

Let us now address with the help of DE analysis the interesting problem of exponential cascade. We want to prove that the DE analysis, through the inspection of the long-time limit, affords a way to distinguish the genuine from the apparent perturbation-induced transition from the Non-Poisson to the Poisson condition. The former kind of transition is illustrated by Fig.(8.5) and the latter by Figs.(8.5) and (8.5). Let us explain why it is so.

Fig.(8.5) illustrates the result of DE analysis in the case of fast non-linear perturbation of μ_0, Eq. (8.12), which produces the inter-spike time distribution of Fig.(8.3).

We see that there exists an extended transition regime with the effective scaling of $\delta' = 1$, but, after this extended transient of the order of T_0, we see the emergence of the ordinary scaling $\delta = 0.5$ rather than of the unperturbed scaling $\delta_0 \simeq 0.83$. According to

the prescription of Eq. (5.21), the scaling $\delta = 0.5$ corresponds to the condition $\mu_0 > 3$. A quite plausible explanation is that the DE analysis is mostly affected by the extended time intervals in which the effective power index $\mu(t)$, given in Eq. (8.13), is greater than 3. This is confirmed by the large value of the average power index $\mu_{eff} \simeq 200$, obtained by considering Eq. (8.19) with the parameters of Fig.(8.5). In conclusion, the exponential cascade of the case illustrated by Fig.(8.3) is the manifestation of a genuine transition from the non-Poisson to the Poisson condition.

Figs.(8.5) and (8.5) show the DE analysis in action in the case of a perturbation affecting the length of the inter-spike times, namely the parameter T_0, by means of Eqs. (8.24) and (8.31).

Fig.(8.5) shows an extended transient regime, of the order of $10\langle\tau\rangle$, with $\langle\tau\rangle$ given by Eq. (8.16). In panel (a) of Fig.(8.5) (fast perturbation) there is an abrupt transition to the asymptotic scaling, and in panel (b) (slow perturbation) this abrupt transition is rendered much smoother by the emergence of an oscillating behavior. In both cases the final scaling regime is found at times larger than T_ω, and in both cases this scaling regime turns out to be $\delta \simeq \delta_0 = 0.7$, in agreement with the interpretation that the model given in Eq. (8.24) does not affect the power index μ_0, which is linked to z by the expressions given in Eqs. (8.21) and (8.22). The result of the DE analysis reported in Fig.(8.5) confirms this prediction, through a well defined slope, which is again $\delta_0 = 0.83$, emerging after a transient that we estimate to be of the order of $10\langle\tau\rangle$.

We recall that the histogram of Fig.(8.4) shows the exponential cascade in the range of short inter-spike times $\tau < T_0$.

This feature is similar to that found for the fast non-linear perturbation of μ_0 (see Fig.(8.3)), but it is important to note that, at variance with that case, the DE now reveals the right unperturbed scaling ($\delta = 0.83$).

This is a crucial difference between the perturbation of T_0 and that of μ_0. The results of Fig.(8.5) and (8.5) fit the theoretical expectation, insofar as the perturbation of T_0 does not affect the power index μ_0, thereby making it natural to predict the emergence of the unperturbed scaling in the long-time regime.

8.6. Why the Exponential-Cascade does not necessarily prove the Poisson Nature of the Neuron Firing Process

.

The research work of this Chapter has been motivated by the experimental results of Ref. [78, 79] and especially by exponential cascade phenomenon. This phenomenon admits a straightforward interpretation as the response of a Poisson process to an external harmonic perturbation [80]. On the contrary, in this work we have shown that this phenomenon does not necessarily imply that the dynamics of neuron firing is a Poisson process. In particular, we have proved:

Result #1. The non-linear perturbation of μ_0, Eqs. (8.12) and (8.13), generates an exponential cascade representing a genuine transition from Non-Poisson to Poisson statistics.

Result #2. The linear perturbation of T_0 may generate the phenomenon of exponential cascade. However, in this case this is not the signature of a genuine transition from Non-Poisson to Poisson statistics, and the adoption of DE analysis shows that the long-time region is still characterized by the same complexity parameter μ_0 as in the unperturbed case.

The original purpose of this research work, aiming at shedding light into the phenomenon of exponential cascade of Refs. [78, 79] led us to a further, unexpected, result:

Result #3. It was found that a relatively weak (linear) harmonic perturbation of μ_0, Eqs. (8.14) and (8.15), either very slow, $R \gg 1$, or very fast, $R \ll 1$, does not affect the system's complexity, which emerges again in the long-time region. However, in the intermediate range $R \sim 10$ ($T_\omega \sim 10\langle\tau\rangle$), a surprising cooperation between perturbation and Non-Poisson dynamics occurs. The effect of this cooperation is the emergence in the long-time limit of the scaling parameter δ with a value significantly larger than the unperturbed complexity parameter δ_0.

Although this research work has been motivated by the neuron firing processes of Refs. [78, 79] we think that the results of this Chapter are of general interest, and provide

interesting indications on the response of non-Poisson processes to external harmonic perturbations.

8.7. Conclusions, Conjectures and Proposals for Future Research Work

In a recent work [102] the observation was made that both the brain and the music composition are non-Poisson renewal processes. The transport of information from music, as a form of weak perturbation, to the brain, is described by a linear response theory [96, 103] adapted to this unusual physical condition. These results can be explained by adopting the conceptual perspective that the interaction among many individual components (neurons) generates non-Poisson renewal events. Therefore, it would be disappointing to be forced to invoke the Poisson condition as the only one compatible with the exponential cascade of Refs. [78, 79].

Actually, half of the data of Ref. [78] comes from the work of Siegel [104], which reports on the response of single electrodes in the primary visual cortex of the cat while the cat received oscillatory visual stimulus from a screen (hence the periodic perturbations of Ref. [78]). Notice however that even though the recordings are from a single electrode, the response of this single electrode ultimately depends on the dynamics of the entire visual cortex (and presumably other regions of the brain as well). This is closely related to the conjecture made in Ref. [102] that a single electrode inherits the complexity of the whole brain. Consequently, the experimental data refer to a collective behavior (even though the signal of a single electrode is analyzed), thereby justifying the adoption of the models yielding the waiting time distribution of Eq. (8.2).

These conjectures are supported by many more recent experimental results. We quote the work by D. Plenz and colleagues, e.g. [105], or the more recent work of Ref. [106]. The experimental results of these authors support the claim of a collective critical regime in the cortex which may be compatible with the non-Poisson assumption made in this manuscript (Eq.(8.2). These conjectures are also supported by recent theoretical papers, see, for instance, [107, 108].

On the basis of all these remarks, we conclude that this article proves that the adoption of a strong invasive perturbation could have the effect of provoking a transition from the non-Poisson to the Poisson condition, thereby annihilating the complexity condition emerging from the collective behavior of a neuron set. This is an incentive to adopt non-invasive perturbations sharing, however, the brain complexity [102]. This requires the study of random perturbations, for instance, dichotomous perturbations that may realistically simulate the influence of a noisy environment [103]. The complexity matching condition invoked by both the authors of Ref. [102] and [103] may be an additional request to make non-invasive the perturbation influence. Thus, the result #3, which is beyond our current understanding may be a consequence of perturbing a system with complexity index μ_0 $(2 < \mu_0 < 3)$ with a simple (deterministic) excitation, thereby creating a significant departure from the condition of complexity matching.

CHAPTER 9

CONCLUSION

In this thesis we have investigated the perturbation of Renewal stochastic processes with regard to their properties concerning the waiting tim distributions and Complexity indices such as scaling coefficient and power law index. The perturbation of Poisson processes appeared to be closed connected to the stochastic resonance phenomena, the essential identity of some basic models for SR with perturbation of Poisson renewal processes has been discussed. It has also been shown that with Poisson and non-Poisson renewal processes, provided that they are in the ergodic regime $\mu > 2$, the power spectral density also displays similar properties to that of SR even sequences.

It has been show with reference to teen data birth Texas analyzed [63] earlier that, a sinusoidal perturbation of Poisson renewal processes may serve as a paradigmatic model where the noise is directly correlated to the seasonal effect itself. This noise although had no auto-correlation as it is, proved to have the same scaling properties as the seasonality effect, namely the signal itself [80]. It was also shown that perturbation induces some kind of a cumulative memory on a Poisson renewal system whose basic identity is to be memory-less. The effect memory on the properties of Renewal aging has been detected by Paradisi et.al.[94],[109]. As for future research we can expect the detection of induced memory by perturbation effects by means of some kind of aging analysis.

The perturbation of non-Poisson renewal processes can be performed by means of linear perturbation or non-linear perturbation, the former being a sub-class of the latter. Also the perturbation might be affecting the transition time to power law T_0 or the power index itself μ_0. We have found out that the linear perturbation of μ_0 leaves the scaling properties unchanged while the diffusion entropy analysis determines the effect of perturbation forming a joint effect of the ordinary scaling of the unperturbed system and an extra effect due to the periodic perturbation. DE using the Asymmetric Jump

Model of walking for diffusion agents based on the time series, detects the correct scaling properties of the system and the effect o perturbation appears in the same way of the superposition of a seasonal effect and a noise affects the scaling condition /citeosman2.

As to the non-linear perturbation of the ergodic non-Poisson system [39] it is detected that this form of perturbation as well as the non-linear perturbation of the Poisson processes [80] forms an exponential cascade akin to the experimental results obtained from neuronal data before [104], [78]. The similarity with the SR models are discussed and it is concluded that unlike the general impression obtained from the exponential decaying envelope of the data, on can not decisively conclude that the system has to be a Poisson system. The work concludes that a non-Poisson system under non-linear perturbation will give us exponential cascade waiting time distributions just as the data does [104], and that, this kind of perturbation can make the statistics of the system to make a transition from non-Poisson to Poisson statistics. This claim has been proved by means of DE-AJM analysis [39]. In conclusion the non-linear perturbation of the rate of a non-Poisson system via μ_0 may cause a transition to Poisson basin of statistics. This may find applications in complex network theory as well as an analysis of neuronal data.

APPENDIX A

NUMERICAL METHOD FOR THE PERTURBATION OF THE RATE OF A

POISSON PROCESS

In a perturbed Poisson process one can reverse engineer the random number

(A-1)
$$\xi = e^{-\left(\int_{t'}^{t'+\tau} r(t'' \, dt'')\right)}$$

under harmonic perturbation of the type

(A-2)
$$r(t) = r_0(1 + \epsilon \cos(\omega t))$$

we can set the equation

(A-3)
$$-\frac{\ln \xi}{r_0} = \tau + \epsilon(\sin(\omega t' + \omega \tau) + \sin(\omega t'))$$

This equation will be solved iteratively by numerical means. Once the equation holds then $t' \rightarrow t' + \tau$ will be set and generating another random number ξ one proceeds for the next τ. This procedure is used only for $\epsilon < 0.5$ for the perturbed Poisson system.

APPENDIX B

NUMERICAL PROCEDURE FOR THE PERTURBATION OF T_0

Let us consider the system described by the following equations:

(B-1)
$$\frac{dy}{dt} = \alpha(t)y^z,$$

(B-2)
$$\alpha(t) = \alpha_0(1 + \epsilon \cos(\frac{2\pi t}{T_\omega}))$$

where ϵ is the perturbation parameter in the range $[0, 1]$ and T_ω is the perturbation period. The variable y is defined in the interval $[0, 1]$. We can derive a relation between the initial condition $y(t') = \xi$ and the exit time τ, defined by $y(t' + \tau) = 1$ and corresponding to the inter-spike time. ξ is a uniform random variable in $[0, 1]$ and t' is the absolute time corresponding to the previous exit from the interval $[0, 1]$. Then, we have:

(B-3)
$$\frac{dy}{dt} = (\alpha_0 + \alpha_0\epsilon \cos(\omega t))y^z.$$

We integrate this expression

(B-4)
$$\int_{y_0}^{y} y^{-z}dy = \int_{t'}^{t'+\tau} \alpha_0 dt'' + \int_{t'}^{t'+\tau} \alpha_0\epsilon \cos(\omega t')dt''$$

and we get

(B-5)
$$\frac{y^{1-z}}{1-z} - \frac{y_0^{1-z}}{1-z} = \alpha_0\tau + \frac{\alpha_0\epsilon}{\omega}(\sin(\omega t' + \omega\tau) - \sin(\omega t')).$$

Substituting $y(t' + \tau) = 1$, we get:

(B-6)
$$\frac{1 - \xi^{1-z}}{\alpha_0(1 - z)} = \tau + \frac{\epsilon}{\omega}(\sin(\omega\tau + \omega t') - \sin(\omega t')).$$

This is the basic relation used in the algorithm. The first step is defined by inserting $t' = 0$ and the first inter-spike time is drawn with the following equation

(B-7)
$$\frac{1 - \xi^{1-z}}{\alpha_0(1 - z)} - \tau_1 = \frac{\epsilon}{\omega}(\sin(\omega\tau_1)).$$

For a given ξ, a numerical solution τ_1 of this equation can be found directly using an iterative procedure, explained below. Then, the first $t' = t_1$ is given by τ_1 and, substituting in Eq. (B-6) $t' = \tau_1$, we compute the second inter-spike time τ_2 and the occurrence time $t_2 = t_1 + \tau_2$. Iterating this procedure, we define, at each step n, $t_n = t_{n-1} + \tau_n$ and, substituting $t' = t_n$ in Eq. (B-6), we compute the next inter-spike time τ_{n+1}.

The iterative procedure used, at each step n, to compute the solution $\tau = \tau_{n+1}$ of Eq. (B-6), is given by the following expression:

(B-8)
$$\tau^{j+1} = \tau_{unp} - B \left(\sin(\omega\tau^j + \omega t') - \sin(\omega t') \right)$$

where:

(B-9)
$$\tau_{unp} = \frac{1 - \xi^{1-z}}{\alpha_0(1 - z)} \quad ; \quad B = \frac{\epsilon}{\omega} \quad ; \quad t' = t_n.$$

In order to avoid numerical problems, the algorithm is written in the following way:

(B-10)
$$\tau^{j+1} = \tau_{unp} - B \left[\sin(\omega\tau^j)\cos(\omega t') + \cos(\omega\tau^j)\sin(\omega t') - \sin(\omega t') \right].$$

Even if this expression is analytically equivalent to the previous one, this expression allows to prevent the effects of the truncations performed in the practical realization of the algorithm, which determine large numerical errors in the evaluation of τ, as t' becomes much larger than τ itself.

The initial condition for the iteration is given by τ_{unp}. The iteration is stopped when:

(B-11)
$$\Delta = \left| \frac{\tau^{j+1} - \tau^j}{\tau^j} \right| < \Delta_0$$

and then we put $\tau_{n+1} = \tau^{j+1}$. The choice of the threshold Δ_0 is a compromise between the accuracy and the program running time, which is a function of ϵ as well.

REFERENCES

[1] Landau L.D. and Lipschitz E.M., Statistical Physics, Pergamon Press, New York (1980).

[2] Barabasi Albert-Laszlo, Linked, Penguin Group Inc., New York (2003).

[3] Taisei K. and Kaizoji M.,*Physica A*, 336, pp.563-570,(2004).

[4] Farmer J.D., Shubik M., Smith E.,*Physics Today*, p.37, September (2005).

[5] L.A. Adamic, B.A. Huberman, *Glottometrics*, 3, pp.143-150,(2002).

[6] Newman.M.E.J., *Contemporary Physics*, 46 no.5, p.323, September-October (2005).

[7] Bak P., How nature works, Springer-Verlag, New York (1996).

[8] Hackett,A.P., 70 years of best sellers 1895-1965, R.R.Bowker Company, New York (1967).

[9] Huberman B.A. and Adamic L.A., Information dynamics in the networked world,in Ben-Naim E.,Frauenfelder H.,Toroczkai Z. (eds.) Complex Networks, # 56 in Lecture Notes in Physics, pp.371-398, Springer, Berlin (2004).

[10] Ebel H.,Mielsch L-I, Bornholdt S., *Phys.Rev.E.*, 66, 035103,(2002).

[11] Marquet P.A.,et.al.,*Journal of Experimental Biology*,208, pp.1749-1769, (2005).

[12] Allegrini P., Barbi F.,Grigolini P., Paradisi P., *Phys.Rev.E*, 73, 046136, (2006).

[13] Tsallis C., *Journal of Statistical Physics*, 52, pp.479-487, (1988).

[14] Barenblatt G.I., Scaling, self-similarity and intermediate asymptotics, Cambridge texts in applied mathematics 14, Cambridge University Press, Cambridge (1996).

[15] Guderley K.G.,*Luftfahrtforschung*, 19, pp.302-312, (1942).

[16] von Weizsaecker C.F. Z.,*Naturforschung*, 9a, pp.269-275,(1954).

[17] Zeldovich Ya. B.,*Sov.Phys.Acoustics*, 2, pp.25-35, 1956.

[18] Barenblatt G.I., Scaling, Cambridge texts in applied mathematics, Cambridge University Press, Cambridge (2003).

[19] Sornette D., Critical phenomena in natural sciences, Springer-Verlag, Heidelberg (2006).

[20] Mandelbrot.B.B., The Fractal Geometry of Nature, W.H.Freeman and Company, New York (1982).

[21] Hecht J., Optics : Light for a New Age, Reed Business Information Inc., New York (1988).

[22] Lesmoir-Gordon N., Rood W.,Edney R., Introducing Fractal Geometry, Totem Books USA, Victoria (2001).

[23] Chaos : the new science, Independent Communications Associates, World edge films production for Channel 4, (1988). Distributed by; New Dimension Media INC, Oregon

[24] Barnsley Michael F., Fractals everywhere, Academic Press, San Diego (1993).

[25] Devaney Robert L., A first course in Dynamical Systems : Theory and experiment, Addison Wesley Publishing Company, (1992).

[26] Hergarten S., Self Organized Criticality in Earth Systems, Springer-Verlag, Heidelberg (2002).

[27] L.F. Richardson, Statistics of deadly quarrels,Ed: Q Wright, C.C. Lienau, Quadrangle Books Inc, London (1960).

[28] B.J.West, B.Deering, The lure of modern science : Fractal thinking, World Scientific, Singapore (1995).

[29] Lowen S.B., Teich M.C., Fractal Based Point Processes, Wiley-Interscience, Hoboken NJ (2005).

[30] Hayes B., *American Scientist*, 90 no:1, pp.10-15, (2002).

[31] Addison P.S., Fractals and Chaos ; an Illustated Course., IOP Publishing Ltd, Bristol (1997).

[32] Aczel A.D., Chance : A guide to gambling, love, the stock market & just about everything else, MJF Books, New York (2004).

[33] Cox D.R., Renewal Theory, Methuen & Co. Ltd Science Paperbacks, London (1967).

[34] Craddock J.M., Statistics in the Computer Age, The English University Press Ltd., London (1968).

[35] Reif F., Fundamentals of Statistical and Thermal Physics, Mc Graw Hill, Singapore (1985).

[36] Jon Ogborn, Simon Collins, Mick Brown,*Physics Education*, 38 issue:5, p.391, (2003).

[37] Rutherford E., Phil.Mag., 20, pp.698-707, (1910).

[38] Jon Ogborn, Simon Collins, Mick Brown,*Physics Education*, 38 issue:5, p.398, (2003).

[39] Akin O.C., Paradisi P., Grigolini P.,Submitted to J.Stat.Mech. (2008).

[40] E.Daly and A.Porporato, *Phys.Rev.E*, 74, 041112, (2006).

[41] Reynolds O.,*Phil.Trans.R.Soc.*, 935 (1983).

[42] Solari H.G.,Natiello.M.A.,Mindlin G.B., Nonlinear Dynamics: a two way trip from physics to math, IOP Publishing Ltd., (1996).

[43] Schuster H.G., Just W., Deterministic Chaos, An Introduction, WILEY-VCH Verlag, Weinheim (2005).

[44] Shapiro A.H., The fluid dynamics of drag, part 4: How to reduce drag?, video recording, Encyclopedia Britannica Educational Corporation,Chicago IL (1960).

[45] Adair R.K., The physics of baseball, Perennial, New York (2002).

[46] Turcotte D.L., Fractals and Chaos in geology and geophysics, Cambridge University Press, Cambridge (1992).

[47] P. Manneville, *J. Phys.*, 41, p.1235 (1980).

[48] Zaslavsky G.M., Physics of Chaos in Hamiltonian systems, Imperial College Press, London (1988).

[49] Giesel T., Thomae S.,*Phys.Rev.Lett.*, 52, p.1936, (1984).

[50] Aquino G.,Grigolini P.,Scafetta N.,Sporadic Randomness, *Chaos Solitons and Fractals*, 12, pp.2023-2038, 2001.

[51] P. Allegrini, V. Benci, P. Grigolini, P. Hamilton, M.Ignaccolo, G. Menconi, L. Palatella, G. Raffaelli, N. Scafetta, M. Virgilio and J. Yang, *Chaos Solitons and Fractals*, 15, p.517, (2003).

[52] Benzi R., Sutera A., Vulpiani A., *J. Phys. A*, 14, L453, 1981.

[53] Benzi R, Parisi G, Sutera A, Vulpiani A, *Tellus*, 34, pp.10-16., (1982).

[54] Harry J.D., Niemi J.B., Priplata A.A., Collins J., Balancing Act,*IEEE Spectrum*, p.1294, April (2005).

http://www.spectrum.ieee.org/apr05/1294

[55] F. Moss, et.al., *Clinical neurophysiology*, pp.267-281, February (2004).

[56] Wellens T., Shatoknin V., Butchleitner A., *Rep.Prog.Phys.*, 67, pp.54-105, (2004).

[57] L. Gammaitoni, P. Hanggi, P. Jung, F. Marchesoni, *Rev.Mod.Phys.*, 70, p.223, (1998).

[58] Papoulis A. Probability Random variables and stochastic processes, Mc-Graw Hill, New York (1965).

[59] P.Radhakrishnan, S.Dinesh,*Chaos Solitons and Fractals*, 27, p.511, (2006).

[60] N.Scafetta, B.J.West, *Geophys. Research Lett.*, 32, L18713 (2005).

[61] M.Ignaccolo, T.Farges, E.Blanc, and M.Füllekrug, arXiv:physics/0508141, in press on Solitons, Chaos and Fractals (2005).

[62] M.Ignaccolo, P. Allegrini, P. Grigolini, P.Hamilton, B.J. West,*Physica A*, 336, p.594, (2004).

[63] M.Ignaccolo, P.Allegrini, P.Grigolini, P.Hamilton, B.J.West, Physica A **336**, 623, (2004).

[64] J.Bellazzini, G.Menconi, M.Ignaccolo, G.Buresti, P. Grigolini, *Phys.Rev.E*, 68, 026126, (2003).

[65] H.Yang, F.Zhao, W.Zhang, Z.Li, *Physica A*, 347, 704, (2005).

[66] A.Longtin, A.Bulsara, F.Moss, *Phys.Rev.Lett.*, 67, 656, (1991).

[67] K.Hu, P.Ch.Ivanov, P.Carpena, H.E. Stanley, *Phys. Rev.*, 64, 011114, (2001).

[68] R.Nagarajan, R.G.Kavasseri, *Chaos Solitons and Fractals*, 26, 777, (2005).

[69] R.Nagarajan, R.G.Kavasseri, *Physica A*, 354, 182, (2005).

[70] N.N.Pang, W.J.Tzeng,*Phys.Rev.E*, 69, 031108, (2004).

[71] L.Gammaitoni, P.Hänggi, P.Jung, F.Marchesoni,*Rev.Mod.Phys.*, 70, 223, (1998).

[72] F.Barbi, M.Bologna, P.Grigolini,*Phys.Rev.Lett.*, 95, 220601, (2005).

[73] N.Scafetta, P.Hamilton, P.Grigolini,*Fractals*, 9, 193, (2001).

[74] P.Grigolini, L.Palatella, G.Raffaelli, *Fractals*, 9, 439, (2001).

[75] T.Zhou, F.Moss. P.Yung, *Phys.Rev.A*, 42, 3161, (1990).

[76] N.Scafetta, P.Grigolini, *Phys.Rev.E*, 66, 036130, (2002).

[77] P. Barat, A. Sarkar, P. Mukherjee, and S.K. Bandyopadhyay, Phys. Rev. Lett. **94**, 055502 (2005).

[78] A.Longtin, A.Bulsara, F.Moss, *Phys.Rev.Lett.*, 67, 656, (1991).

[79] T.Zhou, F.Moss, P.Jung, *Phys.Rev.A*, 42, 3161, (1990).

[80] O.C.Akin, P.Paradisi, P.Grigolini, *Physica A*, 371 issue:2, pp.157-170, (2006).

[81] H.E.Plesser, T.Geisel, *Phys.Rev.E*, 63, 031916, (2001).

[82] L.Lapique, *J.Physiol.*, 9, p.620, (1907);H.C. Tuckwell, *Stochastic Processes in the Neurosciences* (SIAM, Philadelphia, 1989); A.R.Bulsara, T.C.Elston, C.R.Doering, S.B.Lowen, and K.Lindenberg, *Phys.Rev.E* 53, p.3958 (1996); P. Lánský, *Phys.Rev.E*, 55, p.2040, (1997).

[83] M.Schindler, P.Talkner, and P.Hänggi,*Phys.Rev.Lett.*, 93, p.048102, (2004).

[84] P.-L.Gong and J.-X.Xu, *Phys.Rev.E*, 63, p.031906, (2001).

[85] R.FitzHugh, in *Biological Engineering*, Ed: H.P.Schwann, McGraw-Hill, New York, (1962); J.Nagumo, S.Arimoto, and S. Yoshizawa, *Proc. IRE*, 50, p.2061, (1962).

[86] A.L.Hodgkin and A.F.Huxley, *J. Physiol.*, 117, p.500, (1952).

[87] F.Liu, Y.Yu and W.Wang, *Phys.Rev.E*, 63, p.051912, (2001).

[88] I.A.Khovanov and P.V.E.McClintock,*Phys.Rev.E*, 67, p.043901, (2003).

[89] D.T.W.Chik, Y.Wang and Z.D.Wang, *Phys.Rev.E*, 64, p.021913, (2001).

[90] H.Yang, F.Zhao, W.Zhang, Z.Li, *Physica A*, 347, p.704 (2005).

[91] E.Reibold, W.Just, J.Becker, and H.Benner, *Phys.Rev.Lett.*, 78, p.3101, (1997).

[92] C. van Vreeswijk, *Neurocomputing*, 417, pp.38-40, (2001).

[93] R.Baddeley, L.F.Abbott, M.C.A. Booth, F.Sengpiel, T.Freeman, E.A.Wakeman, E.T.Rolls, *Proc.R.Soc.Lond B* 264, p.1775, (1997).

[94] S.Bianco, P.Grigolini, P.Paradisi, *J.Chem.Phys.*, 123, p.174704, (2005).

[95] P.Allegrini, G.Ascolani, M.Bologna, P.Grigolini, cond-mat/0602281.

[96] P.Allegrini, M.Bologna, P.Grigolini, B.J.West,*Phys.Rev.Lett.*, 99, p.010603, (2007).

[97] P.Grigolini, D.Leddon, and N.Scafetta, *Phys. Rev E*, 65, p.046203, (2002).

[98] E. Parzen, Stochastic Processes, Holden-Day Inc., San Francisco, (1962); D.R.Cox and H.D.Miller, The Theory of Stochastic Processes, Chapman & Hall, London UK, first edition (1965).

[99] Devroye L., Non-uniform random variate generation, Springer-Verlag, New York (1986).

[100] P.Allegrini, G.Aquino, P.Grigolini, L.Palatella, A.Rosa, *Phys.Rev.E*, 68, p.056123, (2003).

[101] B. McNamara, K. Wiesenfeld, *Phys.Rev.A*, 39, p.4854, (1989).

[102] S.Bianco, M.Ignaccolo, M.S.Rider, M.J.Ross, P.Winsor, P.Grigolini, *Phys.Rev.E*, 75, p.061911, (2007).

[103] P.Allegrini, M.Bologna, P.Grigolini, B.J.West, arXiv:cond-mat/0612303.

[104] R.M.Siegel, *Physica D*, 42, p.385, (1990).

[105] J.M.Beggs and D.Plenz, *J. Neurosci.*, 23, p.11167, (2003).

[106] D. Plenz and T. C. Thiagarajan,*Trends in Neurosci.*, 30, p.101, (2007).

[107] C. Haldeman and J. M. Beggs, *Phys.Rev.Lett.*, 94, p.058101, (2005).

[108] O. Kinouchi and M. Copelli, *Nature Physics*, 2, p.348, (2006).

[109] P.Allegrini, F.Barbi, P. Grigolini, P. Paradisi, *Phys.Rev.E*, 73, p.046136, (2006).